PhD-FSTM-2024-017
The Faculty of Science, Technology and Medicine

DISSERTATION

Defence held on 05/04/2024 in Luxembourg

to obtain the degree of

DOCTEUR DE L'UNIVERSITÉ DU LUXEMBOURG

EN *BIOLOGIE*

by

JENNIFER PHAN
Born on 13 July 1993 in San Jose, United States

A TRANSCRIPTOME AND PHENOTYPIC ANALYSES BETWEEN EARLY AND LATE PARKINSON'S DISEASE TO UNRAVEL DISEASE MECHANISMS

Dissertation defence committee

Dr Ulf Nehrbass, dissertation supervisor
Professor, Université du Luxembourg
Ceo, Luxembourg Institute of Health

Dr Yong-Jun Kwon, Vice Chairman
Head of Precision Medicine, Luxembourg Institute of Health

Dr Jens Schwamborn, Chairman
Professor, Université du Luxembourg

Dr Arnaud Ogier
Head of Images and Data Mining, KSILINK

Dr Juyong Yoon,
Senior Researcher, KIST Europe

LUXEMBOURG INSTITUTE OF HEALTH
RESEARCH DEDICATED TO LIFE

UNIVERSITÉ DU LUXEMBOURG

DISSERTATION

submitted in partial fulfilment of the requirements for the degree of

Philosophiae Doctor (PhD)

in
Biologie

by
Jennifer Phan

A TRANSCRIPTOME AND PHENOTYPIC ANALYSES BETWEEN EARLY AND LATE PARKINSON'S DISEASE TO UNRAVEL DISEASE MECHANISMS

Degree-awarding institution: *University of Luxembourg*
Host institution: *Luxembourg Institute of Health*

Dissertation defence committee:

Dr. Ulf Nehrbass, dissertation supervisor
Professor, University of Luxembourg
Ceo, Luxembourg Institute of Health

Dr. Yong-Jun Kwon
Head of Precision Medicine, Luxembourg Institute of Health

Dr. Jens Schwamborn
Professor, University of Luxembourg

Dr. Arnaud Ogier
Head of Images and Data Mining, KSILINK

Dr. Juyong Yoon
Senior Researcher, KIST Europe

Defence held on *05/04/2024* in *Luxembourg*

This work was mainly done at:

Developmental and Cellular Biology, LCSB

With collaborators:

LuxGen Genome Center, LNS

Disease Modelling & Screening Platform, LIH

KSILINK

Juntendo

Lubeck University

As part of the doctoral training unit:

Molecular, Organellar and Cellular Quality Control in
Parkinson's Disease and Other Neurodegenerative Diseases (PARK-QC)

This project was funded by:

Ministère de l'Enseignement supérieur et de la Recherche (MESR)

Luxembourg National Research Fund (FNR)

Programme for Research-intensive Doctoral Education (PRIDE)

AFFIDAVIT

I hereby confirm that the Ph.D. thesis entitled “A Transcriptome and Phenotypic Analyses between Early and Late Parkinson’s Disease to Unravel Disease Mechanisms” has been written independently and without any other sources than cited.

Jennifer Phan

Luxembourg, April 2024

ACKNOWLEDGEMENTS

Whew, it has been a wild ride in the past five years. Navigating the numerous connections and faring the repercussions of COVID-19 has certainly made my time in Luxembourg enthralling. Nonetheless, it is a fulfilling experience and a personal growth that I am very grateful for. Along the way, there are MANY people whom I am also grateful for as their help and encouragement have been invaluable.

First, to the Luxembourg Institute of Health or LIH where I first began. To my co-supervisors, Drs. Ulf and Yong-Jun, your unique way of supervising my studies has taught me to be even more self-independent and adaptive as well as reinforcing my communication skills beyond the foreign language barrier. Thank you for taking me on as your student in addition to your many duties and for taking time from your busy schedule to meet with me.

For the team at the LIH Edison building. To Florence, thank you for being the contact person for Ulf. Countless times you have come through to help me at critical points. To Valerie and her HR team, thank you for backing my time in Luxembourg and helping with any of the government-related matters. To Hughes, Jordan, and their IT team, thank you so much for your constant fixes, especially with my laptop(s). Never did I think I would be handling three accounts simultaneously and I should have kept them separate from the beginning.

For the research units within LIH that I approached for cooperation or a simple chat. To Drs. Gunnar, Marta, and the people at Proteomics of Cellular Signalling unit, although the collaboration fell through, thank you for your cheeriness as I made my foray back into the lab at that time. To Nathalie, Elise, and Arnaud from Luxgen, thank you for the fruitful collaboration beyond LCSB. Arnaud, I have thoroughly enjoyed our lengthy discussions and your support has slowly reignited my interest in programming again. To Drs. Bruno, Paul, and their colleagues at the Disease Modelling & Screening platform, thank you for your

tremendous support at LCSB and with that darn Yokogawa instrument. Lastly, to Dr. Feng from the Immune Systems Biology unit, thank you for that insightful conversation on the transcriptomic data. You really have helped me to break down that overwhelming amount of information into something legible.

Next, onto Luxembourg Centre for Systems Biomedicine or LCSB where I mainly worked. To Dr. Jens, thank you for being a gracious lab host. Your multicultural environment has made my time memorable despite the awkwardness from LCSB's constant restructuring. To the people both past and present in his Developmental and Cellular Biology group (Thea, Daniela, Raquel, Ginevra, Michele, Catarina, and Elise), thank you all for being fabulous lab mates. Especially to the postdocs (Gemma, Sarah, Javier, Claudia, Silvia, Jennifer, Kiki, Alise, Graham, Isabel, Sonia, and Henry), thank you for answering my many (and maybe incessant) questions and inquiries however strange they might be for science. To the tight-knit community within LCSB like the Bioimaging platform, thank you for adding to my experiments and experience at the institute.

Then, for the PARK-QC doctoral training unit that I was part of. To all the fellow graduates, thank you for being a wonderful cohort. Despite our few gatherings, we never failed to greet each other when passing by as we roam LCSB or Belval campus. Congratulations on your success and I will continue to root for your journey across the internet.

Onto the left neighbour of Luxembourg and into France or specifically, KSILINK where I had my training. To Dr. Juyong, thank you for your teachings on the neuron cell cultures. I have enjoyed our conversations on the topics of subtle cultural differences and cell culture differences between Europe, USA, and South Korea. To Dr. Arnaud and his team at the Images and Data Mining group, thank you for your tremendous help with the image analysis. You really have come through withstanding the pressing times. And thank you both for being part of the jury members for my defence.

Finally, onto my people from the other side of the world. To my family, thank you for being brave and letting me traverse the Atlantic Ocean for my PhD. Our weekly FaceTime may

have driven me crazy at times, but it was something familiar for me here in a foreign country. Thank you for making the trips across the ocean whenever I did not feel like flying. To my tiny deaf community (Helen, Michelle, and Zeng), thank you for representing the other part of me. Sometimes I looked forward to waking up to the EXTREMELY long chat messages filled with your craziness and occasional gif battles that surprisingly navigate many topics in one night. Thanks for staying up until the crack of dawn to chat with me whenever I popped back up on the messenger. Here's to remaining as travel buddies for the future.

Finally, to all other individuals that are not mentioned here, thank you. Even if it was a smile in a passing moment or a friendly conversation, it contributed to my happy experience in Luxembourg. Who knew meeting so many new people in a new country is such a fun thing to do (so far).

I DID IT! WOOT. 

TABLE OF CONTENTS

LIST OF ILLUSTRATIONS

LIST OF FIGURES

LIST OF TABLES

ABBREVIATIONS

AA	ASCORBIC ACID
AKT	AKT SERINE-THREONINE KINASE
ALCAM	ACTIVATED LEUKOCYTE CELL ADHESION MOLECULE
ASYN	ALPHA SYNUCLEIN
ATP	ADENOSINE TRIPHOSPHATE
BSA	BOVINE SERUM ALBUMIN
CDNA	COMPLEMENTARY DEOXYRIBONUCLEIC ACID
CORIN	ATRIAL NATRIURETIC PEPTIDE-CONVERTING ENZYME
DAMP	DANGER-ASSOCIATED MOLECULAR PATTERN
DBCAMP	DIBUTYRYL CYCLIC ADENOSINE MONOPHOSPHATE
DECTIN-1	DENDRITIC CELL-ASSOCIATED C-TYPE LECTIN-1
DEGS	DIFFERENTIALLY EXPRESSED GENES
DMEM/F-12	DULBECCO'S MODIFIED EAGLE MEDIUM: NUTRIENT MIXTURE F-12
DOD	DAYS OF DIFFERENTIATION
DRP1	DYNAMIN-RELATED PROTEIN 1
E8	ESSENTIAL 8
ESCS	EMBRYONIC STEM CELLS
FACS	FLUORESCENCE-ACTIVATED CELL SORTING
FBS	FETAL BOVINE SERUM
FOXA2	FORKHEAD BOX A2

GBA	GLUCOCEREBROSIDASE
GPCR	G PROTEIN-COUPLED RECEPTORS
GRPS/GRFS	GUANINE RELEASING-PROTEIN/FACTORS
HBDNF	HUMAN BRAIN-DERIVED NEUROTROPHIC FACTOR
HGDNF	HUMAN GLIAL CELL LINE-DERIVED NEUROTROPHIC FACTOR
IKK	IκB KINASE COMPLEX
IKKα	IκB KINASE COMPLEX ALPHA
IKKβ	IκB KINASE COMPLEX BETA
IPSCS	INDUCED PLURIPOTENT STEM CELLS
L-DOPA	L-3,4-DIHYDROXYPHENYLALANINE
LMX1A	LIM HOMEOBOX TRANSCRIPTION FACTOR 1 ALPHA
LRRK2	LEUCINE-RICH REPEAT KINASE 2
LRTM1	LEUCINE RICH REPEATS AND TRANSMEMBRANE DOMAINS 1
MAP2	MICROTUBULE-ASSOCIATED PROTEIN 2
MAPK	MITOGEN-ACTIVATED PROTEIN KINASES
MDNS	MIDBRAIN DOPAMINERGIC NEURONS
NANOG	HOMEOBOX TRANSCRIPTION FACTOR
NESCS	NEUROEPITHELIAL STEM CELLS
NESTIN	NEUROEPITHELIAL STEM CELL PROTEIN
NF-κB	NUCLEAR FACTOR KAPPA-LIGHT-CHAIN-ENHANCER OF ACTIVATED B CELLS
NIK	NF-κB-INDUCING KINASE
OCR	OXYGEN CONSUMPTION RATE
OCT4	OCTAMER TRANSCRIPTION FACTOR 4

OPA1	OPTIC ATROPHY 1 PROTEIN
PARK2	PARKIN E3 UBIQUITIN PROTEIN LIGASE
PAX6	PAIRED BOX 6
PBS	PHOSPHATE-BUFFERED SALINE
PCA	PRINCIPLE COMPONENT ANALYSIS
PCR	POLYMERASE CHAIN REACTION
PD	PARKINSON'S DISEASE
PDL	POLY-D-LYSINE
PFA	PARAFORMALDEHYDE
PI3K	PHOSPHOINOSITIDE 3-KINASE
PINK1	PTEN INDUCED KINASE 1
PMA	PURMORPHAMINE
PS	PENICILLIN-STREPTOMYCIN
PSYN	PHOSPHORYLATED ALPHA SYNUCLEIN
RAS	RAT SARCOMA
RNA	RIBONUCELIC ACID
ROBO	ROUNDABOUT
ROCK	RHO-ASSOCIATED PROTEIN KINASE
SILAC	STABLE ISOTOPE LABELING BY AMINO ACIDS IN CELL CULTURE
SNCA	SYNUCLEIN ALPHA
SOX1	SRY-BOX TRANSCRIPTION FACTOR 1
SOX2	SRY-BOX TRANSCRIPTION FACTOR 2
SSEA4	STAGE-SPECIFIC EMBRYONIC ANTIGEN-4

TGF-β3	TRANSFORMING GROWTH FACTOR BETA-3
TH	TYROSINE HYDROXYLASE
TNFR	TUMOUR NECROSIS FACTOR RECEPTOR
TOMM20	TRANSLOCASE OF OUTER MITOCHONDRIAL MEMBRANE 20
TRA-1-60	T CELL RECEPTOR ALPHA LOCUS
TUBB3	BETA TUBULIN-III

ABSTRACT

Parkinson's (PD) manifests in patients predominately aged 50 and above although, there are cases with younger patients as early as their 20s. This highlighted the diverse age range impacted by the neurodegenerative disease and underscored the need for a nuanced understanding across the various age groups. For this, a side-by-side comparison was made between early-onset and late-onset PD, using stem cell technology to generate midbrain dopaminergic neurons from patients. The two patients had opposite ages of onset and carried mutations in the same gene, PARK2. Transcriptomic and phenotypic analyses were used to find key signatures that set the two etiologies apart. There, we saw two potential signatures: neurite plasticity and neuroinflammation. The drastic decline of the MAP2 expression was observed in late-onset PD patient neurons compared to the early-onset PD patient neurons. Conversely, there was an enrichment of the upregulated RNAs within the noncanonical NF-κB pathway in early-onset PD patient neurons compared to late-onset PD patient neurons. These distinct mechanisms occurring at the cellular level may be among the biological cues signalling the beginning of the neurodegenerative disease at a particular age. Decoding the underlying machinery of PD would further the understanding of the age factor in Parkinson's and unravel the disease mechanisms.

1. INTRODUCTION

With an increasing human lifespan and aging population, the spotlight on age-related diseases remains. Age-related diseases are health conditions that become more prevalent as individuals grow older and can impact different organs of the body, ranging from head to toe and at various levels. Such examples include neurodegenerative, cardiovascular, respiratory, and gastrointestinal diseases, osteoporosis, metabolic disorders, cancer, and so on. Aging is a complex process influenced by a myriad of factors such as genetics, environment, and lifestyle.

From one angle, some clinical researches observe preventive healthcare measures or a certain lifestyle. From another angle, there are biomedical researches that go beyond patient observation. A combination of both types of research is necessary when addressing the intricate system within the human body. After all, the brain is still the great unknown. Two well-known age-related neurodegenerative diseases impact the brain: Parkinson's and Alzheimer's diseases. While both disturb the central nervous system and lead to progressive impairment of cognitive and motor functions, they are distinct in their pathologies. Here, we highlight Parkinson's disease (PD).

1.1. PARKINSON'S DISEASE

Parkinson's disease is associated with the loss of dopaminergic neurons in the substantia nigra region of the brain. (Alexander, 2004.) The exact cause is not fully understood, as there is no specific test for the diagnosis. Instead, it is determined by the exclusion of other possible causes for the symptoms. Back in 1817, a British physician named James Parkinson first described the disease as a gradual loss of neurons that produce dopamine, a neurotransmitter involved in many processes including motor control. (Parkinson, 1817.)

1.1.1. DEMOGRAPHICS

At this time of writing, the Parkinson's Foundation estimated over 10 million people suffer from PD worldwide and that number would continue to increase as time goes on. The demographics of the disease are quite diverse but with some trends. First, most of the patients diagnosed with Parkinson's are in their elderly or their 50s and older. A small percentage of those patients have an earlier age of onset, as young as their 20s. The reason for this is not fully understood, it is thought to be a combination of genetic and environmental factors contributing, perhaps more of the genetic or hereditary factor. (Ferguson, 2016.) (Mehanna R. M., 2014.) As a result, Parkinson's can generally be divided into two categories: early-onset and late-onset PD. Secondly, it is observed that PD is slightly more common in men than women. (Eeden, 2003.) In terms of race and ethnicity, the prevalence varies among the different groups although there are evidences that suggest a low socioeconomic status would increase the risk of PD. (Najafi, 2023.) (Yang, 2016.) The geography and environmental factors can be intertwined, influencing each other toward increasing the risk of PD in certain geographical regions. (Ball, 2019.) (De Miranda, 2022.)

Many genes have been implicated in Parkinson's disease, all ranging in their frequency and biological impact. (**Illustration 1**.) On one end, there are genes whose pathogenic variants are sufficient to cause the disease and are found in familial links through the affected family. (Day, 2021.) (Jankovic, 2020.) Examples include the Synuclein Alpha (SNCA) and Parkin E3 Ubiquitin Protein Ligase (PARK2) genes. On the other end, so far, there are 90 identified variants common among PD patients, contributing a small amount to the risk of the disease. Then in the middle of the spectrum, some variants are somewhat common and pose an intermediate risk. Examples include the Leucine-Rich Repeat Kinase 2 (LRRK2) and Glucocerebrosidase (GBA) genes. Alterations to each of these genes can lead to functional deficits in various aspects within the dopaminergic neurons. For example, the SNCA plays a pivotal role in the alpha synuclein pathology, the PARK2 is involved in protein degradation and the GBA is involved in the lysosomal activity. (Dulski, 2022.) (Huang Y. W., 2023.)

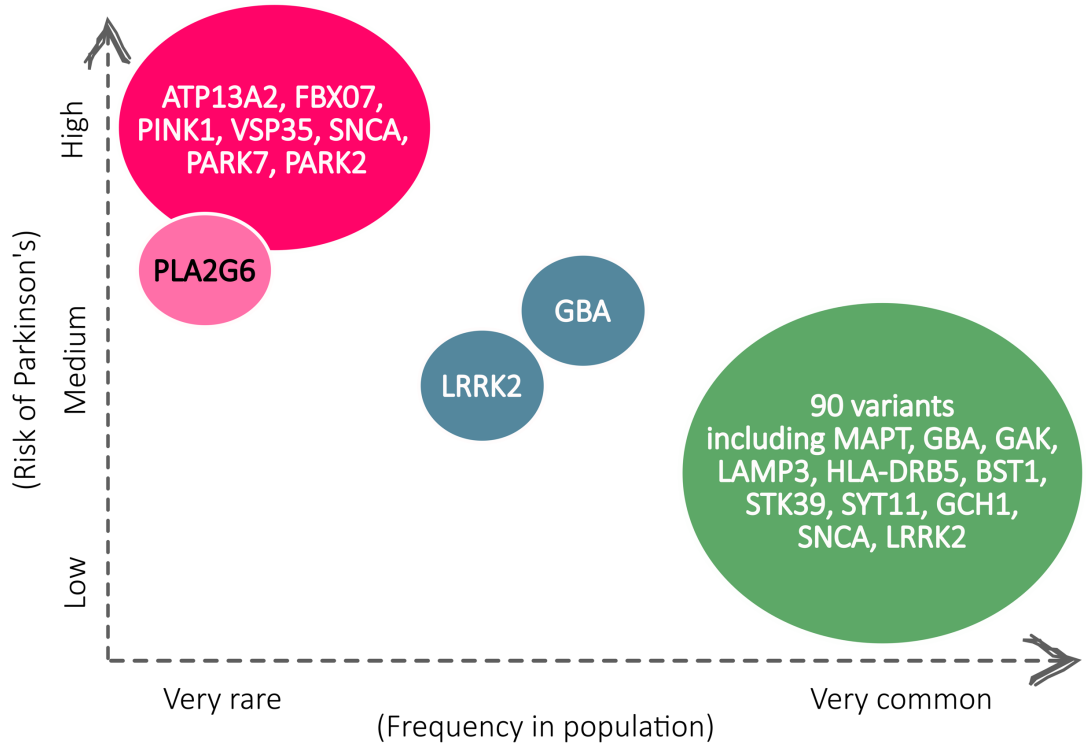

Illustration 1. The genetic blueprint of Parkinson's. A plot with the genes arranged according to their risk and frequency in PD. The Mendelian genes are labelled in pink, except for the PLA2G6 gene. The genes in blue are medium risk and green are low risk but high in frequency.

Adapted from (Day, 2021.)

1.1.2. MOTOR SYMPTOMS

The loss of the dopaminergic neurons greatly affects the smooth and coordinated control of voluntary movements, leading to the visible manifestation of PD. Not all patients will experience the same combination or severity of the motor symptoms but there are cardinal ones. (Akkaoui, 2019.) (Moustafa, 2016.) The most common one is the resting tremors or shaking of hands, fingers, and other extremities that affect the limbs when not moving but decrease in appearance during actual movements. Another is bradykinesia or difficulty initiating and completing voluntary movements such as getting up from a chair. Part of this can also be due to rigidity where there is an increased resistance to the passive movements of the joints. Then there is postural instability where the patient cannot

maintain an upright and balanced position along with shuffling and/or freezing gait in their walking pattern.

While the core motor symptoms are generally similar between early-onset and late-onset PD, there are some distinctions in the manifestation and progression of the symptoms. For early-onset PD, the progression is more gradual and can extend over a long period or the patient may not experience them for many years until their actual appearance. (Post, 2020.) (Riboldi, 2022.) The first symptoms usually show themselves through a combination of rigidity, pain, and cramps, all of which can be mistaken for other related disorders as Parkinson's would not be the first thought. In addition, most of the motor symptoms for young patients could be the aftermath of prolonged drug usage rather than the disease itself. (Wickremaratchi, 2011.) For late-onset PD, the progression is much more rapid over a shorter period and is usually more severe especially when combined with the older age.

1.1.3. NON-MOTOR SYMPTOMS

Aside from the motor symptoms, PD is also associated with a variety of non-motor symptoms that can significantly influence the patient's welfare. These symptoms can appear at different stages of progression and can be challenging to manage. A well-known one is cognitive impairment that consists of difficulty with memory recall, attention span, executive function, and dementia. (Garcia-Ruiz, 2014.) (Piredda, 2019.) Furthermore, the patient can experience sleep disturbances such as insomnia, mood disorders such as depression, and impulse control affliction. Another non-motor symptom is the gastrointestinal issues that range from constipation and ingestion to difficulty in swallowing or dysphagia. (Klann, 2021.) (Tan, 2022.) While these issues are associated with Parkinson's, they can also be a result of long-term medications for their motor symptoms.

The non-motor symptoms exhibit variations between early-onset and late-onset PD. The young patients have a slower progression of the symptoms yet because of that extended time, the impact on the quality of life can be much more significant. (Mehanna R. &., 2019.)

In addition, the manifestation of certain symptoms is likely in one etiology over the other such as dementia being less likely for early-onset PD or gastrointestinal issues being more likely for late-onset PD. (Heetun, 2012.) (Hely, 2008.)

1.1.4. TREATMENT&CARE

Although there is no cure for Parkinson's disease, there are treatments available to manage the symptoms and improve the patient's well-being. The treatments are often multidisciplinary, including medication, dietary changes, therapies, and support groups. An example of the medication is levodopa, a dopamine replacement agent. (Armstrong, 2020.) An example of nutritional changes can be an increased fibre intake and hydration to help with constipation. (Knight, 2022.) Physical, occupational, and speech therapies are all beneficial to improve daily functioning. (Pigott, 2022.) Finally, there are support groups to provide emotional support for the patients and their caregivers. (Gerritzen, 2022.) The strength of a well-built community is essential for patients with PD. Then there is the ongoing neuroscience research in effort to advance our understanding of the disease.

1.2. NEURON BIOLOGY

The brain itself is a very complex organ that acts as a control centre for the central nervous system. Its function arises from the interactions and connectivity of the neurons within, which are responsible for processing and transmitting signals throughout the body. In this section, we return to the beginning and see how the neurons are formed then delve further into the neurons themselves, examining both their normal function and the disruptions seen in Parkinson's.

1.2.1. THE CENTRAL NERVOUS SYSTEM DEVELOPMENT

Early in embryonic development, the embryo undergoes gastrulation, organizing itself into three germ layers: the ectoderm, mesoderm, and endoderm. (Zhai, 2022.) Each layer will go on to develop specific cell types and tissues, but the central nervous system is formed from the ectoderm through neurulation or neural plate formation. (**Illustration 2**.) First, the ectoderm begins by folding inward into the middle, creating the neuroectoderm that pinches off within the mesoderm. The result is a neural tube adjacent to the ectoderm, with a group of neural crest cells in between. (Sadler, 2005.) The neural crest cells are dedicated to the peripheral nervous system and other related cell types from the upper portion of the human body. For the neural tube, the anterior portion will give rise to the brain while the posterior portion shapes into the spinal cord. Brain development continues as different regions and structures occur, such as the forebrain, midbrain, hindbrain, and so on. Finally, neurogenesis occurs in these regions, leading to the generation of different types of neurons such as dopaminergic neurons in the midbrain. (Kinter, 2022.) (Prakash, 2006.) The neuron connectivity also establishes itself, creating a circuit throughout the human body and installing the brain as the control centre of the central nervous system.

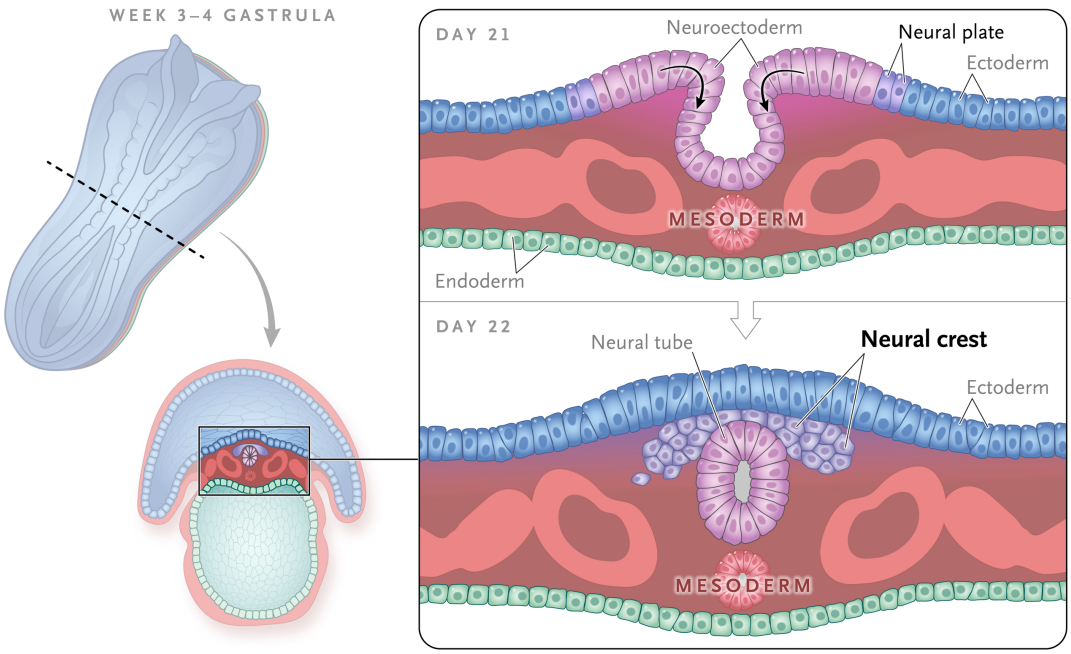

Illustration 2. The neural crest formation. A visual depiction of the gastrulation shown. On the left is the gastrula between weeks 3 and 4 of the embryonic development. On the right, a cross-section of the three germ layers within the gastrula shows the neurulation.

1.2.2. NEURON ANATOMY AND NORMAL FUNCTION

Despite the different types of neurons in the brain, its anatomy generally remains the same. (**Illustration 3**.) It has a cell body with its nucleus and dendrites branching outward to receive the signals from neighbouring neurons. At their end, the cell body has an axon projecting outward with sections of myelin sheath wrapped around it. This projection conducts the electrical impulses away from the cell body and toward the axon terminals, sending the signal to other neighbouring neurons. Evidently, a neuron is efficient in its anatomy for connectivity and any disturbances to it would cause dysfunction.

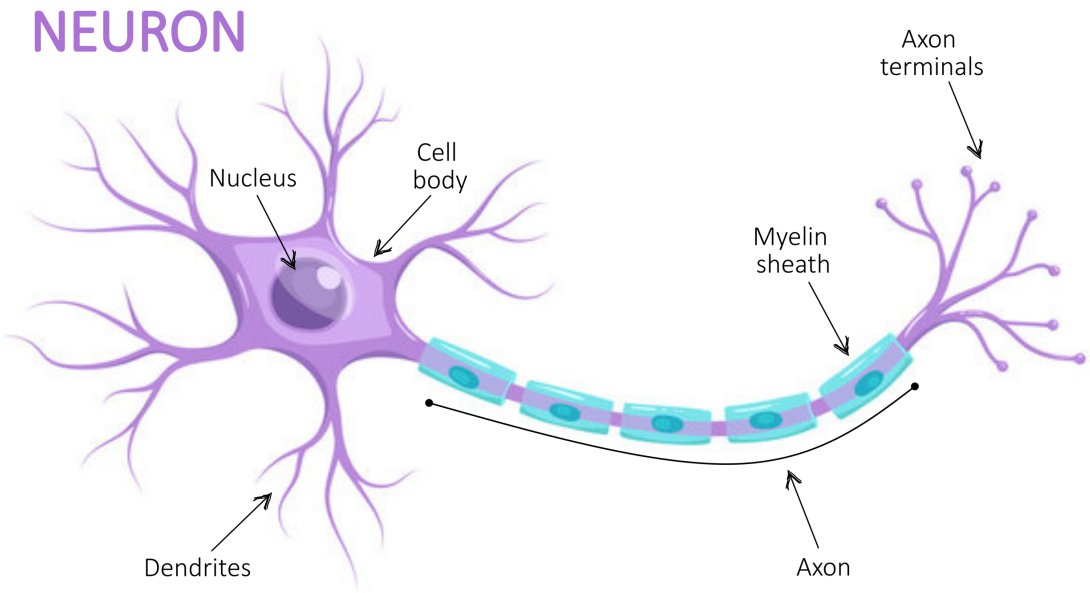

Illustration 3. The neuron anatomy. A visual depiction of neuron anatomy with parts pointed out: cell body, nucleus, dendrites, axon, myelin sheath, and axon terminals.

A neuron is usually at its resting state. Once it receives a stimulus exceeding a threshold, the neuron generates an action potential where an electrical signal traverses the axon. (Nelson, 2017.) That action potential is regulated by different factors, such as the ion channels and gradients that polarize or depolarize the axon membrane. The myelin sheath also contributes to the efficiency of the action potential propagation across the axon. Still, there are unmyelinated neurons such as those in the peripheral nervous system. (Saab, 2017.) Once the electrical signal reaches the axon terminal, the neuron forms a synapse junction with another neuron and the neurotransmitters are released into the junction. The reception of the neurotransmitters induces a postsynaptic action potential that is a combination of excitatory and inhibitory signals to determine if the signal continues onto other neurons. (Maynard, 2023.) If not, the termination of the signal is dictated by the clearing of the neurotransmitters through reuptake or degradation. (Sheng, 2002.) As a result, neuronal communication is established within the junction between the axon terminals of one neuron and the dendrites of another neuron.

Aside from signalling, the neuron engages in other activities as well to maintain the overall function and health of the central nervous system. Examples can include metabolic functions where glucose metabolism and mitochondrial activity are conducted to provide the necessary energy for neural activities, synaptic plasticity where the synapses adapt structurally and functionally in response to experience as well as axonal transport where necessary molecules are delivered to distant parts of the brain for maintenance or repair. (Bélanger, 2011.) (Cooke, 2006.) (Zheng, 2019.)

1.2.3. NEURON DYSFUNCTION IN PARKINSON'S DISEASE

The focal point of Parkinson's is the dysfunction of the neurons. (Sulzer, 2013.) At the cellular level, the dysfunction begins with the loss of the midbrain dopaminergic neurons (mDNs), leading to the deficiency of dopamine. This cardinal feature creates a drastic impact on the regulation of voluntary movement.

From the shortfall of dopamine, this disruption continues onto the neurites beyond synaptic gaps. The defective synaptic junctions impacting the communication between neurons are just one part of the wide range of consequences coming from the constraints on the neurites. (Bellucci, 2016.) The neurites are the long thin projections within the neural network that include the axon and dendrites. Their flaws can start from inefficient dendritic integration of signals where the neurons would have an altered response, or the dendritic spine dynamics change to the point where the strength of the synaptic connection is affected/lost. (Picconi, 2012.) (Villalba, 2010.) The flaws continue onto the axon compartment where an accumulation of misfolded proteins or damaged organelles can occur as well as non-functioning cytoskeletal/motor proteins compromising the axon trafficking system. (Mishra, 2022.) (Tagliaferro, 2016.) More importantly, the defective neurites can influence the balance between the excitatory and inhibitory signalling that makes up the neural communication, leading to a faulty neural circuitry. (Gonzalez-Suarez, 2022.) (Haxhiu, 2005.)

Delving deeper, there is the proteinaceous culprit, alpha synuclein, a pathogenic hallmark of PD. Alpha synuclein is involved in regulating the synaptic vesicles and the subsequent release of neurotransmitters. (Bendor, 2013.) In their abnormal state, the alpha synuclein accumulates, leading to the formation of Lewy bodies. Not only that, their phosphorylated isoforms are also much more prone to the misfolding and aggregations. (Kawahata, 2022.) This pathology can affect the organelles, overtake the neuron, and spread from one neuron to another, thus contributing to the progressive nature of the disease. (Bernal-Conde, 2020.) Eventually, those intracellular deposits disturb the neuron homeostasis and lead to their death.

Following the same logic, there can be deficits in the cellular machineries responsible for clearing the malformed proteins such as the ubiquitin-proteasome system. (**Illustration 4**.) Several genes have been implicated in this machinery including the PARK2 and PTEN Induced Kinase 1 (PINK1) genes. (Olanow, 2006.) The ubiquitin-proteasome system is a highly regulated cellular process that selectively degrades ubiquitin-tagged proteins. Once tagged, the proteins are directed to the proteasome for digestion into peptides. In the PD

neurons, the deformed alpha synuclein (phosphorylated ones as well) are often targeted for ubiquitination therefore the dysfunction of that machinery can lead to Lewy body formation as well. (McNaught, 2001.) Aside from the cytoplasmic clearing of the misfolded proteins, the ubiquitin-proteasome system also influences the fate of other cellular structures such as the endoplasmic reticulum, plasma membrane, and cytoskeleton. (Amm, 2014.) (Pohl, 2019.)

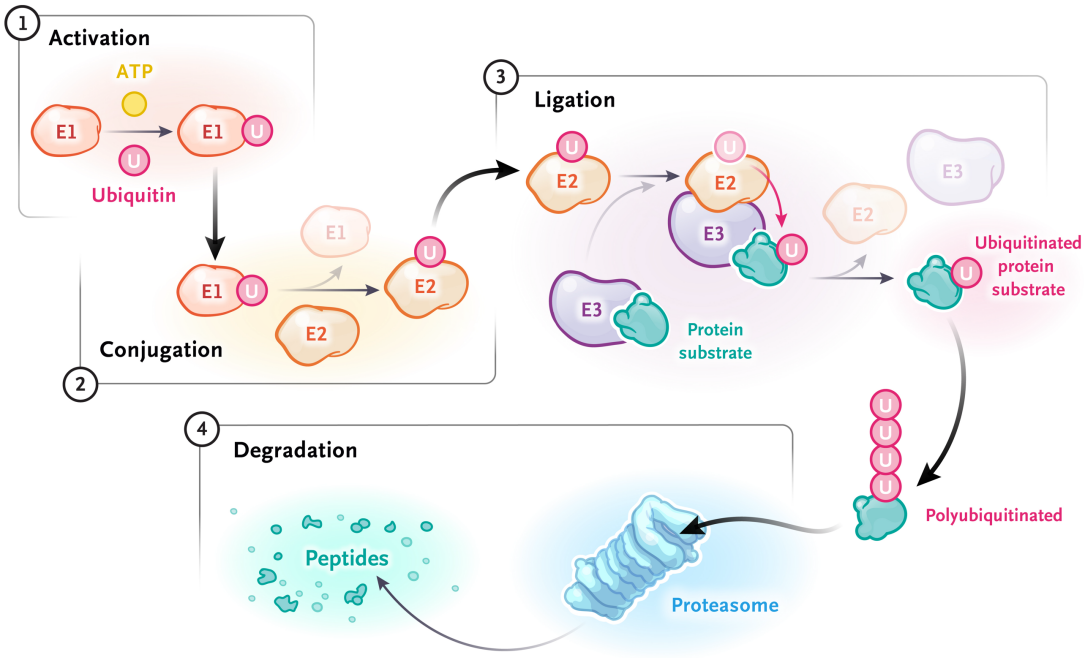

Illustration 4. The ubiquitin-mediated protein degradation process. A visual depiction of the ubiquitin-proteasome system and its inner workings. Tagging the malformed proteins with ubiquitin takes part in three stages: activation, conjugation, and ligation. Lastly, the ubiquitin-tagged protein is directed to the proteasome for digestion.

Mitochondria, as hubs of oxidative phosphorylation, are also susceptible to the damaging effect of deformed proteins. About the PD-implicated genes, there is a particular interplay between PARK2, PARK7, and PINK1 genes that influences the mitochondrial quality control. (Hauser, 2017.) (Truban, 2017.) Damages can include defects in the respiratory chain,

leading to a reduced adenosine triphosphate (ATP) production or an increase of the reactive oxygen species, which leads to increased oxidative stress on other organelles thereby overwhelming the neurons. This is especially true in the brain, an organ with high-energy demands and abundant oxidative molecules. In addition, any alterations to mitochondrial dynamics such as fission and fusion activities and mitophagy can cause the organelle to contribute to neurodegeneration. (Ganley, 2022.) (Lim, 2012.)

Deciphering the intricacies of neuron dysfunction in Parkinson's provides the foundation for discovering potential therapeutic targets, especially with the stem cell technology emerging in biomedical research.

1.3. STEM CELL TECHNOLOGY

The concept of stem cells has been around for quite some time, but the true understanding of their abilities began in the early 1960s, when Canadian researchers, Ernest McCulloch and James Till, made their groundbreaking discovery of hematopoietic stem cells in the bone marrow. (Becker, 1963.) The stem cells are characterized by two abilities: self-renewal or the ability to proliferate and pluripotency or the ability to differentiate into other cell types. (Zakrzewski, 2019.) They can be categorized by their potency such as the multipotent somatic stem cells that can give rise to only cell types relating to their tissue of origin. Those cells play a crucial role in maintaining and repairing the tissues they reside in. Another type is pluripotent embryonic stem cells (ESCs) which can form cells from all three germ layers of the gastrula. (Martello, 2014.)

The embryonic stem cells are present in the embryo as early as the first week of development after the ovum egg is fertilized. (Mu, 2022.) (Weatherbee, 2021.) The zygote continues to develop into a blastocyst, which consists of an outer layer of trophoblasts that give rise to the placenta and an inner cell mass that becomes the embryo proper. (**Illustration 5**.) This is where embryonic stem cells are found, using their pluripotency ability to form the diverse tissues and organs of the human body.

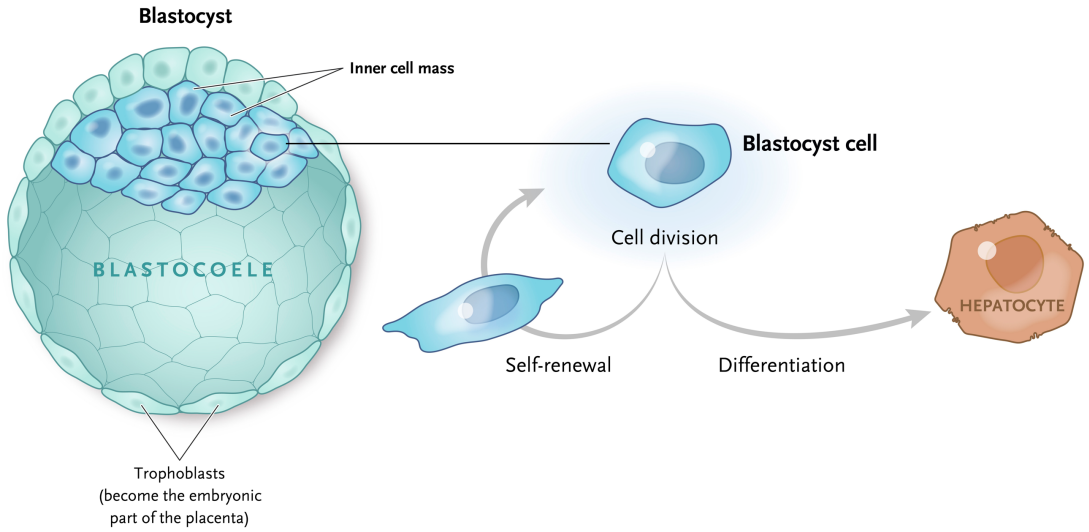

Illustration 5. The embryonic stem cells within the blastocyst. A visual depiction of the zygote during embryonic development. The first few stages of the development are shown, leading up to the blastocyst formation where the embryonic stem cells are found in the inner cell mass.

In a strictly controlled cell culture environment, the researchers can direct the ESCs to differentiate into desired cell types such as the neurons; however, there are ethical concerns regarding their source. (Juengst, 2000.) (Keller, 2005.) (Wert, 2003.) This led the researchers to consider other avenues for obtaining the stem cells such as using mesenchymal stem cells (adult stem cells) instead. (Pittenger, 2019.)

1.3.1. INDUCED PLURIPOTENT STEM CELL TECHNOLOGY

The induced pluripotent stem cell (iPSC) technology represents the next groundbreaking development in stem cell research. (Shi, 2017.) In 2007, a Japanese researcher, Shinya Yamanaka, and his team reprogrammed adult human fibroblasts back to their pluripotency state, essentially creating embryonic-like stem cells. (**Illustration 6**.) (Takahashi, 2007.) Analogously, the four reprogramming transcription factors: OCT3/4, SOX3, KLF4, and c-MYC, are coined as the Yamanaka factors. This is often the approach used

to reconfigure the somatic cells from various sources such as skin or blood; hereby circumventing the ethical issues that come with ESCs. (Buganim, 2013.)

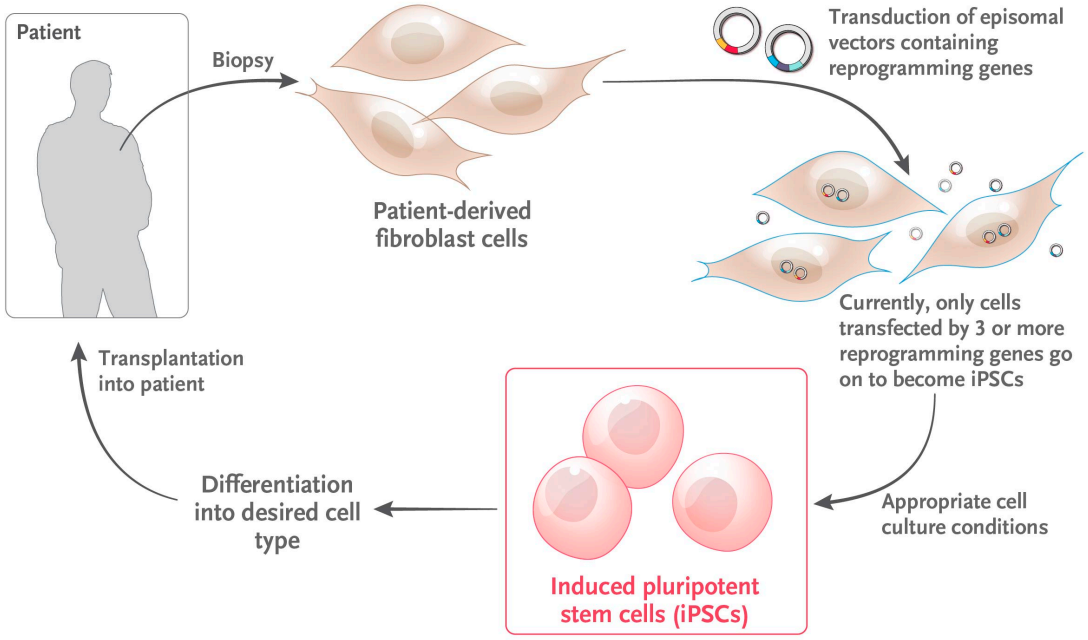

Illustration 6. The reprogramming of fibroblasts into induced pluripotent stem cells. A visual depiction of the iPSC generation. The fibroblasts derived from the patients are transduced with the reprogramming genes to revert them back into their pluripotency state. Then the iPSCs can be cultured, differentiated, and potentially transplanted back into the patient.

Once reprogrammed, the iPSCs exhibit pluripotency, meaning they can differentiate into other cell types of all three germ layers; however, quality controls must be in place, which include checking their genomic integrity. (Rohani, 2018.) This is an unfortunate side to the stem cells, tumorigenicity or the tendency to form tumour cells and genomic aberrations increase the likelihood of the stem cells turning into tumour cells. (Knoepfler, 2009.) That aside, the differentiation process can be terminal, meaning the cell fate is set and cannot be reversed. Or the iPSCs can be directed to progenitor cells that are multipotent. Those progenitors can give rise to other cell types only within their lineage. (Birbrair, 2021.) For

example, the iPSCs are differentiated into neuroepithelial stem cells (NESCs) found in the neural tube of the gastrula. Then all derivatives of the NESCs afterward are specifically of neural cell types. This approach is beneficial because neurons are post-mitotic and cannot proliferate, while the NESCs retain the self-renewal property. (Kreutz, 2023.) This iPSC technology solves the ethical concerns of using the ESCs and opens new possibilities for personalized medicine, drug discovery, and disease modelling.

1.3.2. PATIENT-BASED DISEASE MODELING

Patient-based disease modelling is a transformative approach toward biomedical research, leveraging stem cell technology to create in vitro systems mimicking the disease in the patient. This allows for a closer look into the cellular and molecular processes, providing valuable insights into the disease mechanisms, progression, and potential therapeutic targets.

Using animal models or immortalized cell lines do not fully capture the complexity of a disease. In that capacity, the stem cell technology is fully utilized especially with the iPSCs originating from the patient. (Doss, 2019.) Once obtained, the iPSCs can differentiate into the afflicted cell types of the disease such as neurons for neurodegenerative disorders, cardiomyocytes for heart conditions, or hepatocytes for liver inflammation. Previously, cell culture has been two-dimensional or a monolayer of cells within a tissue culture dish; however, this does not quite capture the true presentation of the disease. (Liu C. O., 2018.) To that end, the increasingly popular three-dimensional culture known as organoids is used to create a system that mimics physiological changes and recapitulate the complexity of the disease in the human body. (**Illustration 7**.) (Sharma, 2020.)

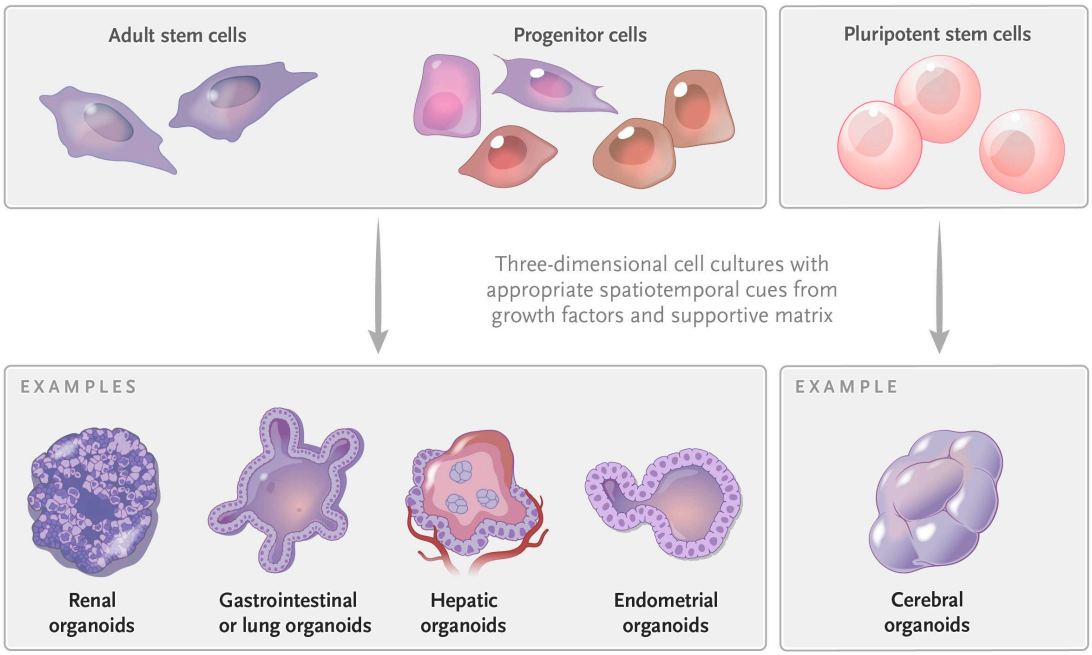

Illustration 7. Organoids, the three-dimensional patient-based disease models. A visual depiction of the many different types of organoids. The fate of the organoids is determined by the cell types used to generate them.

Aside from unravelling disease mechanisms, patient-based disease models are also beneficial for drug screening and precision medicine. (Loewa, 2023.) (Park S. G., 2023.) The principle is to tailor treatments toward the patients based on their genetic and molecular makeup. Potential therapeutic compounds can be tested on cells that closely mirror the patient's own cells and have their outcome evaluated, allowing for a personalized approach to treatment. Any adverse effects are anticipated, and the positive reactions are closely monitored for further tailoring.

The field of regenerative medicine continues to evolve as researchers explore more ways to harness the regenerative abilities of stem cells to treat a myriad of medical conditions including neurodegenerative disorders. One of which is Parkinson's disease.

Parkinson's is a complex and progressive neurodegenerative disease that affects millions of people worldwide. Each patient's journey is unique as the disease manifests differently in terms of motor and non-motor symptoms. Support from healthcare professionals, caregivers, family, and friends is an essential part for the patient navigating life with PD. Ongoing neuroscience research continues to further our understanding of the disease's causes and progression. Altogether, raising awareness and advocating for the current research are part of the collective effort to advance our knowledge of Parkinson's to find more effective treatments and, ultimately a cure.

2. AIMS&OBJECTIVES

Although many patients have late-onset PD, there are cases with those having early-onset PD. This distinction underscored the interplay between genetics, environment, and age-related factors during the development of Parkinson's. So far, numerous clinical-pathological studies have been conducted, where the patients were assessed for their motor and non-motor conditions or familial relations. (Ferguson, 2016.) Their medical assessment also taken, looking into their brain connectivity or fluid composition. (Schirinzi, 2020.) All this was done, but little inquiry has been made at the cellular and molecular levels.

Here, we attempt to fill the gap between the physical manifestation of the two PD etiologies and their underlying cause at the cellular level.

In detail, the aims & objectives of this project were to do:

1. Transcriptomic analysis – starting the comparison at the RNA level and finding the differentially expressed genes

2. Proteomic analysis – continuing the comparison onto protein level and finding the differentially expressed peptides to integrate with transcriptomic data

3. Phenotypic analysis – continuing the comparison onto the morphology to observe different cellular characteristics

4. Functional assessment – continuing the comparison onto the functional capacity to see how the molecular changes impact the organelles such as the mitochondria

3. MATERIALS&METHODS

3.1. EXPERIMENTAL DESIGN

This project intended to do a comparison between early-onset and late-onset PD iPSC-derived neurons with a time course experiment. Three time points were specified for the dopaminergic neuron culture, each ending with a collection of materials for the downstream assays. (**Illustration 8**.) The DOD or days of differentiation was used to discern the "age" of those neuron cultures.

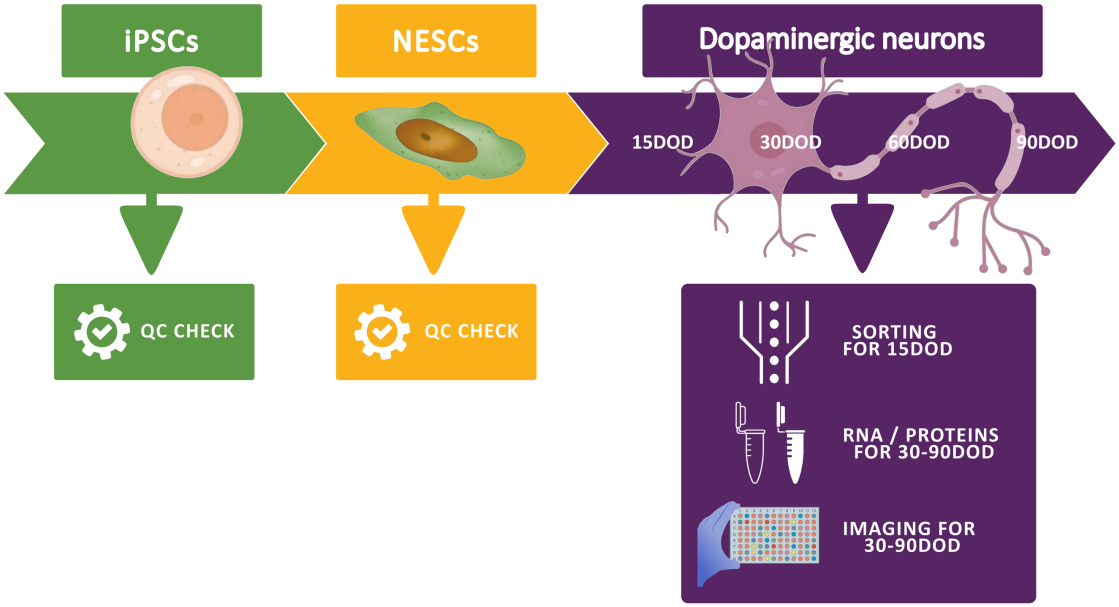

Illustration 8. The project's experimental design. The outline of the entire cell culture shown, starting from the iPSCs to dopaminergic neurons. Endpoints indicated for neuron culture were for when they were collected for assays.

Eppis and culture plate sourced from © Irfan_setiawan and Julee Ashmead/Adobe Stock

3.2. INDUCED PLURIPOTENT STEM CELL CULTURE

A pair of patient and healthy iPSCs were used for comparisons between the late-onset PD (Pair 1: PA.2 and WTA.2) and early-onset PD (Pair 2: PB and WTB). (**Table 1**.) The criterion was age of onset for the patient lines (PA.2 and PB) which were 64 and 28 respectively. The healthy lines (WTA.2 and WTB) were gender-matched and sampling age-matched to their patient counterparts (A's and B's).

Three of these lines were obtained as iPSCs for their starting culture but the PA.2 line was obtained as NESCs, so this culture was not started as iPSCs and was an exception to some of the following protocols. Aside from these four lines, a healthy control line was used only to troubleshoot some of the new protocols or adapt previous protocols for 2D neuron culture.

		MUTATION	AGE OF ONSET	AGE OF SAMPLING	GENDER
PAIR 1	Patient A (PA.2)	PARK2 Exon 7 deletion and c.1072T deletion	64	75	M
	Wild type A (WTA.2)	-	-	75	M
PAIR 2	Patient B (PB)	PARK2 Exon 6 and 7 Homozygous deletions	28	50	M
	Wild type B (WTB)		-	45	M
CTRL	K7		-	81	F

Table 1. Information for the five cell lines in this project. The two pairs had a patient and healthy cells to portray a certain PD pathology: Pair 1 for late-onset PD and Pair 2 for early-onset PD. The last line was the control cell line used for troubleshooting.

The medium used to culture the iPSCs was complete Essential 8 (E8) medium with two different compositions, determined by weekday or weekend feeding. For weekday feeding, it was E8 basal medium (Gibco, A1517001) supplemented with 1X of E8 supplement and 1% volume/volume of penicillin-streptomycin (PS) (Gibco, 15140122). For the weekend feeding, it was E8 FLEX basal medium (Gibco, A2858501) supplemented with 1X of E8 FLEX supplement and 1% volume/volume of PS.

When the iPSCs were obtained from the cryostorage, they were thawed in a warm water bath long enough for the frozen pellet to come loose then resuspended in pre-warmed Dulbecco's Modified Eagle Medium: Nutrient Mixture F-12 (DMEM/F-12) medium (Gibco, 21331046) in a 15mL conical falcon tube. The tubes were centrifuged at 300xg for 3 minutes, where a pellet was visible at the bottom of the tube. The supernatant was aspirated, and the pellet was gently resuspended in pre-warmed E8 supplemented medium with 10µM rho-associated protein kinase (ROCK) inhibitor (CliniSciences, A11001-50). Afterward, the iPSCs were seeded onto pre-warmed Matrigel-coated (Corning, 354277) tissue-culture treated 6-well plates. The medium was completely replaced daily with freshly supplemented E8 medium, except using E8 FLEX supplemented medium before the weekends or any two-day periods. When reaching 80% confluency, the iPSCs were passaged by dissociating from the old plate with slightly pre-warmed Accutase (StemCell, 7922). The dissociation was stopped with pre-warmed DMEM/F-12 medium in a 15mL conical falcon tube and then centrifuged at 300xg for 3 minutes, where a pellet was visible at the bottom of the tube. After the supernatant was aspirated, the iPSCs were gently resuspended in pre-warmed and freshly supplemented E8 medium with 10µM ROCK inhibitor then seeded onto a new Matrigel-coated plate.

The iPSC quality control check was done after a period of stable culture with at least three passages made. This was done by karyotyping and immunofluorescence staining. The karyotyping was performed through ThermoFisher KaryoStat+ service along with a sample of the PA.2 (LATE PD) NESCs included. The immunofluorescence staining of the pluripotency markers was done with iPSCs cultured onto Matrigel-coated 12mm glass coverslips.

The iPSCs were fixed with 4% paraformaldehyde (PFA) solution (Merck, 1004965000) for 15 minutes at room temperature then washed thrice with phosphate-buffered saline (PBS) buffer for five minutes each time. Permeabilization was done with 0.5% Triton X-100 (Carl Roth, 3051.3) for 15 minutes at room temperature then washed thrice with PBS buffer for five minutes each time. Blocking was done with 10% foetal bovine serum (FBS) (Gibco, 10500064) in PBS solution for 1 hour at room temperature. Afterward, the iPSCs were stained with primary antibodies in 10% FBS in PBS solution overnight at 4°C. (**Table 2**.) On the next day, the iPSCs were washed thrice with PBS buffer at room temperature for five minutes each time then stained with secondary antibodies in 10% FBS in PBS solution for 1 hour at room temperature and in the dark. (**Table 2**.) Finally, the coverslips were washed thrice with PBS buffer at room temperature for five minutes each time and then mounted onto glass slides. The image acquisition was done using the AxioVert.A1 camera with the Zeiss confocal laser scanning microscope 710 and 20X objective.

	MARKER	COMPANY	CATALOG NO
1° ABs	NANOG	Cell Signalling	5232
	OCT4	Cell Signalling	5677
	SOX2	Cell Signalling	23064
	SSEA4	Millipore	MAB4304
	TRA-1-60	Millipore	MAB4360
	TRA-1-81	Millipore	MAB4381
2° ABs	GOAT ANTI-MOUSE, ALEXA FLUOR 488	ThermoFisher	A11001
	GOAT ANTI-RABBIT, ALEXA FLUOR 647	ThermoFisher	A21244
	HOECHST	ThermoFisher	62249

Table 2. Antibodies for the iPSC pluripotency markers.

3.3. NEUROEPITHELIAL STEM CELL DIFFERENTIATION

A previously described protocol was followed to derive neuroepithelial stem cells from the iPSCs. (Reinhardt, 2013.) Two basal mediums were used: embryoid and N2B27. The embryoid basal medium had knockout DMEM medium (Gibco, 10829018), 20% knockout serum replacement (Gibco, 10828028), 1% PS, 1% GlutaMax (Gibco, 35050061), 1% Minimum Essential Medium Non-Essential Amino Acids solution (Gibco, 11140050), and 100µM beta-mercaptoethanol (Gibco, 31350010). The N2B27 basal medium had 48% DMEM/F-12 medium, 48% Neurobasal medium (Gibco, 21103049), 1%PS, 1% GlutaMax, 1% B27 supplement without vitamin A (Gibco, 12587001), and 0.5% N2 supplement (Gibco, 17502001).

Small molecules were freshly added on certain days accordingly. (**Illustration 9**.) The embryoid medium was supplemented with 10µM ROCK inhibitor, 3µM CHIR99201 (Axon Medchem, CT99021), 10µM SB431542 (Abcam, ab120163), 1µM dorsomorphin (Tocris, 3093), and 0.75µM purmorphamine (PMA) (Enzo, ALX420045M005). The N2B27 NESC patterning medium was the N2B27 basal medium supplemented with 3µM CHIR99201, 10µM SB431542, 1µM dorsomorphin, and 0.75µM PMA. The N2B27 NESC maintenance medium was the N2B27 basal medium supplemented with 150µM ascorbic acid (AA) (Sigma, A4544), 3µM CHIR99201, and 0.5µM PMA.

Derivation began by preparing a well of the Aggrewell-400 microwell culture plate (StemCell, 34450) coated with the anti-adherent solution according to the manufacturer's protocol. The well was pre-warmed with 500µL supplemented embryoid medium in the 37^{o}C incubator while the iPSCs were prepared. Approximately 1.2 million iPSCs were collected with the same dissociation method as previously described, except the iPSCs were resuspended with supplemented embryoid medium then added to the prepared well of Aggrewell-400 plate. Gentle pipetting was done within well to ensure an even distribution of cells across the microwells. The embryoids formed overnight and were transferred to a well of an ultra-low attachment 6-well plate with additional supplemented embryoid medium for another day. Then the medium was changed to supplemented N2B27 NESC

patterning medium for the next two days. Finally, the medium was exchanged for supplemented N2B27 NESC maintenance medium for the rest of the NESC culture. After two days in maintenance medium, neural tube formation was confirmed within the embryoids then broken up with vigorous pipetting in a 15mL falcon conical tube. The clumps were seeded onto the Matrigel-coated 12-well plate with supplemented N2B27 NESC maintenance medium at different densities according to the sizes of the clumps. Afterward, the culture was checked frequently for NESC-like cells and passaged until a homogenous NESC culture was obtained.

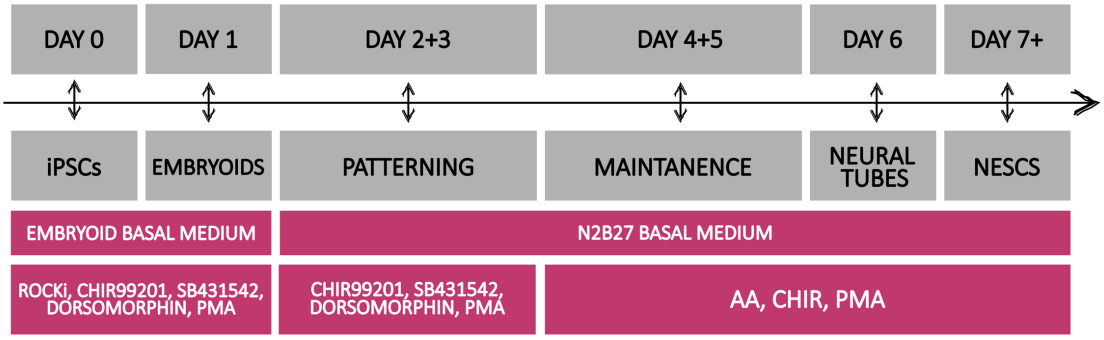

Illustration 9. Neuroepithelial stem cell differentiation protocol. The details were described above. Here, the different stages of differentiation were outlined along with the basal mediums and small molecules used to direct cell fate.

The NESC quality control was done after a period of stable culture, where at least five passages were made resulting in a clean and homogenous NESC culture each time. The dissociation method resembled what was described for iPSCs but without the ROCK inhibitor. The quality control was done by staining for their multipotency markers.

The immunofluorescence staining was done with NESCs cultured on Matrigel-coated 12mm glass coverslips. The NESCs were fixed with 4% PFA solution for 15 minutes at room temperature and then washed thrice with PBS buffer for five minutes each time. Next, the cells were permeabilized with 0.5% Triton X-100 for 15 minutes at room temperature then

washed thrice with PBS buffer for five minutes each time. Blocking was done with 10% FBS in PBS solution for 1 hour at room temperature. Afterward, the NESCs were stained with primary antibodies in 10% FBS in PBS solution overnight at 4°C. (**Table 3**.) On the next day, the NESCs were washed thrice with PBS buffer at room temperature for five minutes each time then stained with secondary antibodies in 10% FBS in PBS solution for 1 hour at room temperature and in the dark. (**Table 3**.) Finally, the coverslips were washed thrice with PBS buffer at room temperature for five minutes each time then mounted onto glass slides. The image acquisition was done using the AxioVert.A1 camera with the Zeiss confocal laser scanning microscope 710 and 20X objective.

	MARKER	COMPANY	CATALOG NO
1° ABs	FOXA2	Santa Cruz	sc-101060
	SOX1	R&D Systems	AF3369
	SOX2	R&D Systems	AF2018
	LMX1A	ABCAM	ab139726
	NESTIN	ABCAM	ab22035
	PAX6	Biolegend	901301
2° ABs	DONKEY ANTI-MOUSE, ALEXA FLUOR 488	ThermoFisher	A32766
	DONKEY ANTI-RABBIT, ALEXA FLUOR 555	ThermoFisher	A32794
	DONKEY ANTI-GOAT, ALEXA FLUOR 647	ThermoFisher	A32849
	HOECHST	ThermoFisher	62249

Table 3. Antibodies for the NESC multipotency markers.

3.4. MIDBRAIN DOPAMINERGIC DIFFERENTIATION

For the derivation of the dopaminergic neuron from NESCs, the N2B27 basal medium was used here. The composition was as previously described: 48% DMEM/F-12 medium, 48% Neurobasal medium, 1% penicillin-streptomycin, 1% GlutaMax, 1% B27 supplement without vitamin A, and 0.5% N2 supplement. Small molecules were used to supplement the N2B27 basal medium accordingly. (**Illustration 10**.) The N2B27 mDN differentiation medium was supplemented with 200µM ascorbic acid, 500µM dibutyryl cyclic adenosine monophosphate (dbCAMP) (Santa Cruz, sc-201567), 10ng/mL human brain-derived neurotrophic factor (hBDNF) (PeproTech, 450-02), 10ng/mL human glial cell line-derived neurotrophic factor (hGDNF) (PeproTech, 450-10), 1ng/mL transforming growth factor beta-3 (TGF-β3) (PeproTech, 100-36E), and 1µM PMA. The N2B27 mDN maintenance medium was supplemented similarly to the differentiation medium but without PMA.

The mDN derivation began by seeding NESCs onto Geltrex-coated (Gibco, A1413201) T75 tissue culture flasks at densities according to the total number of dopaminergic neurons needed for each time point. The cells were cultured with supplemented N2B27 mDN differentiation medium and completely replaced every other day for the first six days. Afterward, the medium was changed to supplemented N2B27 mDN maintenance medium where half volume was exchanged for freshly supplemented maintenance medium every two days. A total of 12 T75 flasks were maintained: one flask for a cell line then a time point. At each time point, four flasks containing the four lines were used for the endpoint assays.

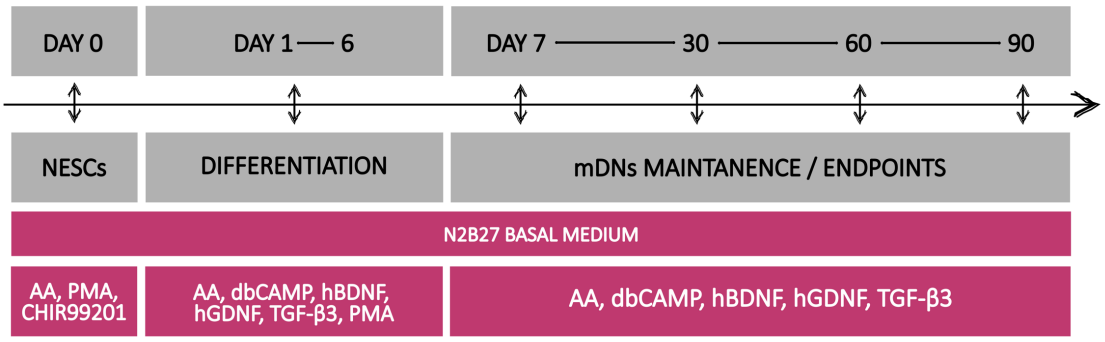

Illustration 10. Dopaminergic neuron differentiation protocol. The details were described above. Here, the different stages of differentiation were outlined along with the basal mediums and small molecules used to direct cell fate.

The mDN quality control was done 14 days after terminal differentiation. This was done by staining for their neuronal markers. The neurons were dissociated from the flask, where the differentiation took place, with slightly pre-warmed Accutase supplemented with 200mM sodium pyruvate (Gibco, 11360070). The dissociation was stopped with pre-warmed DMEM/F-12 medium in a 50mL conical falcon tube and then centrifuged at 500xg for 5 minutes, where a pellet was visible at the bottom of the tube. The neurons were seeded onto Matrigel-coated black clear-bottom 96-well plates (PerkinElmer, 6055300) in supplemented N2B27 mDN maintenance medium with 10µM ROCK inhibitor. A week of recovery was left for the neurons with half-volume medium exchange every two days before immunofluorescence staining.

The neurons were fixed with 4% PFA solution for 15 minutes at room temperature and then washed thrice with PBS buffer for five minutes each time. Next, the cells were permeabilized with 0.5% Triton X-100 for 15 minutes at room temperature and then washed thrice with PBS buffer for five minutes each time. Blocking was done with 10% FBS in PBS solution for 1 hour at room temperature. Afterward, the mDNs were stained with primary antibodies in 10% FBS in PBS solution overnight at 4°C. (**Table 4**.) On the next day, the mDNs were washed thrice with PBS buffer at room temperature for five minutes each time then stained with secondary antibodies in 10% FBS in PBS solution for 1 hour at room temperature and in the dark. (**Table 4**.) Finally, the wells were washed thrice with PBS buffer at room temperature for five minutes each time and then stored in fresh PBS buffer. The image acquisition was done using the AxioVert.A1 camera with the Zeiss confocal laser scanning microscope 710 and 20X objective.

	MARKER	COMPANY	CATALOG NO
1° ABs	ALPHA SYNUCLEIN	Santa Cruz	sc-12767
	PHOSPHORYLATED ALPHA SYNUCLEIN	Cell Signalling	23706S
	TUBB3	Millipore	AB9354
	TH	ABCAM	ab112
	MAP2	Biolegend	822501
2° ABs	DONKEY ANTI-MOUSE, ALEXA FLUOR 488	ThermoFisher	A32766
	DONKEY ANTI-RABBIT, ALEXA FLUOR 555	ThermoFisher	A32794
	DONKEY ANTI-GOAT, ALEXA FLUOR 647	ThermoFisher	A32849
	HOECHST	ThermoFisher	62249

Table 4. Antibodies for the neuronal markers.

3.5. RNA SEQUENCING AND ANALYSIS

The extraction of the total ribonucleic acid (RNA) materials was performed with the RNeasy kit (Qiagen, 74106), following the manufacturer's protocol. To summarize, first, the mDNs were rinsed with ice-cold PBS buffer twice to ensure complete removal of the culture medium. The neurons were then lysed with a mixture of RLT buffer and 10% beta-mercaptoethanol. Total lysate collection was ensured with a cell scrapper and the lysis material was frozen in an Eppendorf tube overnight at-80^{o}C. On the next day, the lysates were thawed then homogenized with a QIAshredder spin column. An equal volume of 70% ethanol was added to each lysate and gently mixed, then loaded onto a RNeasy spin column. The column membrane was washed with RW1 buffer and then treated with DNase digestion (Qiagen, 79254) for 15 minutes. Another wash with RW1 buffer was done to the column membrane then twice again with the RPE buffer. Finally, the RNA material was eluted from the membrane with RNase-free water. All buffers and columns were provided

with the RNeasy kit. The RNA concentrations were measured with the Nanodrop. At this point, the RNA samples were handed to the Luxgen platform for sequencing.

Ethanol precipitation was done to the RNA samples to ensure maximum number of impurities was removed before sequencing library preparation, following the author's protocol. (Green, 2016.) To summarize, the concentration of the monovalent cations was first adjusted with sodium acetate. Ice-cold glycogen and ethanol were then mixed into the samples and stored overnight at -20^{o}C. The RNA materials were recovered with centrifugation at 12,000xg for 10 minutes at 4^{o}C. With the supernatant aspirated, the pellets were washed with ice-cold 70% ethanol. The samples were centrifuged at maximum speed for 10 minutes at 4^{o}C. Again, the supernatant was aspirated, and any remaining liquid was left to evaporate on the bench at room temperature. The RNA pellets were dissolved in RNase-free water for library preparation.

The library was prepared with the Illumina Stranded Total RNA Prep, Ligation with Ribo-Zero Plus kit (Illumina, 20040529), following the manufacturer's protocol. To summarize, first, each sample were diluted into each well of a polymerase chain reaction (PCR) plate using nuclease-free ultrapure water. The library preparation began by depleting ribosomal RNA from the sample plate as well as any remaining salts and solutions. Next, the purified total RNAs were fragmented and denatured, priming them for complementary deoxyribonucleic acid (cDNA) synthesis. After the double stranded cDNA fragments were synthesized, adenine nucleotides were adenylated onto the 3' end of the fragments, also known as poly (A) tails. Lastly, the cDNA fragments underwent amplification, resulting in a final RNA library for sequencing before their final clean-up. All mixtures and solutions used for PCR were provided with the Total RNA Prep kit. The specific thermocycler programs were described in the manufacturer's protocol. Finally, sequencing was performed with the Illumina NextSeq 550 system.

The analysis was performed with the R software, using DESeq2 package for significance analysis and ggplot2 package for visualization. (Love, 2014.) (Wickham, 2016.) The REACTOME database was used for pathway analysis.

3.6. DOPAMINERGIC NEURON POPULATION SORTING AND ANALYSIS

The derived dopaminergic neuron populations were assessed with fluorescence-activated cell sorting (FACS), using the BD LSR Fortessa Cell Analyzer instrument. At least one million neurons per line were collected after each time point. The neurons were dissociated from the flask with slightly pre-warmed Accutase supplemented with 200mM sodium pyruvate. The dissociation was stopped with pre-warmed DMEM/F-12 medium in a 50mL conical falcon tube and then centrifuged at 500xg for 5 minutes, where a pellet was visible at the bottom of the tube. After the supernatant was aspirated, the neurons were resuspended in PBS buffer.

Dead cells were distinguished from live cells with a fixable viability dye (Invitrogen, 65-0863-18), following the manufacturer's protocol. In short, the neurons were washed twice with PBS buffer. 1µL of the fixable viability dye was added to the neurons suspended in 1mL of PBS buffer and incubated for 30 minutes at 4°C in the dark. Next, the neurons were washed twice with PBS buffer, fixed with 4% PFA solution for 15 minutes at room temperature, then washed twice with PBS buffer. Permeabilization was done next with 0.05% saponin (Sigma, 47036) and 1% bovine serum albumin (BSA) (Roth, 8076.3) in PBS solution for 20 minutes on a rotator at 4°C. Afterward, the samples were stained with primary antibodies in 0.05% saponin and 1% BSA in PBS solution for 45 minutes on a rotator at 4°C. (**Table 5**.) The samples were washed twice with 10% FBS in PBS solution and stained with secondary antibodies in 0.05% saponin and 1% BSA in PBS solution for 30 minutes on a rotator at 4°C. (**Table 5**.) Finally, the samples were washed in 10% FBS in PBS solution and then resuspended in 1% FBS in PBS solution in FACS polystyrene tubes for sorting.

The BD FlowJo software was used to view the flow cytometric data and identify the percentage of the populations of interest. The GraphPad Prism software was used to plot out the results and do significance analysis.

	MARKER	COMPANY	CATALOG NO
1° ABs	TH	ABCAM	ab112
	MAP2	Biolegend	822501
2° ABs	DONKEY ANTI-RABBIT, ALEXA FLUOR 488	ThermoFisher	A21206
	DONKEY ANTI-CHICKEN, ALEXA FLUOR 647	ThermoFisher	A78952

Table 5. Antibodies for assessing the neuron population.

3.7. PHENOTYPIC STAINING AND ANALYSIS

The phenotypes of dopaminergic neurons were checked using the high-throughput screening with Yokogawa CV8000 microscope. The black clear-bottom 96-well plates were coated with 10% poly-d-lysine (PDL) in PBS solution overnight in the 37°C cell incubator then washed thrice with sterile PBS buffer. Any remaining liquid was aspirated, and the plates were left to dry in the cell culture laminar hood. Afterward, the plates were coated with Geltrex overnight in the 37°C cell incubator.

The NESCs were differentiated into dopaminergic neurons in Geltrex-coated T75 flasks up to each time point where the neurons were collected. They were dissociated from the flask with slightly pre-warmed Accutase supplemented with 200mM sodium pyruvate. The dissociation was stopped with pre-warmed DMEM/F-12 medium in a 50mL conical falcon tube and then centrifuged at 500xg for 5 minutes, where a pellet was visible at the bottom of the tube. The neurons were seeded onto the PDL/Geltrex-coated black clear-bottom 96-well plates in supplemented N2B27 mDN maintenance medium with 10µM ROCK inhibitor. A week of recovery was left for the neurons with half-volume medium exchange every two days before immunofluorescence staining.

The neurons were fixed with 4% PFA solution for 15 minutes at room temperature then washed thrice with PBS buffer for five minutes each time. Next, they were permeabilized

with 0.5% Triton X-100 for 15 minutes at room temperature then washed thrice with PBS buffer for five minutes each time. Blocking was done with 10% FBS in PBS solution for 1 hour at room temperature. Afterward, the neurons were stained with primary antibodies in 10% FBS in PBS solution overnight at 4°C. (**Table 6**.) The next day, the neurons were washed thrice with PBS buffer at room temperature for five minutes each time then stained with secondary antibodies in 10% FBS in PBS solution for 1 hour at room temperature and in the dark. (**Table 6**.) Finally, the plates were washed thrice with PBS buffer at room temperature for five minutes each time and then stored in fresh PBS buffer.

	MARKER	COMPANY	CATALOG NO
1° ABs	ALPHA SYNUCLEIN	Santa Cruz	sc-12764
	PHOSPHORYLATED ALPHA SYNUCLEIN	Cell Signalling	23706S
	TOMM20	Santa Cruz	sc-17764
	MAP2	ABCAM	ab92434
2° ABs	DONKEY ANTI-MOUSE, ALEXA FLUOR 488	ThermoFisher	A32766
	DONKEY ANTI-CHICKEN, ALEXA FLUOR 555	ThermoFisher	A78949
	DONKEY ANTI-RABBIT, ALEXA FLUOR 647	ThermoFisher	A32795
	HOECHST	ThermoFisher	62249

Table 6. Antibodies for the dopaminergic neuron phenotypes.

The image acquisitions were performed on Yokogawa CV8000 microscope in a scanning confocal mode using a dual Nipkow spinning disk. All four solid lasers were used (405nm, 488nm, 561nm, and 640nm) to acquire the images in zigzag fashion per row. A single Z-plane 5x5 image was taken from the centre of each well through a 40X objective. Image segmentation and feature extraction were performed with KSILINK's software. (Vuidel, 2022.)

3.8. OXYGEN CONSUMPTION RATE MEASUREMENTS (INCOMPLETED)

An attempt was made to determine the neurons' mitochondria function using the Seahorse XF Cell Mito Stress kit (Agilent, 103015-100). The Seahorse XFe96 Pro Cell Culture 96-well microplates were coated with 10% PDL in PBS solution overnight in a 37°C incubator and then washed thrice with sterile PBS buffer. Any remaining liquid was aspirated, and the plates were left to dry in the cell culture laminar hood. Afterward, the plates were coated with Geltrex overnight in the 37°C cell incubator.

The dopaminergic neurons were seeded onto the PDL/Geltrex-coated plate in supplemented N2B27 mDN maintenance medium with 10µM ROCK inhibitor as previously described. A week of recovery was left for the neurons with half-volume medium exchange every two days.

The oxygen consumption rate was measured using the Seahorse XFe96 Extracellular Flux Bioanalyzer, following the manufacturer's protocol. In summary, the XF sensor cartridge plate was hydrated with a calibrant solution in a CO_2-free incubator the night prior. On the day of analysis, the cell culture plate was rinsed twice with XF assay medium and then left to acclimate to XF assay medium in a CO_2-free incubator for an hour. During this time, the sensor cartridge plate was prepared with the toxins as described and in order following the manufacturer's protocol. (**Table 7**.) When the acclimation finished, the cell culture plate was combined with the sensor cartridge plate and then run on the bioanalyzer to measure the oxygen consumption rate. After measurement, the neurons were fixed with 4% PFA solution for 15 minutes at room temperature and then washed thrice with PBS buffer. The nucleus was stained with Hoechst in PBS buffer for 1 hour at room temperature in the dark. The total number of nuclei was determined with the BioTek Cytation 5 cell imaging multimode reader, using the DAPI fluorescence cube.

TOXIN	CONCENTRATION	COMPANY	CATALOG NO
OLIGOMYCIN	2µM	SIGMA	75351
FCCP	250nM	ABCAM	ab12008
ANTIMYCIN A	5µM	ABCAM	ab1419041
ROTENONE	5µM	SIGMA	R8875

Table 7. Toxins for the Seahorse Cell Mito Stress test.

The Seahorse Wave Desktop software was used to view the metabolism data from XF analyser and identify the oxygen consumption measurements. The GraphPad Prism software was used to plot out the results and do significance analysis.

3.9. YOUNG DOPAMINERGIC NEURON SORTING AND STAINING (INCOMPLETED)

An attempt was made at extracting a population of young dopaminergic neurons with live fluorescence-activated cell sorting, using the BD FACSAria III Cell Sorter instrument. Young K7 dopaminergic neurons at 15DOD were collected by dissociating them from the flask with slightly pre-warmed Accutase supplemented with 200mM sodium pyruvate. The dissociation was stopped with pre-warmed DMEM/F-12 medium in a 50mL conical falcon tube and then centrifuged at 500xg for 5 minutes, where a pellet was visible at the bottom of the tube. After the supernatant was aspirated, the neurons were resuspended in PBS buffer.

First, dead cells were distinguished from live cells with a live viability dye (Invitrogen, L34955) following the manufacturer's protocol. In short, the neurons were washed once with PBS buffer. 1µL/mL of the viability dye was added to the neurons suspended as 1 million cells per 1mL of PBS buffer and incubated for 30 minutes in the cell culture laminar hood without lights. Next, the neurons were washed twice with wash buffer, which was

N2B27 basal medium with 10µM ROCK inhibitor. The neurons were stained with primary antibodies in PBS buffer on a rotator for 20 minutes at 4°C. (**Table 8**.) Afterward, they were washed twice with wash buffer and then stained with secondary antibodies in PBS buffer on a rotator for 30 minutes at 4°C. (**Table 8**.) Finally, they were washed twice and then resuspended in the fresh wash buffer in FACS polystyrene tubes for sorting.

	MARKER	COMPANY	CATALOG NO
1° ABs	ALCAM PE-CONJUGATED	R&D Systems	FAB6561P
	LRTM1 647-CONJUGATED	R&D Systems	FAB10046R
	CORIN	R&D Systems	MAB2209
2° ABs	DONKEY ANTI-RATE, ALEXA FLUOR 488	ThermoFisher	A48269

Table 8. Antibodies for young dopaminergic neuron sorting.

The BD FACSDiva software was used to view the flow cytometric data real time and identify the live neurons of interest. During collection, the neurons were kept on ice and in fresh wash buffer. When all the tubes were sorted, the young neurons were immediately transferred to a 15mL conical falcon tube and centrifuged at 300xg for 3 minutes where a pellet was visible at the bottom of the tube. The supernatant was aspirated, and the pellet was gently resuspended in pre-warmed N2B27 mDN supplemented maintenance medium with 10µM ROCK inhibitor. The neurons were seeded onto a pre-warmed Matrigel-coated black clear-bottom 96-well plate.

After a week of recovery, the neurons were fixed with 4% PFA solution for 15 minutes at room temperature then washed thrice with PBS buffer for five minutes each time. Next, the neurons were permeabilized with 0.5% Triton X-100 for 15 minutes at room temperature then washed thrice with PBS buffer for five minutes each time. Blocking was done with 10%

FBS in PBS solution for 1 hour at room temperature. Afterward, the neurons were stained with primary antibodies in 10% FBS in PBS solution overnight at 4°C. (**Table 9**.) On the next day, the neurons were washed thrice with PBS buffer at room temperature for five minutes each time then stained with secondary antibodies in 10% FBS in PBS solution for 1 hour at room temperature and in the dark. (**Table 9**.) Finally, the plates were washed thrice with PBS buffer at room temperature for five minutes each time and then stored in fresh PBS buffer. The image acquisition was done using the AxioVert.A1 camera with the Zeiss confocal laser scanning microscope 710 and 20X objective.

	MARKER	COMPANY	CATALOG NO
1° ABs	TH	ABCAM	ab112
	MAP2	Biolegend	822501
	TUBB3	Millipore	AB9354
2° ABs	DONKEY ANTI-RABBIT, ALEXA FLUOR 488	ThermoFisher	A21206
	DONKEY ANTI-CHICKEN, ALEXA FLUOR 555	ThermoFisher	A78949
	HOECHST	ThermoFisher	62249

Table 9. Antibodies for the young dopaminergic neuron markers.

3.10. STABLE ISOTOPE LABELLING BY AMINO ACIDS IN CELL CULTURE (FAILED)

An attempt was made to extract the human-specific peptides from dopaminergic neurons at different time points with stable isotope labelling by amino acids in cell culture (SILAC). 12 days before collection, the dopaminergic neurons were switched into SILAC N2B27 supplemented mDN maintenance medium. The key difference between the SILAC and normal N2B27 medium was the absence of arginine and lysine amino acids, which was

achieved in the basal mediums. The SILAC N2B27 basal medium had 48% DMEM/F-12 medium (Athena Enzyme System, AE-0423) and 48% Neurobasal medium (Athena Enzyme System, AE-0428), both of which were lacking the arginine and lysine amino acids. Medium and heavy arginine and lysine amino acids were added into the basal medium separately. (**Table 10**.) The rest of the basal medium remained the same as normal N2B27 basal medium: 1% PS, 1% GlutaMax, 1% B27 supplement without vitamin A, and 0.5% N2 supplement. The SILAC N2B27 supplemented maintenance medium had the same small molecules as well: 200µM ascorbic acid, 500µM dbCAMP, 10ng/mL hBDNF, 10ng/mL hGDNF, and 1ng/mL TGF-β3.

	AMINO ACID	COMPANY	CATALOG NO
HEAVY	L-lysine·2HCl:$^{13}C_6$-$^{15}N_2$	CAMBRIDGE LAB	CNLM-291-H
	L-arginine·HCl:$^{13}C_6$-$^{15}N_4$	CAMBRIDGE LAB	CNLM-539-H
MEDIUM	L-lysine·2HCl:D_4	CAMBRIDGE LAB	DLM-2640
	L-arginine·HCl:$^{13}C_6$	CAMBRIDGE LAB	CLM-2265-H

Table 10. Differentially labelled amino acids for the SILAC basal mediums.

The SILAC was set up using the heavy and medium arginine and lysine amino acids to label the human peptides of each sample within a pair in a forward-reverse manner. (**Illustration 11**.) To achieve this, differentially labelled amino acids were added to the N2B27 basal medium to create two conditions: medium basal mediums (L-lysine·2HCl:D_4 and L-arginine·HCl:$^{13}C_6$) and heavy basal mediums (L-lysine·2HCl:$^{13}C_6$-$^{15}N_2$ and L-arginine·HCl:$^{13}C_6$-$^{15}N_4$) All the amino acids were added at final concentration of 0.1mg/mL in the basal mediums.

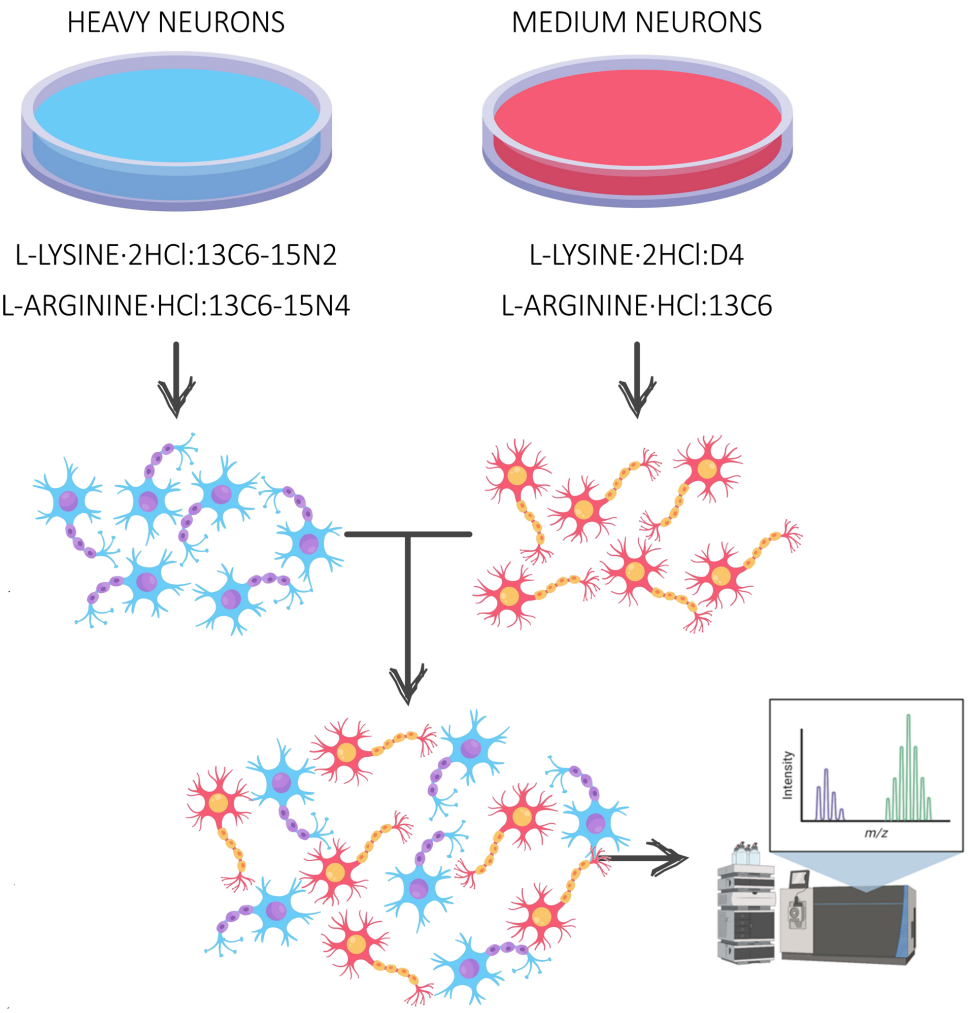

Illustration 11. The SILAC experimental setup. A visual depiction of neuron culture with the labelling mediums and preparation of peptide samples before measurement.

Once the neurons were switched to the SILAC N2B27 supplemented maintenance medium, the medium was replenished by half volume exchange every other day until the designated time point. Then the neurons were dissociated from the flask with slightly pre-warmed Accutase, supplemented with 200mM sodium pyruvate. The dissociation was stopped with pre-warmed SILAC DMEM/F-12 medium in 50mL conical falcon tube then centrifuged at 500xg for 5 minutes, where a pellet was visible at the bottom of the tube. After the supernatant was aspirated, the neurons were resuspended in PBS buffer. Centrifugation

was repeated, the supernatant was discarded, and the pellet was frozen at-80^{o}C before peptide extraction.

The pellet was slightly thawed at room temperature on the bench, digested in 8M urea buffer in 50mM ammonium bicarbonate, then homogenized with a sonicator. The protein concentration was measured using the EZQ Protein Quantification kit (Molecular Probes, R33200) and the BMG LABTECH CLARIOstar Plus plate reader instrument. Each protein samples were resuspended with 8M urea buffer to achieve a final concentration of 1µg/µL and a total of 20µg of protein. They were reduced with 15mM dithiothreitol in 50mM ammonium bicarbonate on a shaker for 30 minutes at 37^{o}C. After cooling to room temperature, the disulfide bonds were alkylated with 55mM iodoacetamide in 50mM ammonium bicarbonate on a shaker for 30 minutes at room temperature and in the dark. Lastly, the samples were diluted with 50mM ammonium bicarbonate to a final concentration of 1M urea. Trypsin was added at an enzyme-to-substrate ratio of 1:50 to each sample and incubated overnight on a shaking thermocycler at 37^{o}C. The next day, the digestion was stopped with 10% formic acid to achieve a final pH of 3 or lower. Peptide desalting and purification were done with Empore solid-phase extraction cartridges C-18-SD. All buffers, solutions, and instruments were generously provided by Proteomics of Cellular Signalling group at LIH. At this point, the peptide samples were handed to them for mass spectrometry.

4. RESULTS

4.1. INDUCED PLURIPOTENT STEM CELLS QUALITY CONTROL

The quality control of the iPSCs is imperative to ensure their reliability and reproducibility as many factors can influence their identity such as the reprogramming with viral vectors or long-term storage and cell culture. There are many ways to check the identity of the iPSCs. In this case, we checked for presence of embryonic stem cell pluripotency markers and normal karyotype.

Through immunofluorescence staining, six conventional embryonic stem cell markers can be checked for: homeobox transcription factor (NANOG), octamer transcription factor 4 (OCT4), SRY- box transcription factor 2 (SOX2), podocalyxin-like protein-1 (TRA-1-81), T cell receptor alpha locus (TRA-1-60), and stage-specific embryonic antigen-4 (SSEA4). Three of them are nuclear: NANOG, OCT4, and SOX2. They are transcription factors that work to preserve the necessary gene expression of the pluripotency and self-renewal abilities of ESCs. (Swain, 2020.) (Verneri, 2020.) Obviously, changes in those molecules occur when the iPSCs lose their pluripotency and turn into lineage selection. The rest are surface markers: TRA-1-81, TRA-1-60, and SSEA4. They are used to define a population of undifferentiated iPSCs with their expressions lost upon their derivation or tumorigenesis. (Abujarour, 2013.) (Malecki, 2012.) (Henderson, 2002.)

After thawing and a period of stable culture, the pluripotency markers was checked for the three iPSC lines. (**Figure 1**.)

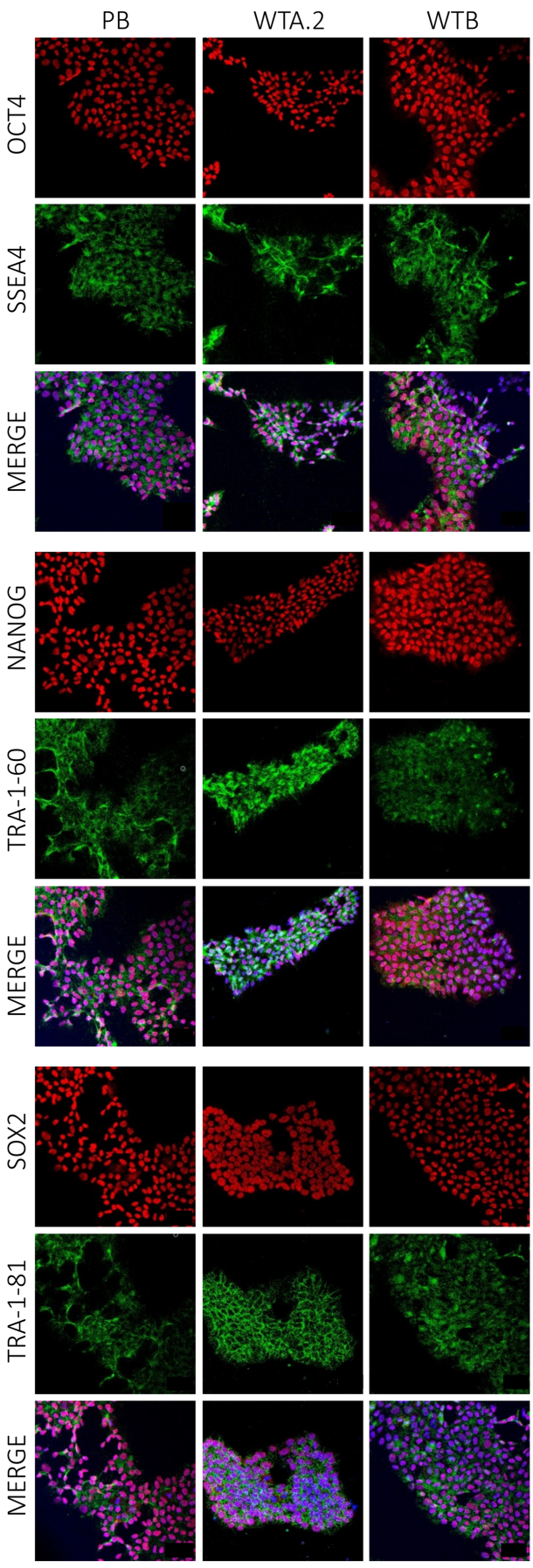
PB
WTA.2
WTB
OCT4
SSEA4
MERGE
NANOG
TRA-1-60
MERGE
SOX2
TRA-1-81
MERGE

Figure 1. The pluripotency markers of iPSCs. The NANOG, OCT4, SOX2, SSEA4, TRA-1-60, and TRA-1-81 markers showed positive expression for all iPSC lines and at their usual locations. The NANOG, OCT4, and SOX2 were within the nucleus. The SSEA4, TRA-1-60, and TRA-1-81 were within the plasma membrane.

Next, their karyotypes were checked for any chromosome aberrations. This was to ensure a clean reprogramming of the cells as well as their good health after the long-term storage in the cryostorage. Normal karyotypes were confirmed for the three iPSC lines as well as the PA.2 (LATE PD) NESC line. (**Figure 2**.)

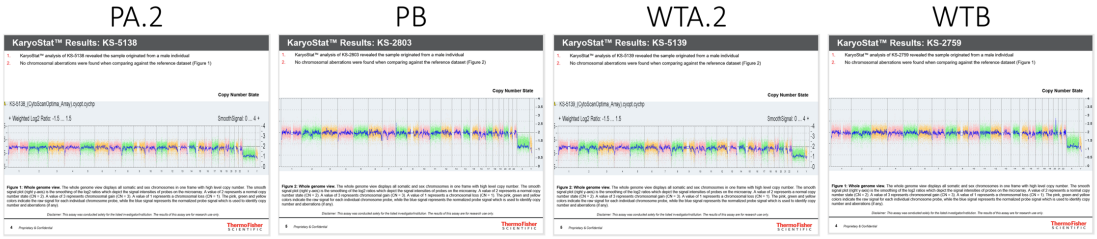

Figure 2. Karyotypes of the four lines. Normal karyotypes were established for all four lines. The PB, WTB, and WTA.2 were iPSCs while the PA.2 were NESCs. This service was rendered from ThermoFisher KaryoStat+.

4.2. NEUROEPITHELIAL STEM CELLS QUALITY CONTROL

A previously described NESC differentiation protocol was followed for the neural progenitor cells derivation from the iPSCs. (**Figure 3**.) (Reinhardt, 2013.) This approach was done for the expansion and storage of the NESCs to retain a low number of passages. Neural tubes were the visual indication for a successful derivation. In addition, PA.2 (LATE PD) NESCs were confirmed to have been derived with the same protocol.

Under the microscope, the progenitors organized themselves into neural rosette structures much like a normal NESC morphology and appeared to look like clean cultures. Observantly, the patient NESCs showed smaller colonies compared to the wild types with several elongated bodies of cells in between, not to be mistaken for spontaneously differentiated cells.

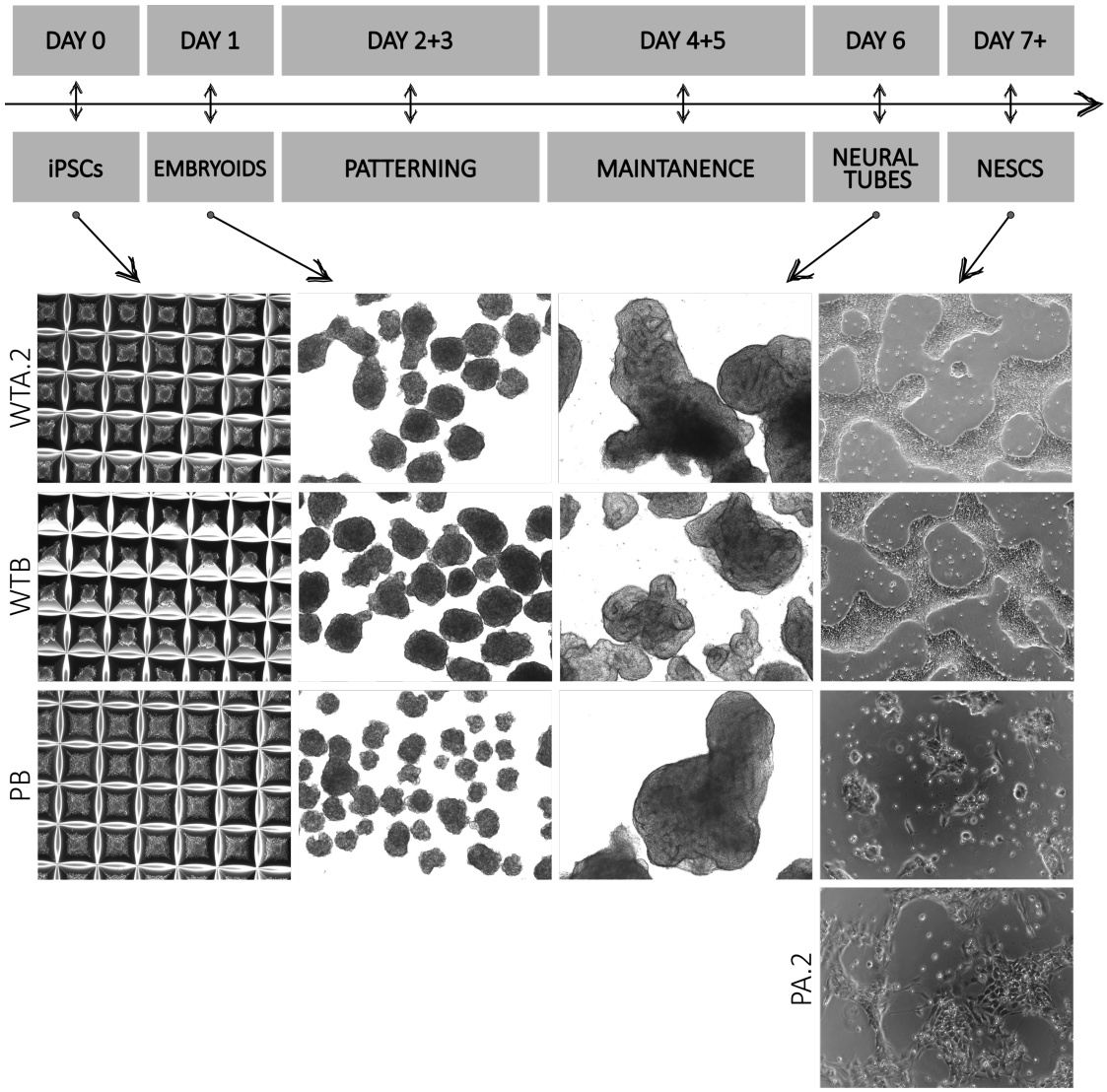

Figure 3. The neuroepithelial stem cell differentiation. The different stages of differentiation were shown with brightfield images of the culture. The final morphology of the derived NESCs were checked out for all four lines at the end.

Through immunofluorescence staining, six conventional neural stem cell markers can be checked for: SOX2, SRY-box transcription factor 1 (SOX1), forkhead box A2 (FOXA2), LIM homeobox transcription factor 1 alpha (LMX1A), paired box 6 (PAX6), and neuroepithelial stem cell protein (NESTIN). These markers act together in conjunction to maintain the precursor identity of NESCs that is in between iPSCs and dopaminergic neurons. From iPSCs, the SOX2 expression is carried over to NESCs, suppressing further differentiation to a terminal neural fate. At the same time, their family member, SOX1, which is specific to neural stem cells, helps to maintain their state by counteracting with the pro-neural molecules. (Li M. Z., 2016.) (Pagin, 2021.) (Verneri, 2020.) The pro-neural molecules include FOXA2 and LMX1A transcription factors, both of which have the check-balance interactions with SOX1 and SOX2 factors. (Doucet-Beaupré, 2015.) (Gale, 2008.) (Tian, 2015.) Lastly, the PAX6 transcription factor and NESTIN filaments are present for maintaining NESCs themselves. (Park D. X., 2010.) (Thakurela, 2016.)

All six markers were present in the four lines. (**Figure 4**.) Except for NESTIN being cytoskeletal proteins, all markers were transcriptional factors so they should be in the nucleus. Observantly, the FOXA2 marker in both patient NESCs appeared to be translocated to the cytosol, indicating a change to their metabolic state. According to the literature, the nuclear export of FOXA2 was promoted by insulin signalling via phosphorylation through the phosphoinositide 3-kinase/AKT serine-threonine kinase (PI3K/AKT) pathway. (Howell, 2009.) (Wolfrum C. B., 2003.) As a result, the FOXA2 transcription factor become inactive, and the metabolic state was enhanced as one of the roles of FOXA2 was to maintain glucose and lipid homeostasis. This may be a component of the gut-brain axis as previous studies have investigated the functional capacity of FOXA2 in metabolism within pancreatic cells. (Sund, 2001.) (Wang H. G.-J., 2002.) (Wolfrum C. A., 2004.) These implications could carry over as the patient NESCs continue to differentiate to dopaminergic neurons. Nonetheless, the translocation of the FOXA2 marker do not affect the identity of the neural progenitor cells. The rest of the markers were present and at their usual location, thereby confirming the NESCs.

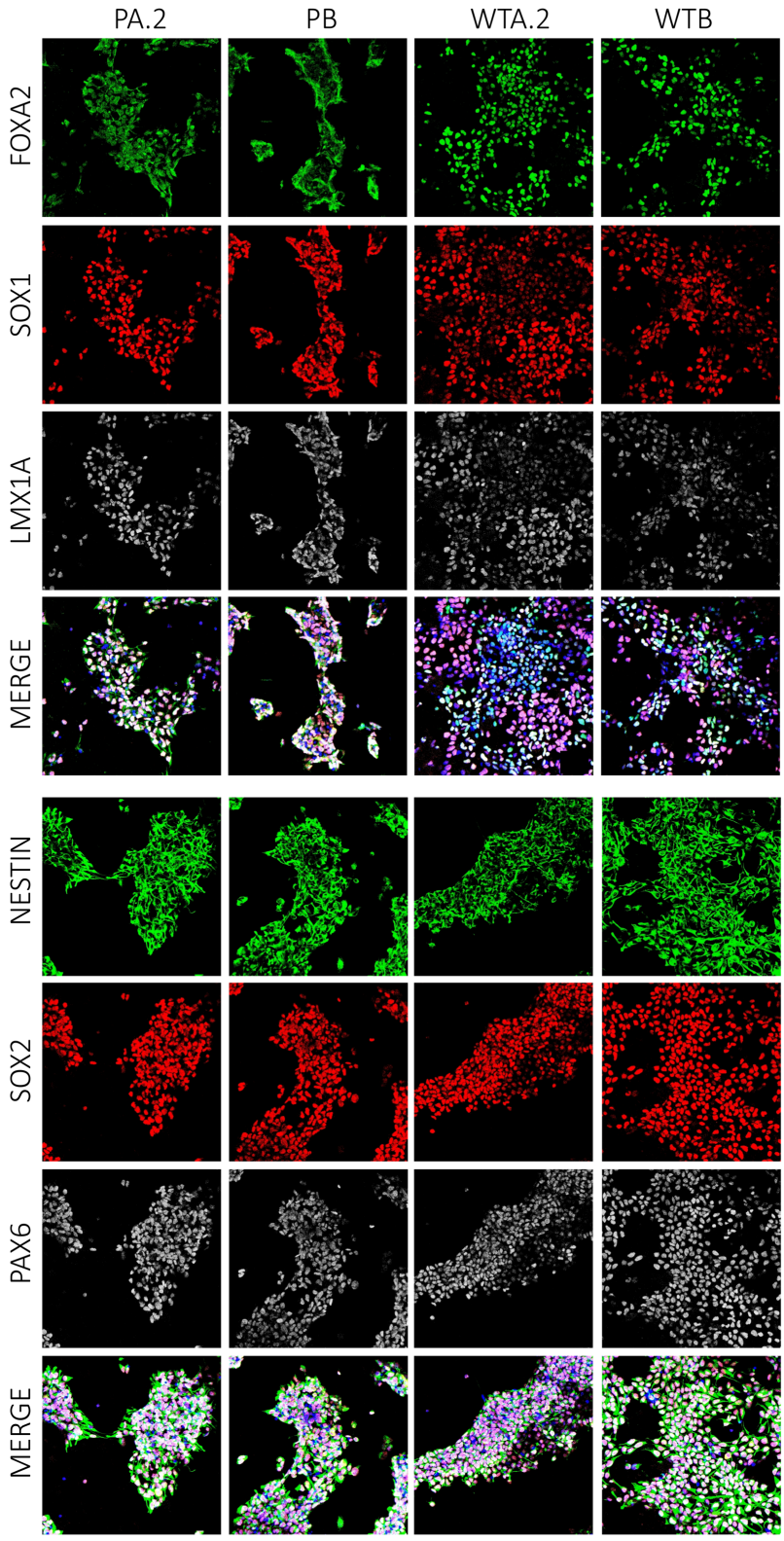

Figure 4. The multipotency markers of NESCs. FOXA2, SOX1, SOX2, LMX1A, NESTIN, SOX2, and PAX6 markers showed positive expression for all NESC lines. Most of the markers were transcription factors, therefore nuclear. NESTIN was a cytoskeletal marker. The FOXA2 showed translocation to the cytoplasm for the patient NESCs, indicating different metabolic states compared to the wild types.

4.3. NEURON POPULATION ASSESSMENT

Any differentiation process will yield a heterogeneous population, even when directed toward a specific cell type. During dopaminergic neuron differentiation, other glial types can arise such as the astrocytes or oligodendrocytes. Brightfield images were taken of the dopaminergic neurons after differentiation for visual inspection. (**Figure 5A**.) The images showed relatively clean cultures, with some spontaneously differentiated cells underneath the neuronal layer for the patient neurons.

Through the fluorescence-activated cell sorting, two markers were used to determine the percentage of the dopaminergic neurons: tyrosine hydroxylase (TH) and microtubule-associated protein 2 (MAP2). TH is a rate-limiting enzyme that converts tyrosine into L-3,4-dihydroxyphenylalanine (L-DOPA). (Du D. S., 2022.) This molecule is a precursor to three types of neurotransmitters of the central nervous system: dopamine, norepinephrine, and epinephrine. (Daubner, 2011.) (Weihe, 2006.) MAP2 are the neuron-specific cytoskeletal proteins abundant in the dendrites and cell body to mediate long-term potentiation. (Kim, 2020.)

All four mDN lines showed double-positive expression of TH and MAP2, with a decreasing expression over time. (**Figure 5B**.) The PA.2 (LATE PD) neurons showed significant differences in the TH+, MAP2+, and TH+/MAP2+ expression levels between 30DOD and 90DOD. This confirmed the physiological difference between late-onset and early-onset PD, the latter having a slower and steady neuron degeneration. From the cell culture point of view, there was no significant difference in the differentiation rate between the four lines at each time point. (**Figure 5C**.) This indicated a similar rate of differentiation between all lines and similar numbers of dopaminergic neurons at each time point.

Through the immunofluorescence staining, five markers associated with the PD dopaminergic neurons were checked for: TH, MAP2, beta tubulin-III (TUBB3), alpha synuclein (ASYN), and phosphorylated alpha synuclein (PSYN). (**Figure 6**.) Aside from MAP2,

TUBB3 are another neuron-specific tubulin proteins abundant throughout the neuron. The ASYN and PSYN are the proteins implicated in Parkinson's.

The four mDN lines showed positive expression for all markers. MAP2 expression was faint compared to TUBB3, indicating the immaturity of the neurons as staining was about two weeks after differentiation.

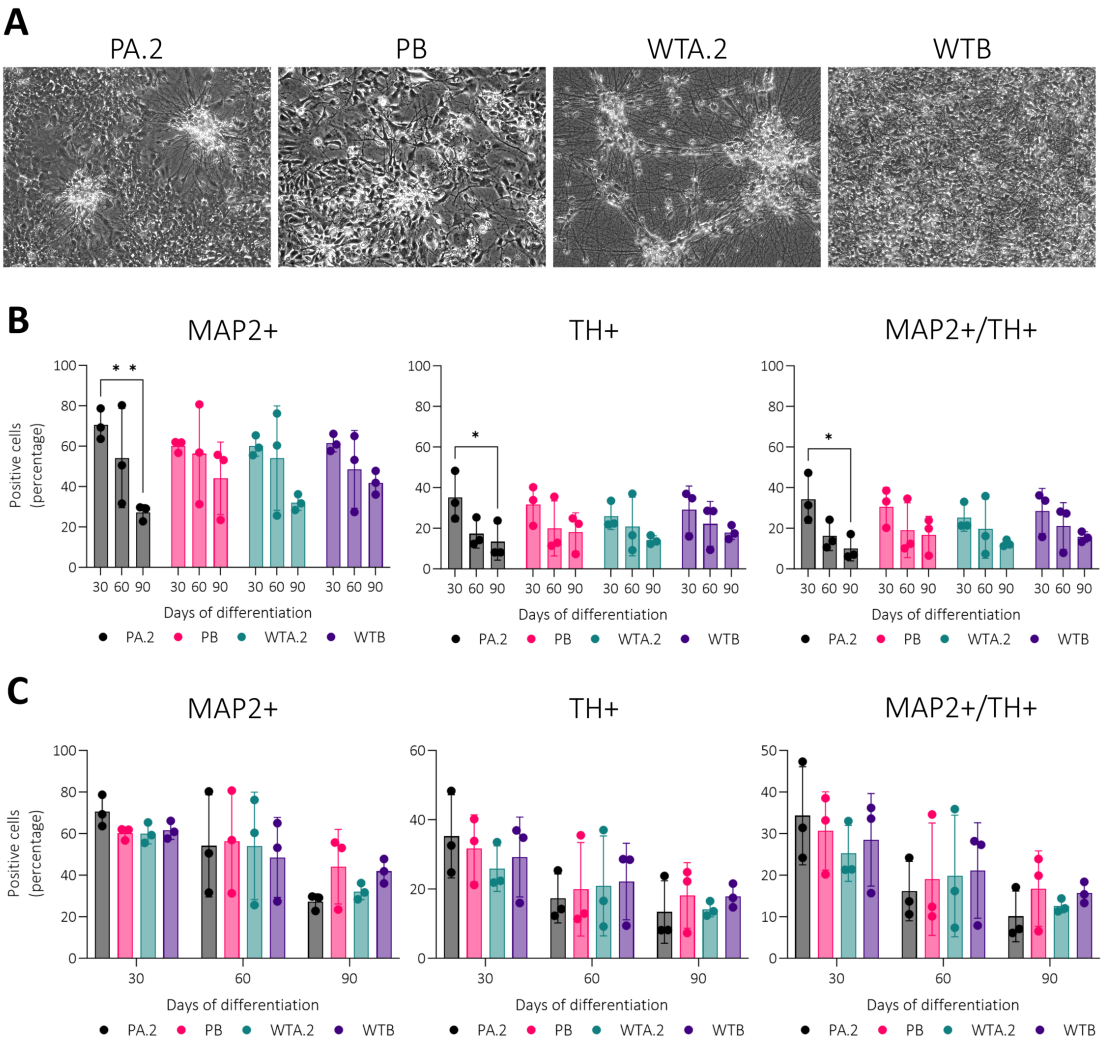

Figure 5. The dopaminergic neurons after differentiation. (A) showed the brightfield images of the neurons in culture. (B) and (C) showed the percentage of neurons positive for TH and MAP2 markers individually and together, with (B) displaying the cell lines on the y-axis and (C) displaying the time points. Significance was determined with Tukey's multiple comparison test. * p≤0.05; ** p≤0.01

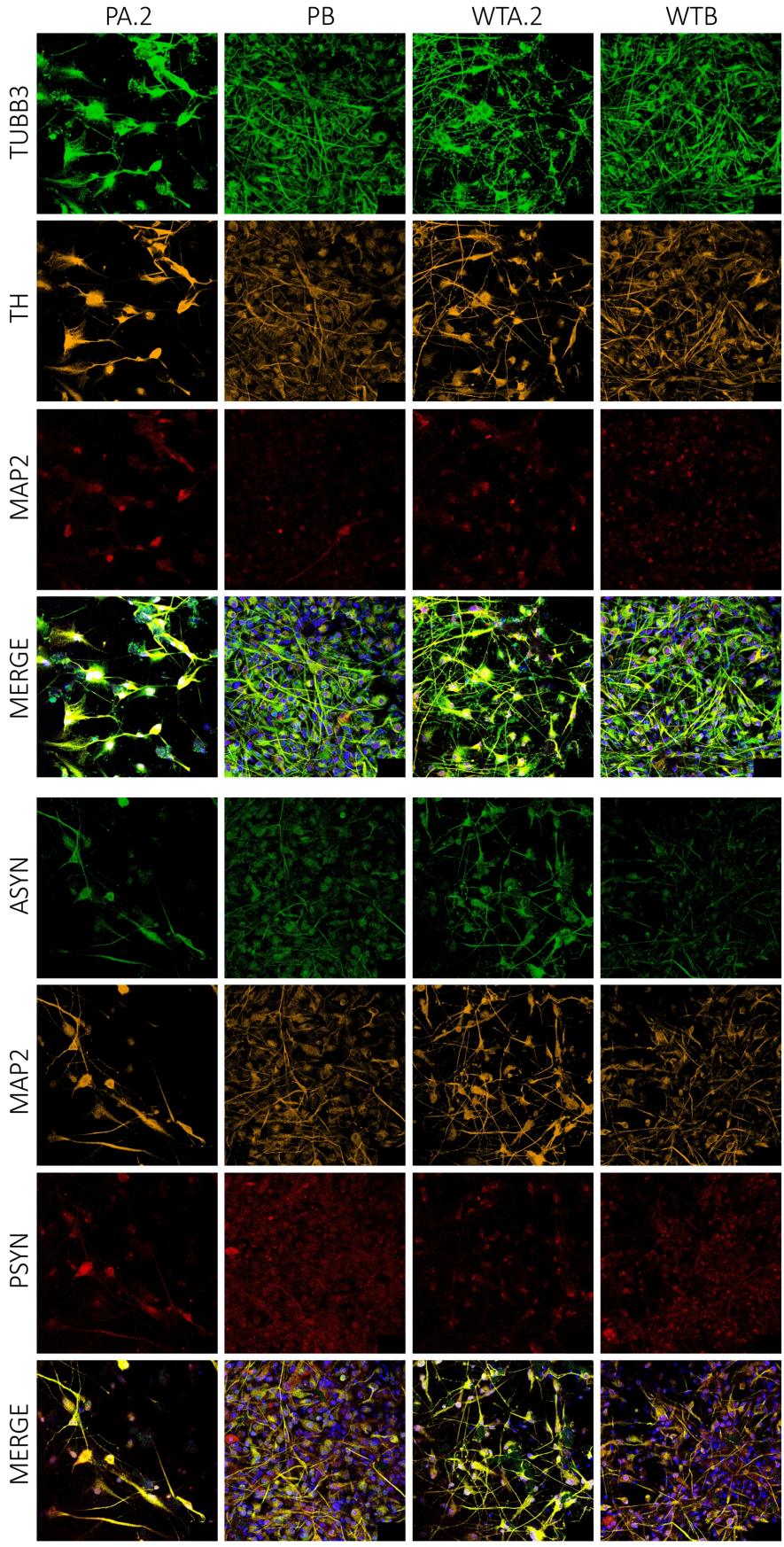
PA.2
PB
WTA.2
WTB
TUBB3
TH
MAP2
MERGE
ASYN
MAP2
PSYN
MERGE

Figure 6. The neuronal markers of mDNs. TH, TUBB3, MAP2, ASYN and PSYN markers showed positive expressions for all four mDN lines. The faint MAP2 staining indicate the immaturity of the neurons.

4.4. TRANSCRIPTOMIC ANALYSIS

To start the comparison, we began with the nucleic acids namely RNA materials. After sequencing, the quality check of the reads was done. (**Figure 7**.) (Ewels, 2016.)

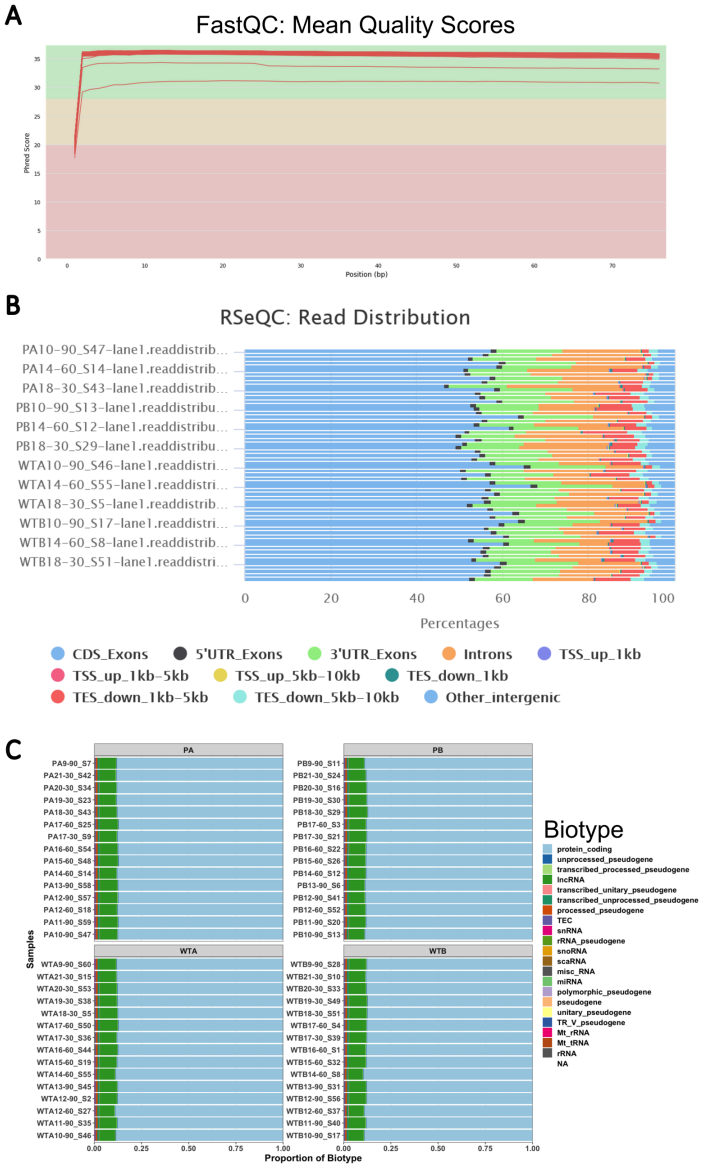

Figure 7. The RNA sequencing quality check. Sections from the QC reports on RNA sequencing reads shown. (A) showed the mean quality scores of all reads. (B) showed the read distribution for the representative sequences, revealing the presence of other regulatory sequences. (C) showed a biotype plot of the RNA species present, majority being protein-coding.

Another element of the quality check was the batch-to-batch variation, referring to the systematic differences between the replicates arising from cell culture conditions and sample processing. To check this, the principal component analysis (PCA) was used, and the two conditions were the sample replicates and time. (**Figure 8**.) In either circumstance, the replicates showed tight grouping following a linear behaviour so the variance between replicates could be considered minimized. Furthermore, the two wild types, WTA.2 and WTB neurons, showed tighter groupings compared to the patient neurons so it could be said that they were comparable for the transcriptomic analysis.

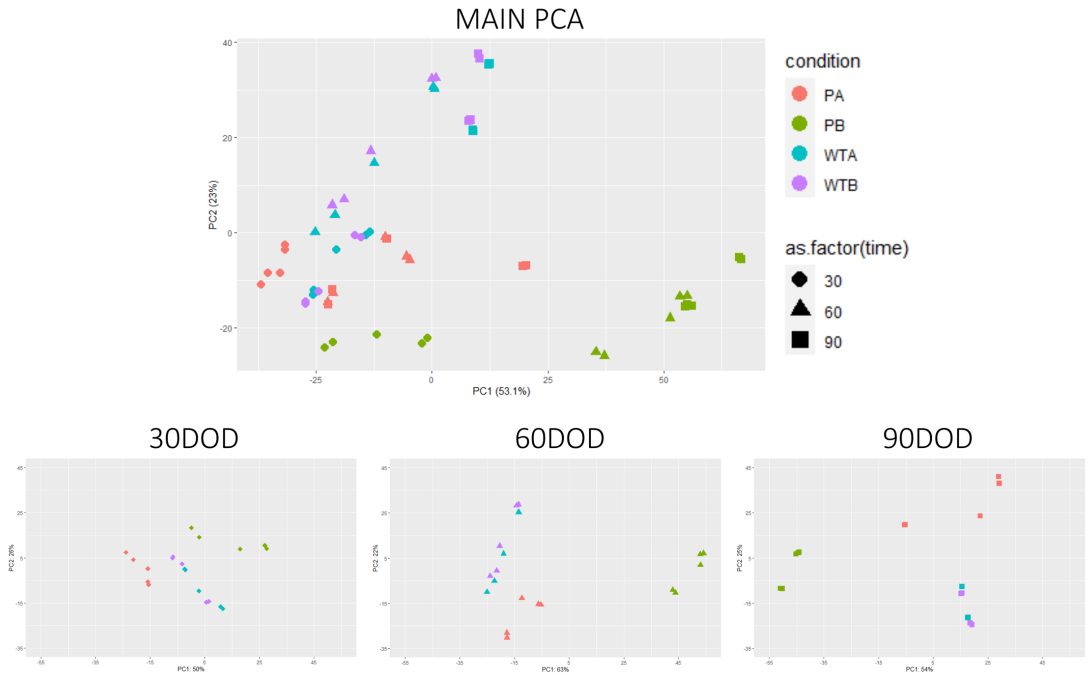

Figure 8. PCA for the batch-to-batch variations. Different PCA plots were shown while assessing two conditions: sample replicates and time. The main plot had both conditions displayed and then broken down into each time point separately. The tight groupings of the wild types showed they were comparable for this analysis.

The initial screening for the differentially expressed genes (DEGs) was done with a p-value of 0.01 and counted in different ways. (**Figure 9**.) In the figure, the upset plot could be separated to three sections, with four data bars each.

The first section of the upset plot was for the singular datasets, meaning DEGs found for each cell line:

- 4463 DEGs for PB (EARLY PD) neurons
- 1679 DEGs for PA.2 (LATE PD) neurons
- 532 DEGs for WTB (HEALTHY) neurons
- 455 DEGs for WTA.2 (HEALTHY) neurons

Then the next section or the next four data bars were for datasets with DEGs that were in common between two cell lines:

- 2751 DEGs for PA.2 (LATE PD) and PB (EARLY PD)
- 2199 DEGs for WTA.2 (HEALTHY) and WTB (HEALTHY)
- 1567 DEGs for PB (EARLY PD) and WTB (HEALTHY)
- 1137 DEGs for PA.2 (LATE PD) and WTA.2 (HEALTHY)

The last section or the last four data bars of the upset plot were for datasets with DEGs that were in common between three cell lines:

- 2975 DEGs for the PA.2 (LATE PD), WTA.2 (HEALTHY), and WTB (HEALTHY)
- 1862 DEGs for the PB (EARLY PD), WTA.2 (HEALTHY), and WTB (HEALTHY)
- 584 DEGs for the PA.2 (LATE PD), PB (EARLY PD), and WTA.2 (HEALTHY)
- 444 DEGs for the PA.2 (LATE PD), PB (EARLY PD), and WTB (HEALTHY)

In the end, we targeted three different datasets from the second section that to serve as comparisons between the different PD etiologies in question:

- Late-onset PD: PA.2 (LATE PD) versus WTA.2 (HEALTHY)
- Early-onset PD: PB (EARLY PD) versus WTB (HEALTHY)
- PD itself: PA.2 (LATE PD) versus PB (EARLY PD)

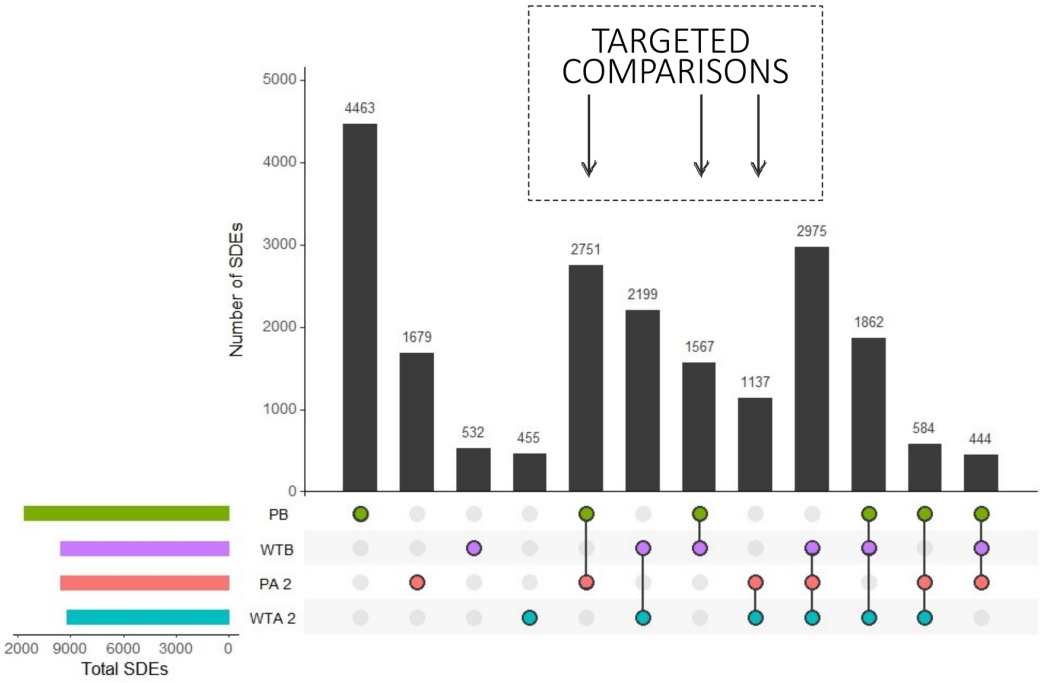

Figure 9. The initial preview of DEGs. An upset plot showing the number of DEGs and could be separated into three sections, with four data bars each. The first four bars were for each cell lines, the second four were for DEGs in common between two cell lines and the last four were DEGs in common between three cell lines. The targeted comparisons were highlighted. Significance was determined with Wald's test and p-value of 0.01.

Advanced modelling for the three targeted comparisons was done using DESeq2 package that considered genotype, patient or healthy, and time. (Love, 2014.) For each DEG, two expressions over time were mapped out according to the samples within the pair, and significance was determined by the difference of expression levels between the two samples in at least one time point. Top 20 significant DEGs were found for each of the comparisons. (**Figure 10A**.)

After modelling the DEGs individually, hierarchical clustering was applied with a threshold of 0.01 to create an overall expression profile each comparison. (**Figure 10B**.) With this first clustering, 1642 DEGs were found for late-onset PD (PA.2 versus WTA.2), 2655 DEGs for early-onset PD (PB versus WTB), and 4120 DEGs for PD itself (PA.2 versus PB). There were concerns about the false positives skewing the data, DEGs whose level of expression could

be low compared to the rest of the DEGs but still having a significant difference in expressions between the samples. Therefore, to find more functionally meaningful DEGs, the p-value was increased to 0.0001. (**Figure 10C**.) After this adjustment, the DEGs for late-onset PD were 485, 1063 DEGs for early-onset PD, and 1281 DEGs for PD itself.

The final genetic expression profiles had several clusters displaying conspicuous behaviours such as those unmistakably diverging in expression from day 30 or those converging in expression at day 90. All clusters were categorized in three ways: divergent, convergent, and variant behaviours. (**Figure 11A**.) The divergent and convergent behaviours were further organized as upregulation or downregulation based on the topmost level of expression at a certain time point, day 90 for divergent and day 60 for convergent behaviours. The variant behaviours were set aside since they could not be explained straightforwardly. After this restructuring, the divergent behaviour was present in all comparisons therefore that category of DEGs was focused on for pathway analysis. As followed, six sets were used. The three targeted comparisons earlier had another two sets of pairs within, a sample's DEGs upregulated over the other and vice versa. For example, within the late-onset PD pair, there was a subset with the PA.2 (PATIENT) DEGs upregulated and then another subset with WTA.2 (HEALTHY) DEGs upregulated instead.

To state the numbers, for late-onset PD, there were 150 DEGs upregulated in PA.2 (PATIENT) and 156 DEGs for WTA.2 (HEALTHY) neurons. Then for early-onset PD, there were 506 DEGs for PB (PATIENT) and 557 DEGs for WTB (HEALTHY). Lastly for PD itself, there were 760 DEGs for PA.2 (LATE PD) and 471 DEGs for PB (EARLY PD).

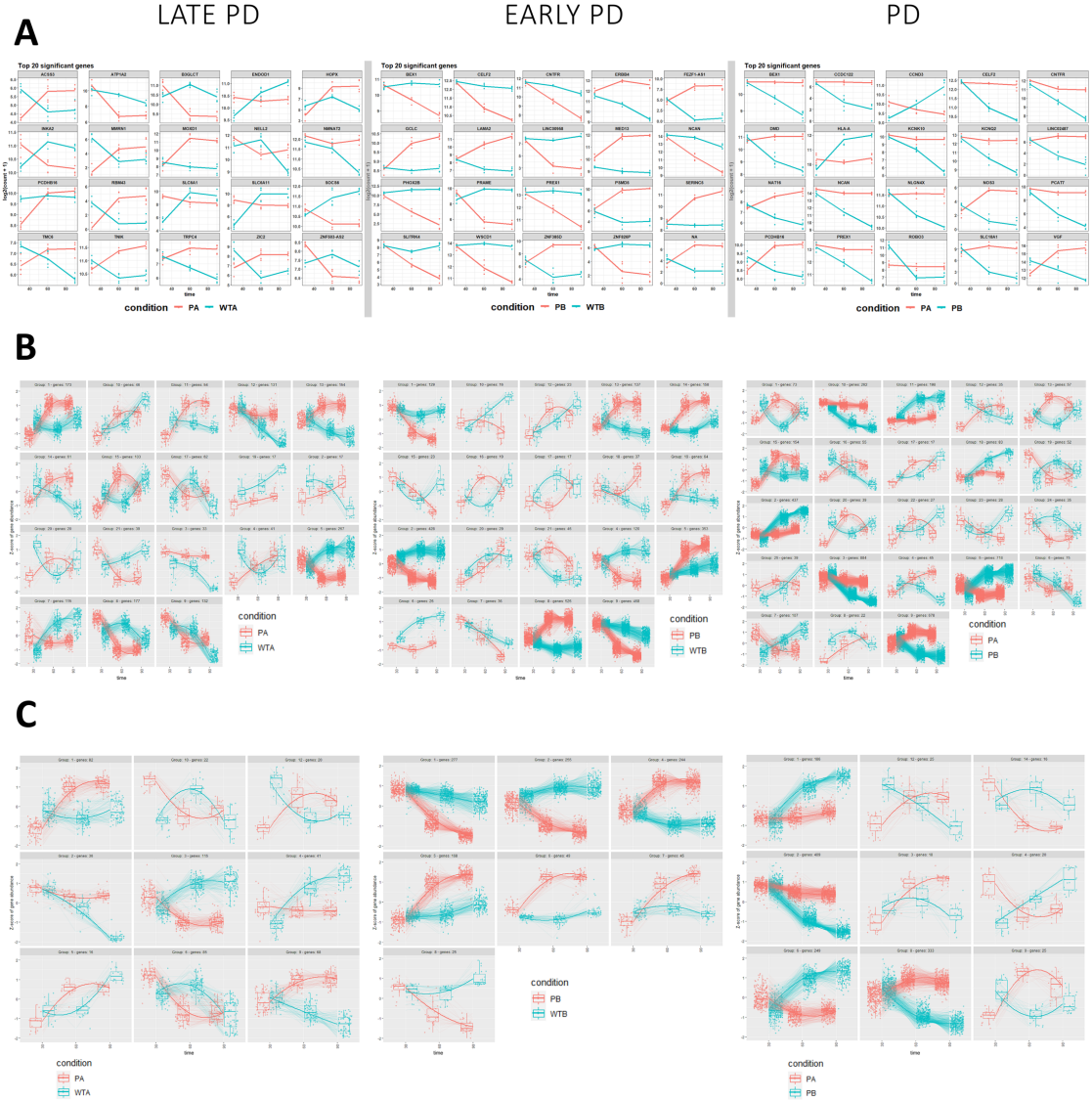

Figure 10. The advanced modelling of the RNA expression profiles. DESeq2 was used to create the expression profile for each comparison. (A) showed the modelling of individual DEGs. (B) showed the first hierarchical clustering of DEGs to create the expression profile, with a p-value of 0.01. (C) showed final clustering for the expression profile, with a p-value of 0.0001. Significance was determined with Wald's test.

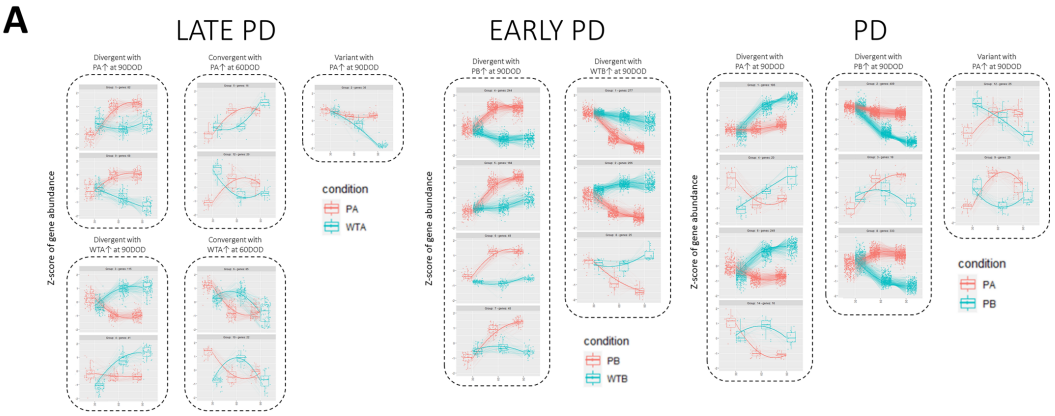
A
LATE PD
EARLY PD
PD
Divergent with PA↑ at 90DOD
Convergent with PA↑ at 60DOD
Variant with PA↑ at 90DOD
Divergent with WTA↑ at 90DOD
Convergent with WTA↑ at 60DOD
Divergent with PB↑ at 90DOD
Divergent with WTB↑ at 90DOD
Divergent with PA↑ at 90DOD
Divergent with PB↑ at 90DOD
Variant with PA↑ at 90DOD
Z-score of gene abundance
condition
PA
WTA
PB
WTB

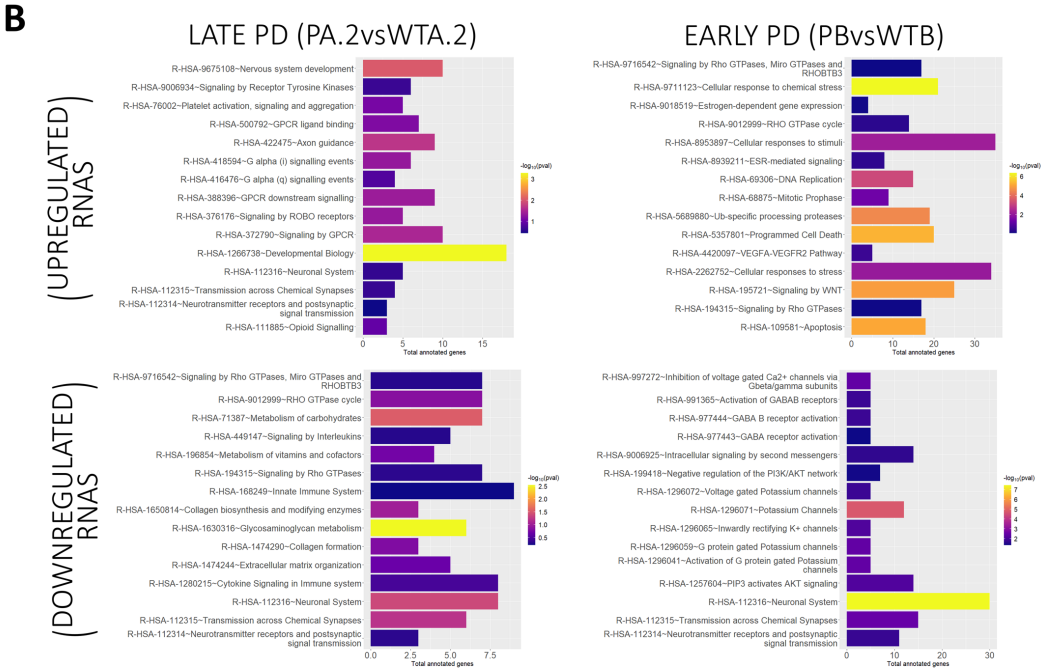
B
LATE PD (PA.2vsWTA.2)
EARLY PD (PBvsWTB)
(UPREGULATED RNAS)
(DOWNREGULATED RNAS)
R-HSA-9675108~Nervous system development
R-HSA-9006934~Signaling by Receptor Tyrosine Kinases
R-HSA-76002~Platelet activation, signaling and aggregation
R-HSA-500792~GPCR ligand binding
R-HSA-422475~Axon guidance
R-HSA-418594~G alpha (i) signalling events
R-HSA-416476~G alpha (q) signalling events
R-HSA-388396~GPCR downstream signalling
R-HSA-376176~Signaling by ROBO receptors
R-HSA-372790~Signaling by GPCR
R-HSA-1266738~Developmental Biology
R-HSA-112316~Neuronal System
R-HSA-112315~Transmission across Chemical Synapses
R-HSA-112314~Neurotransmitter receptors and postsynaptic signal transmission
R-HSA-111885~Opioid Signalling
R-HSA-9716542~Signaling by Rho GTPases, Miro GTPases and RHOBTB3
R-HSA-9711123~Cellular response to chemical stress
R-HSA-9018519~Estrogen-dependent gene expression
R-HSA-9012999~RHO GTPase cycle
R-HSA-8953897~Cellular responses to stimuli
R-HSA-8939211~ESR-mediated signaling
R-HSA-69306~DNA Replication
R-HSA-68875~Mitotic Prophase
R-HSA-5689880~Ub-specific processing proteases
R-HSA-5357801~Programmed Cell Death
R-HSA-4420097~VEGFA-VEGFR2 Pathway
R-HSA-2262752~Cellular responses to stress
R-HSA-195721~Signaling by WNT
R-HSA-194315~Signaling by Rho GTPases
R-HSA-109581~Apoptosis
R-HSA-71387~Metabolism of carbohydrates
R-HSA-449147~Signaling by Interleukins
R-HSA-196854~Metabolism of vitamins and cofactors
R-HSA-168249~Innate Immune System
R-HSA-1650814~Collagen biosynthesis and modifying enzymes
R-HSA-1630316~Glycosaminoglycan metabolism
R-HSA-1474290~Collagen formation
R-HSA-1474244~Extracellular matrix organization
R-HSA-1280215~Cytokine Signaling in Immune system
R-HSA-997272~Inhibition of voltage gated Ca2+ channels via Gbeta/gamma subunits
R-HSA-991365~Activation of GABAB receptors
R-HSA-977444~GABA B receptor activation
R-HSA-977443~GABA receptor activation
R-HSA-9006925~Intracellular signaling by second messengers
R-HSA-199418~Negative regulation of the PI3K/AKT network
R-HSA-1296072~Voltage gated Potassium channels
R-HSA-1296071~Potassium Channels
R-HSA-376176~Signaling by ROBO receptors
R-HSA-1296065~Inwardly rectifying K+ channels
R-HSA-1296059~G protein gated Potassium channels
R-HSA-1296041~Activation of G protein gated Potassium channels
R-HSA-1257604~PIP3 activates AKT signaling
Total annotated genes
-log10(pval)

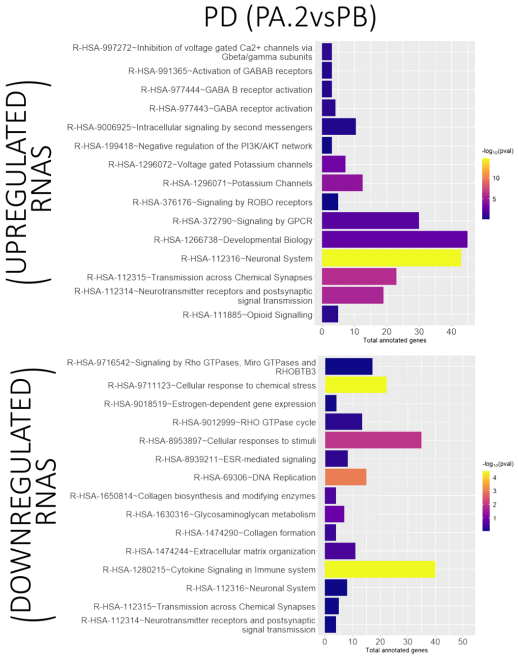
PD (PA.2vsPB)
(UPREGULATED RNAS)
(DOWNREGULATED RNAS)
R-HSA-997272~Inhibition of voltage gated Ca2+ channels via Gbeta/gamma subunits
R-HSA-991365~Activation of GABAB receptors
R-HSA-977444~GABA B receptor activation
R-HSA-977443~GABA receptor activation
R-HSA-9006925~Intracellular signaling by second messengers
R-HSA-199418~Negative regulation of the PI3K/AKT network
R-HSA-1296072~Voltage gated Potassium channels
R-HSA-1296071~Potassium Channels
R-HSA-376176~Signaling by ROBO receptors
R-HSA-372790~Signaling by GPCR
R-HSA-1266738~Developmental Biology
R-HSA-112316~Neuronal System
R-HSA-112315~Transmission across Chemical Synapses
R-HSA-112314~Neurotransmitter receptors and postsynaptic signal transmission
R-HSA-111885~Opioid Signalling
R-HSA-9716542~Signaling by Rho GTPases, Miro GTPases and RHOBTB3
R-HSA-9711123~Cellular response to chemical stress
R-HSA-9018519~Estrogen-dependent gene expression
R-HSA-9012999~RHO GTPase cycle
R-HSA-8953897~Cellular responses to stimuli
R-HSA-8939211~ESR-mediated signaling
R-HSA-69306~DNA Replication
R-HSA-1650814~Collagen biosynthesis and modifying enzymes
R-HSA-1630316~Glycosaminoglycan metabolism
R-HSA-1474290~Collagen formation
R-HSA-1474244~Extracellular matrix organization
R-HSA-1280215~Cytokine Signaling in Immune system
R-HSA-112316~Neuronal System
R-HSA-112315~Transmission across Chemical Synapses
R-HSA-112314~Neurotransmitter receptors and postsynaptic signal transmission
Total annotated genes
-log10(pval)

Figure 11. Behaviour categories and the subsequent pathway analysis. (A) showed expression profiles categorized based on divergent, convergent or variant behaviours. The details of the organization were described above. (B) showed pathway analysis for DEGs with divergent behaviour. Significance of pathway analysis was determined with Fisher's Exact test and p-value of 0.01.

The REACTOME database was used to find pathways enriched with DEGs from the six sets. The top 15 significant pathways were found for each, and some motifs were immediately noticeable. (**Figure 11B**.) For late-onset PD, the signalling-related pathways were enriched with upregulated RNAs in PA.2 (PATIENT) such as GPCR or ROBO signalling. G protein-coupled receptors or GPCRs are a large family of cell surface receptors that transduce a variety of external signals into intracellular downstream effectors. (Hilger, 2018.) Roundabout or ROBO receptors are transmembrane receptors that regulate cell functions such as axon guidance and angiogenesis. (Tong, 2019.)

On the opposite end, the metabolism and immune related pathways were enriched with upregulated RNAs in WTA.2 (HEALTHY) such as glycosaminoglycan metabolism or immune cytokine signalling. For early-onset PD, the stress response-related pathways were enriched with upregulated RNAs in PB (PATIENT) such as apoptosis or ubiquitin-specific processing proteases metabolism. Then on the opposite end, the channels/receptors in signalling pathways were enriched with upregulated RNAs in WTB (HEALTHY) such as potassium channel or GABA receptor. Lastly for PD itself, the results could almost be taken from the patient and healthy comparisons. Several signalling-related pathways were enriched with upregulated RNAs in PA.2 (LATE PD) such as ROBO or potassium signalling. Then stress and immune related pathways were enriched with upregulated RNAs in PB (EARLY PD).

Seeing the similarity in results from the initial pathway analysis, we wondered if we could correlate the patient-healthy pairs with the patient-patient pair. (**Figure 12A**.) First, we started with the entire dataset of DEGs of a patient, PA.2 (LATE PD) or PB (EARLY PD). Then we derived only the upregulated DEGs for each patient in comparison to their healthy counterpart (A's and B's). The same was done for downregulated DEGs for each patient in

comparison to their healthy counterpart. Finally, the DEGs were further trimmed down into upregulated DEGs in comparison to the opposing patient. Again, the same was done for the downregulated DEGs. With all that said, we come to the "final" four sets of RNAs. To state the numbers, there were 212 upregulated DEGs and 211 downregulated DEGs for late-onset PD. Then there were 258 upregulated DEGs and 316 downregulated DEGs for early-onset PD. The following pathway analysis yield similar motifs to the initial analysis, but the significance was increased between the patient lines (PA.2 versus PB). (**Figure 12B**.)

By appearance, signalling was a major theme for late-onset PD and immune response was for early-onset PD. Related pathways for both themes were extracted from the pathway analysis. (**Figure 13**.) For the signalling motif, what was present were kinases of RHO family as well as GPCRs. The RHO kinases are responsible for a myriad of activities within a neuron including the axon plasticity while the GPCRs are the ones interpreting the incoming signals. (Huang Y. &., 2015.) (Ng, 2004.) (Spillane, 2014.)

For the immune motif, it appeared that the nuclear factor kappa-light-chain-enhancer of activated B cells (NF-κB) pathway was highly enriched with upregulated DEGs especially the ones with the noncanonical activation. Interestingly, mitogen-activated protein kinase (MAPK) pathways were enriched with downregulated PB (EARLY PD) RNAs. Overall, we have a comprehensive view of the transcriptomic landscape between early-onset and late-onset PD.

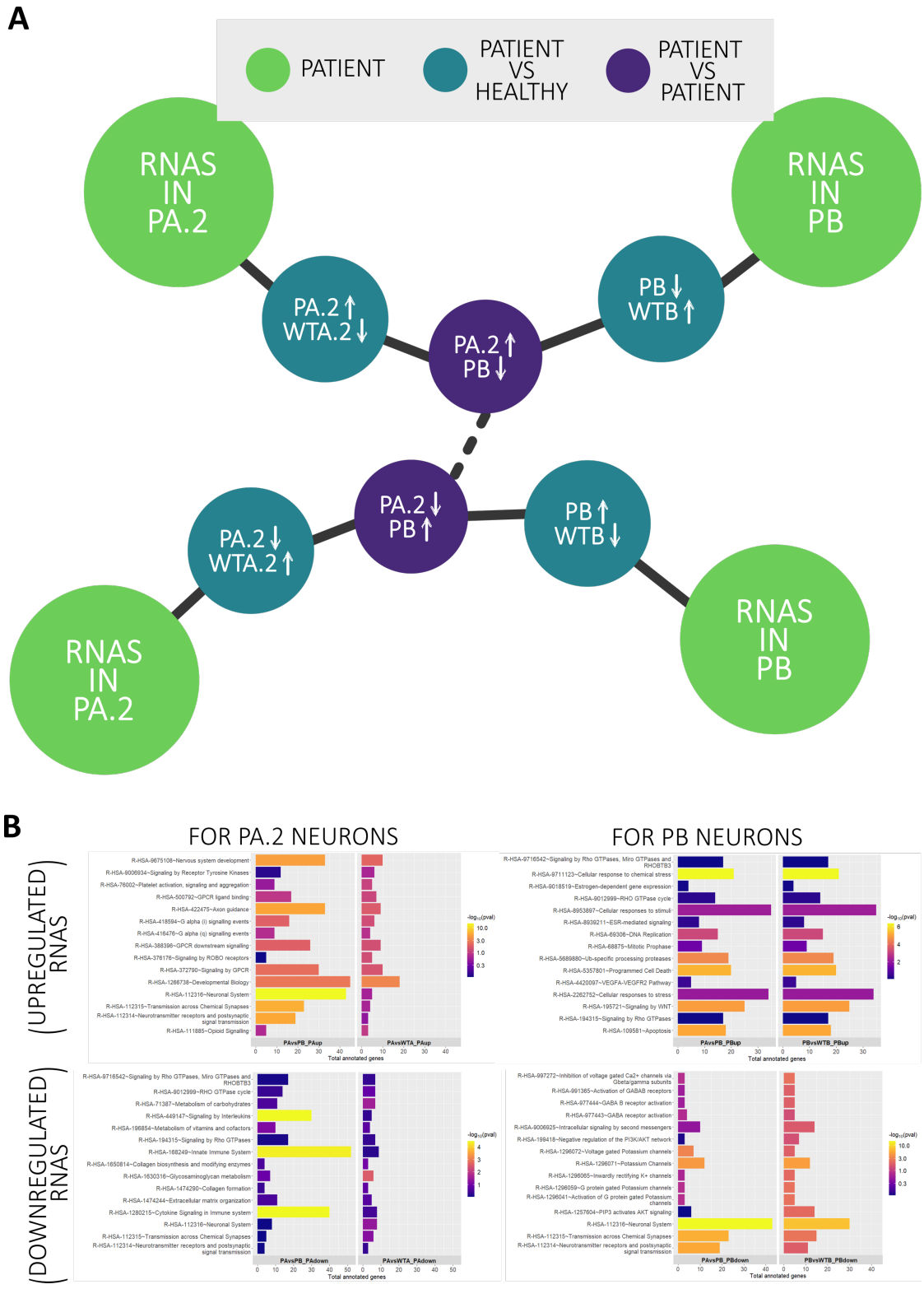

Figure 12. Correlations between the pairs and the subsequent pathway analysis. (A) showed the relationship map between patient-healthy and patient-patient pairs. (B) showed the pathway analysis for the "final" four sets. Significance was determined with Fisher's Exact test and p-value of 0.01.

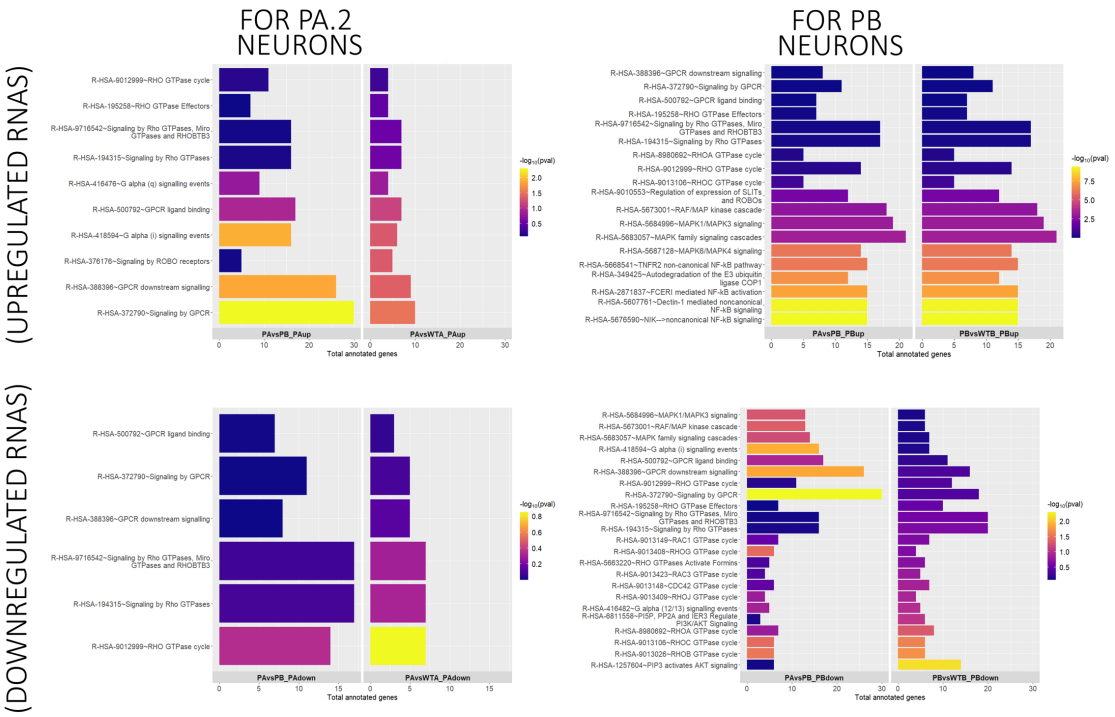

Figure 13. Signalling and immune related pathways present in the "final" four sets. All the related pathways to the signalling and immune motifs were extracted and shown here.

4.5. PHENOTYPIC ANALYSIS

The second part of the comparison was observing different morphological features within the dopaminergic neurons. Four phenotypes were chosen: total alpha synuclein, phosphorylated alpha synuclein, neurites, and mitochondria. For the immunofluorescence staining, four markers were used: ASYN, PSYN, MAP2, and translocase of outer mitochondrial membrane 20 (TOMM20) respectively to the phenotypes. (**Figure 14A&B**, **Figure 15A&B**, **Figure 16A&B**, **Figure 17A&B**.) Interestingly, each phenotype showed similar expression levels over time to varying degrees of significance. The neurite length and the number of total alpha synuclein and mitochondrial components showed an increasing expression over time while the number of phosphorylated alpha synuclein showed a bell-shaped behaviour. (**Figure 14C**, **Figure 15C**, **Figure 16C**, **Figure 17C**.)

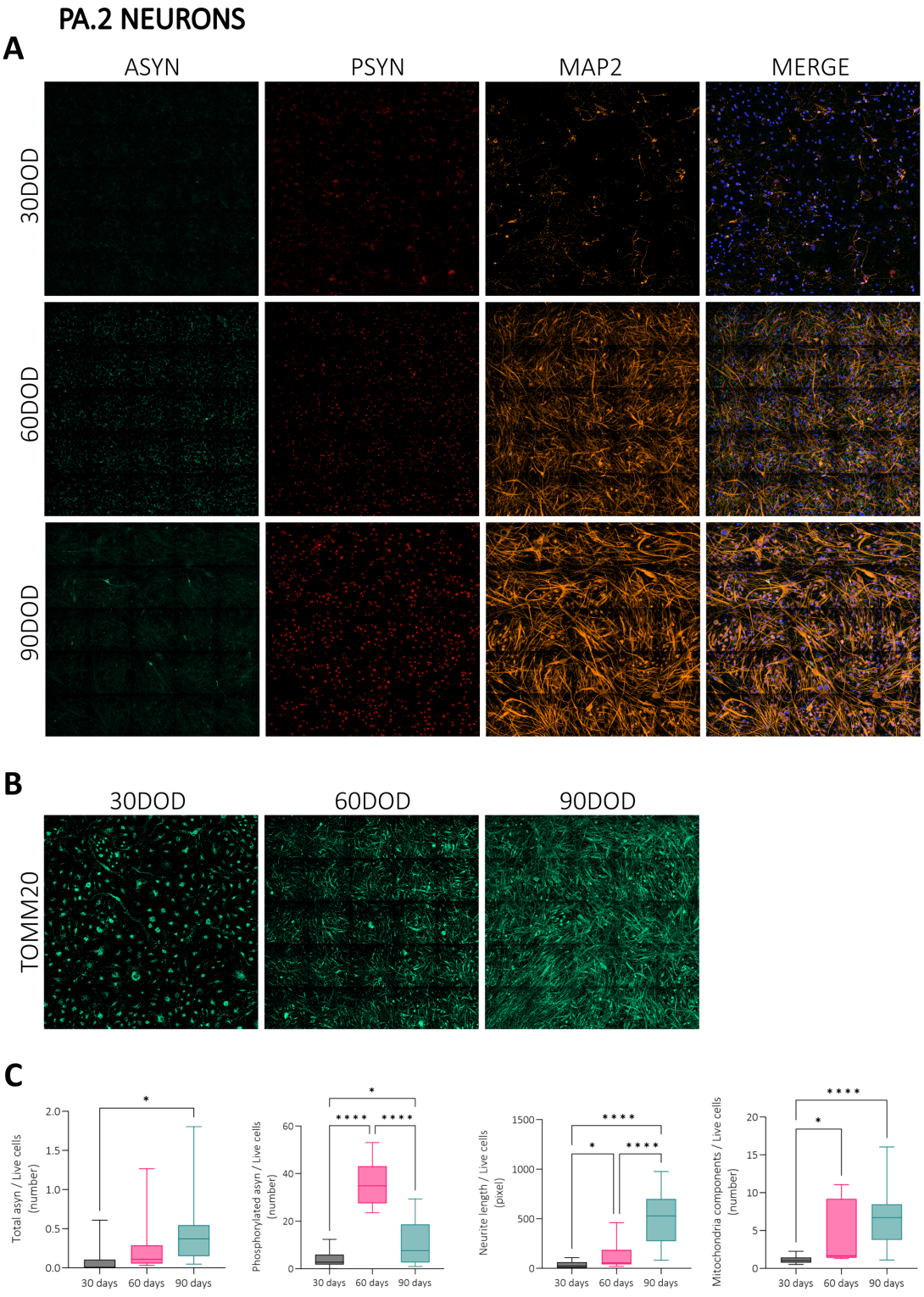

Figure 14. The phenotypic staining and analysis of PA.2 dopaminergic neurons. ASYN, PSYN, MAP2, and TOMM20 markers showed their expression across three time points. (A) showed ASYN, PSYN, and MAP2 markers. (B) showed TOMM20 marker. (C) showed the expression level over time for each marker. Significance was determined with Dunnett's T3 multiple comparison test. * p≤0.05; **** p≤0.0001

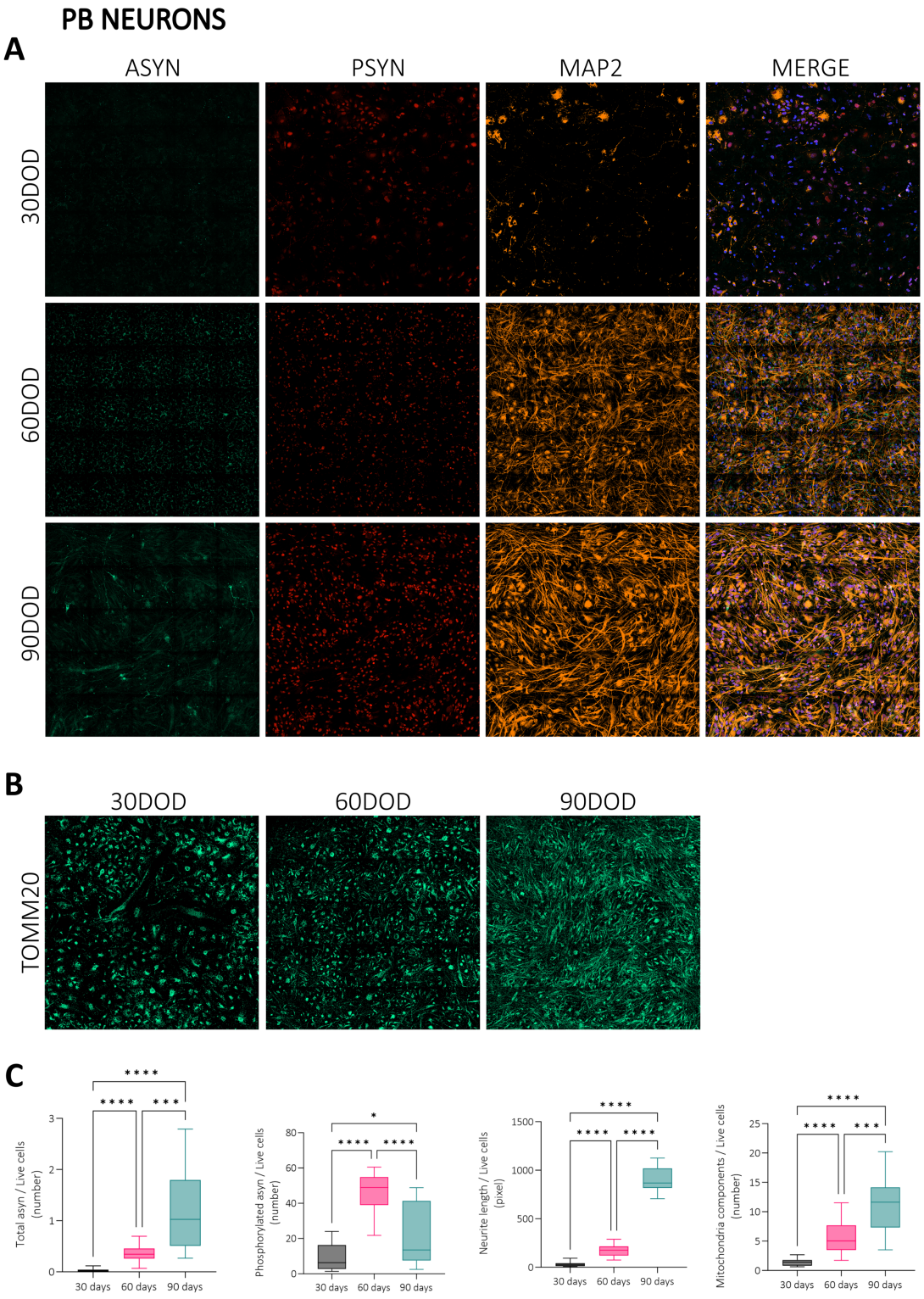

Figure 15. The phenotypic staining and analysis of PB dopaminergic neurons. ASYN, PSYN, MAP2, and TOMM20 markers showed their expression across three time points. (A) showed ASYN, PSYN, and MAP2 markers. (B) showed TOMM20 marker. (C) showed the expression level over time for each marker. Significance was determined with Dunnett's T3 multiple comparison test. * p≤0.05; *** p≤0.001; **** p≤0.0001

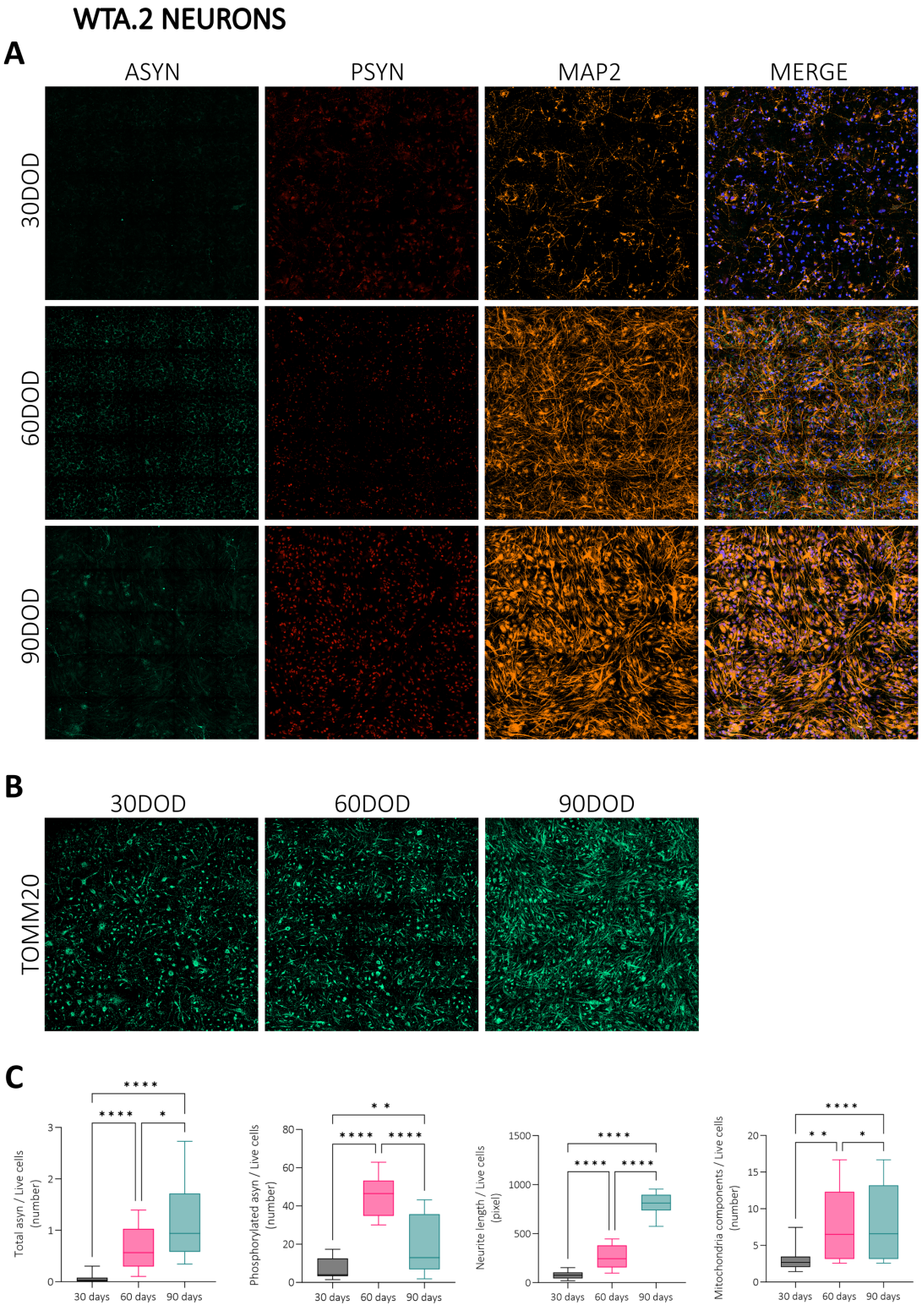

Figure 16. The phenotypic staining and analysis of WTA.2 dopaminergic neurons. ASYN, PSYN, MAP2, and TOMM20 markers showed their expression across three time points. (A) showed ASYN, PSYN, and MAP2 markers. (B) showed TOMM20 marker. (C) showed the expression level over time for each marker. Significance was determined with Dunnett's T3 multiple comparison test. * p≤0.05; ** p≤0.01; **** p≤0.0001

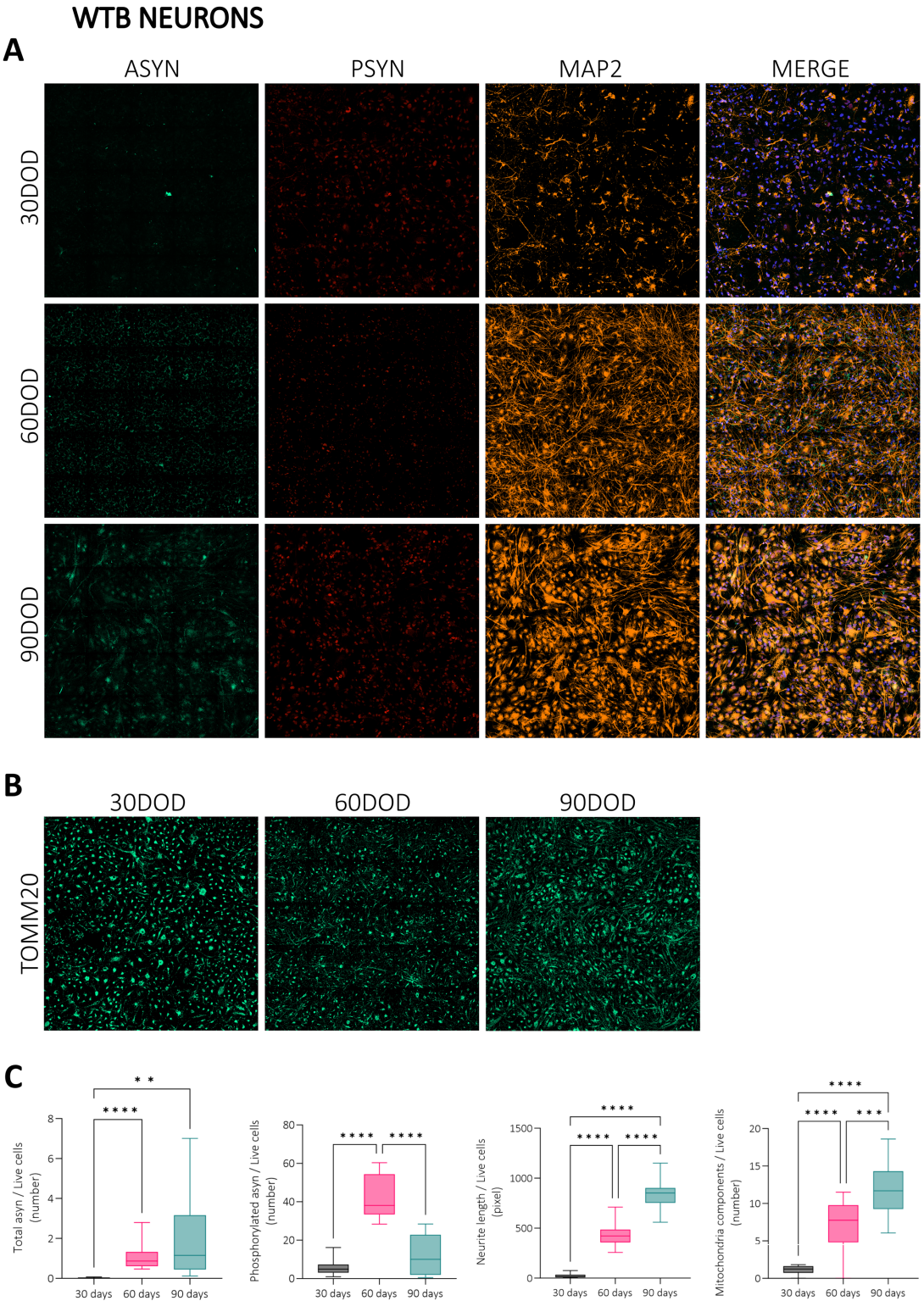

Figure 17. The phenotypic staining and analysis of WTB dopaminergic neurons. ASYN, PSYN, MAP2, and TOMM20 markers showed their expression across three time points. (A) showed ASYN, PSYN, and MAP2 markers. (B) showed TOMM20 marker. (C) showed the expression level over time for each marker. Significance was determined with Dunnett's T3 multiple comparison test. ** p≤0.01; *** p≤0.001; **** p≤0.0001

4.5.1. NEURITES

The MAP2 staining was used for neurite morphology and several related features were extracted. They were neurite length, branches, branch points, branch starting points, branch ending points, and synapses. A representative image showed how each of the neurite feature was assessed based on the MAP2 staining. (**Figure 18B, E, H, K, N & Q**.)

Each feature was compared between all four lines for each time point. (**Figure 18A, D, G, J, M & P**.) For neurite length, the patient neurons started with significantly shorter lengths compared to the wild type neurons, but the patients had no significant difference between each other until day 90. (**Figure 18A**.) At day 90, the PA.2 (LATE PD) neurons had a significant decrease in their length compared to PB (EARLY PD) and wild type neurons, while the neurite length was comparable between the last three lines. Similar observations were seen for synapses, except significance started at day 60 where the wild type neurons had a higher number of synapses than patient neurons. (**Figure 18D**.) Then, at day 90, PA.2 (LATE PD) neurons had a lower number of synapses compared to PB (EARLY PD) and wild type neurons with no differences between the last three lines.

The significant changes observed in the neurite length were the same in branches, branch points, branch starting points, but not the branch ending points. (**Figure 18G, J, M & P**.) Instead, for the ending points, at day 90, PA.2 (LATE PD) neurons had significantly lower number compared to PB (EARLY PD) and one of the wild types. Although slightly different, the results of this feature do not contradict with other features. Overall, the neurites were substantially weaker for late-onset PD compared to early-onset PD and the healthy counterparts at day 90. Lack of alterations in the features within PB (PATIENT) for the early-onset PD did confirm the slow decline of the neurites, where any significant difference from the healthy counterparts were yet to be seen.

For a more targeted comparison, the pairs from the transcriptomic analysis were used here as well: late-onset PD (PA.2 versus WTA.2), early-onset PD (PB versus WTB), and PD itself (PA.2 versus PB). (**Figure 18C, F, I, L, O & R**.) For late-onset PD, all neurite features were

significantly compromised in PA.2 (PATIENT) compared to WTA.2 (HEALTHY) neurons. Interestingly, the features had a converging behaviour between PB (EARLY PD) and WTB (HEALTHY) neurons. In the patient neurons, the MAP2 marker had a decline in expression between day 30 and 60 but a recovery was seen at day 90 where its expression was comparable to the healthy counterpart. Lastly, the PA.2 (LATE PD) had significantly impaired neurite morphology compared to PB (EARLY PD) neurons at day 90. These three results showed how the neurites change within each etiology as well as in comparison with each other, reinforcing the collective understanding on neuron behaviour: the axonal and dendritic projections were significantly affected for patients with late-onset PD but not to the same extent for those with early-onset PD.

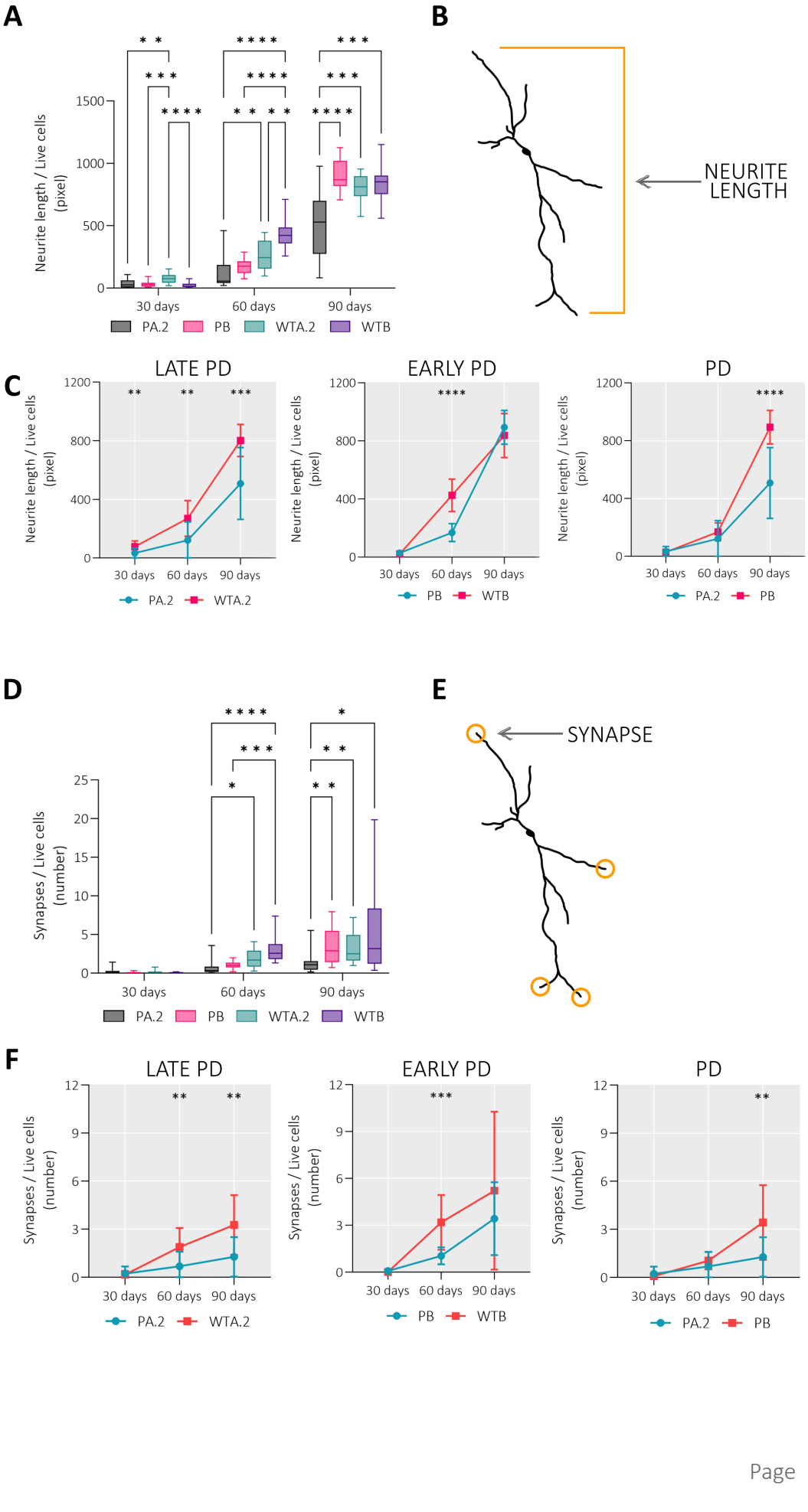
A
B
C
D
E
F
Neurite length / Live cells (pixel)
1500
1000
500
0
30 days
60 days
90 days
PA.2
PB
WTA.2
WTB
NEURITE LENGTH
LATE PD
EARLY PD
PD
1200
800
400
Synapses / Live cells (number)
25
20
15
10
5
12
9
6
3
SYNAPSE

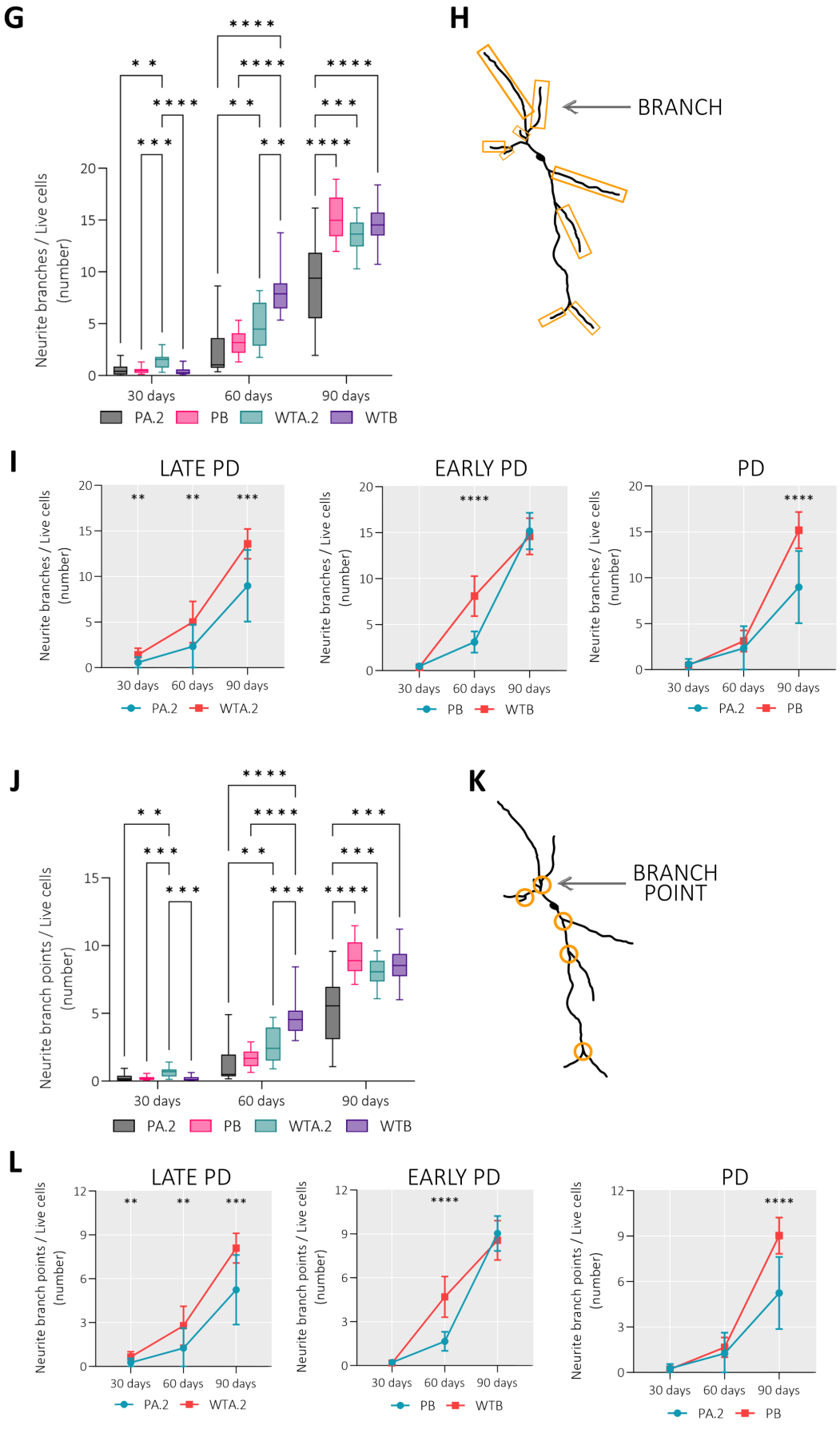
G
H
BRANCH
Neurite branches / Live cells (number)
30 days
60 days
90 days
PA.2
PB
WTA.2
WTB
I
LATE PD
EARLY PD
PD
J
K
BRANCH POINT
Neurite branch points / Live cells (number)
L

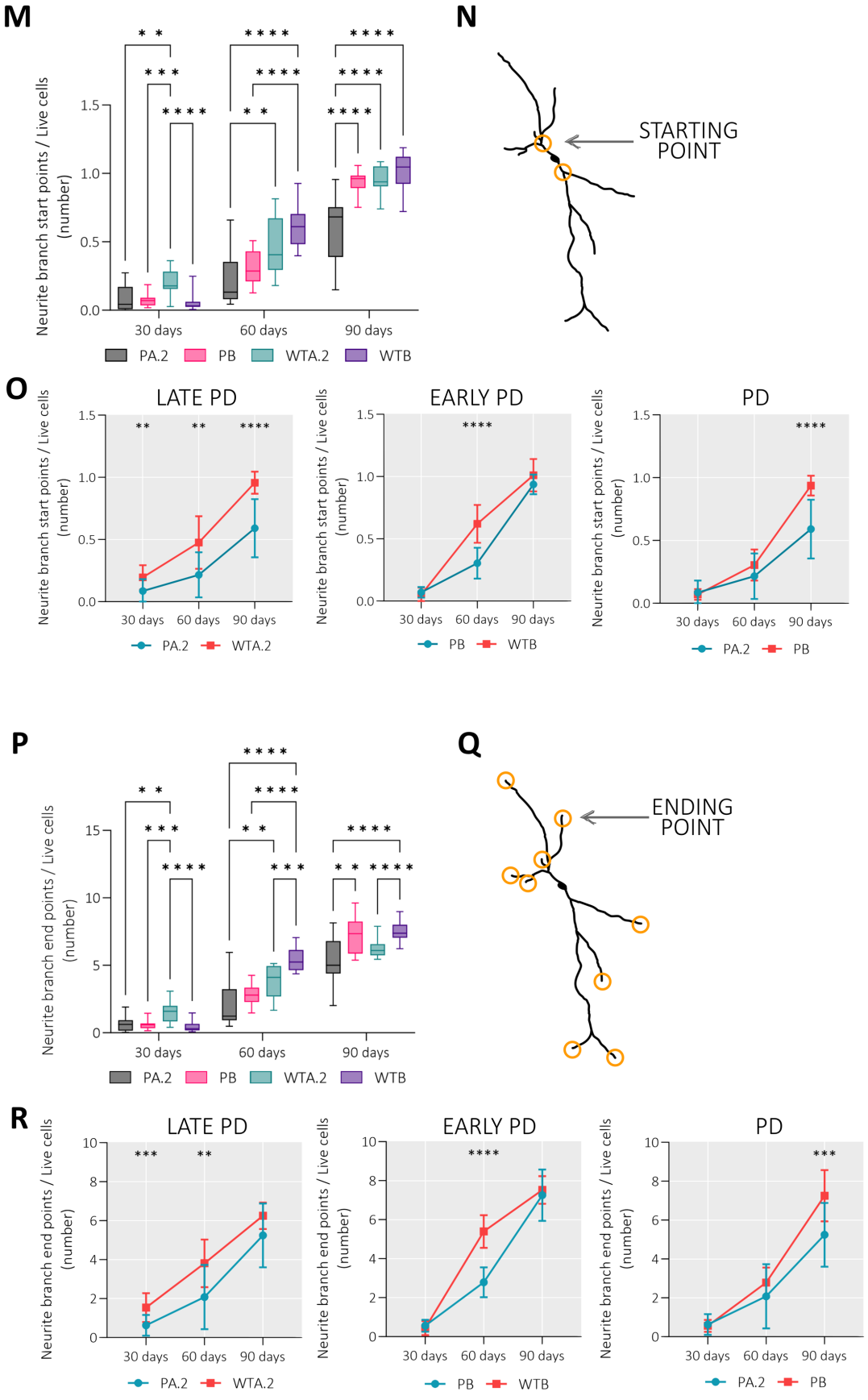
M
N
Neurite branch start points / Live cells (number)
STARTING POINT
30 days
60 days
90 days
PA.2
PB
WTA.2
WTB
O
LATE PD
EARLY PD
PD
P
Neurite branch end points / Live cells (number)
Q
ENDING POINT
R

Figure 18. Analysis of the different neurite features. Based on the MAP2 staining, six neurite features were extracted: (A, B, C) for length; (D, E, F) for synapses; (G, H, I) for branches; (J, K, L) for branch points; (M, N, O) for branch starting points; (P, Q, R) for branch ending points. Each had three plots: (B, E, H, K, N, Q) showing a visual example of the feature; (A, D, G, J, M, P) showing all four lines compared; (C, F, I, L, O, R) showing the patient-healthy and patient-patient comparisons. Significance was determined for all four lines with Tukey's multiple comparison test, then for the pairs with Šídák's multiple comparison test. * p≤0.05; ** p≤0.01; *** p≤0.001; **** p≤0.0001

Black neuron sourced from Oriol Pavon/SciDraw

4.5.2. ALPHA SYNUCLEIN

The ASYN staining was used for the total alpha synuclein morphology. The number of alpha synuclein within an overlay mask of MAP2 was totalled for each line. (**Figure 19B**.) Between the four lines, the wild type neurons had significantly higher amount of alpha synuclein compared to the patient neurons, more so when compared to PA.2 (LATE PD). (**Figure 19A**.) Then at day 90, there was a significant increase of the protein within PB (EARLY PD) neurons comparable to the wild types. Ergo, the PA.2 (LATE PD) neurons continued having low amounts compared to the rest of the lines. For the comparisons between the targeted pairs, the significance observed here was synonymous with what was seen for the neurites.

Considering that the alpha synuclein pathogenesis was the norm for Parkinson's, perhaps this was not the case here. An increase of alpha synuclein do not necessarily imply an increase of their aberrant isoforms. Instead, it could be an increase of their usual form within the synaptic terminals that work with the neurotransmitter trafficking. (Burré, 2015.) Therefore, it would stand that the wild type neurons have healthier synaptic structures and higher level of alpha synuclein expression compared to the patient neurons. The same could be said for PB (EARLY PD) compared to PA.2 (LATE PD) neurons.

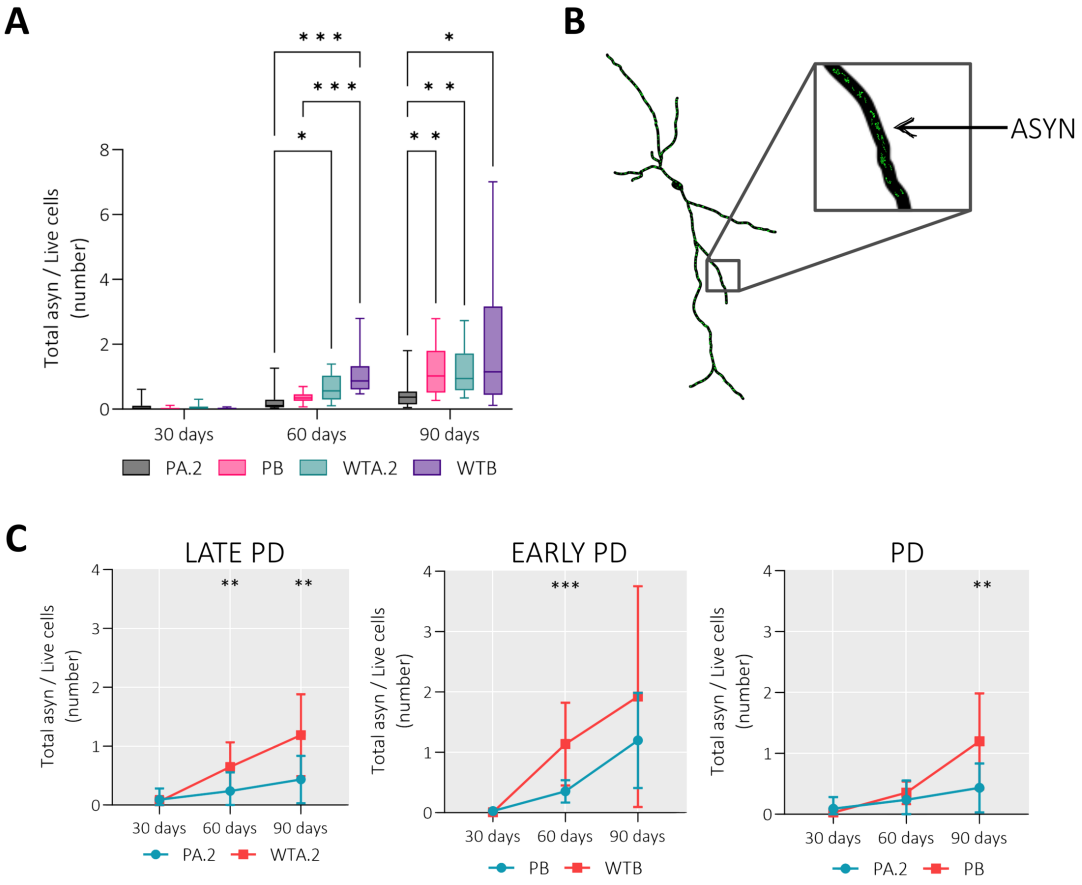

Figure 19. Analysis of the alpha synuclein phenotype. Based on the ASYN staining with MAP2 mask, the total number of alpha synuclein was extracted. (B) showed how the phenotype was analysed. (A) showed four lines compared at each time point. (C) showed the patient-healthy and patient-patient comparisons. Significance was determined for all four lines with Tukey's multiple comparison test, then for the pairs with Šídák's multiple comparison test. * p≤0.05; ** p≤0.01; *** p≤0.001; **** p≤0.0001

Black neuron sourced from Oriol Pavon/SciDraw

The PSYN staining was used for phosphorylated alpha synuclein morphology. The number of phosphorylated alpha synuclein within an overlay mask of MAP2 was totalled for each line. (**Figure 20B**.) A bell-shaped behaviour was observed when comparing the four lines. (**Figure 20A**.) Significance was seen between PA.2 (LATE PD) and PB (EARLY PD) at day 30 and again at day 60 in addition to the late-onset pair. The bell-shaped behaviour was also observed in the comparisons among the targeted pairs. For late-onset PD, the WTA.2 (HEALTHY) had more phosphorylated alpha synuclein than PA.2 (PATIENT) neurons and

significantly at day 60. For early-onset PD, it was the PB (PATIENT) having a bit more of the phosphorylated proteins compared to WTB (HEALTHY) neurons. Then for PD, PB (EARLY PD) had significant levels of the proteins compared to PA.2 (LATE PD) consistently throughout.

Following similar interpretations for the alpha synuclein morphology, an increase of phosphorylated alpha synuclein may not be pathogenic. Although the normal function of this isoform is not fully understood, it is thought to regulate the balance between the excitatory and inhibitory signals since it normally localizes in the presynaptic axon terminals. (Kontaxi, 2023.)

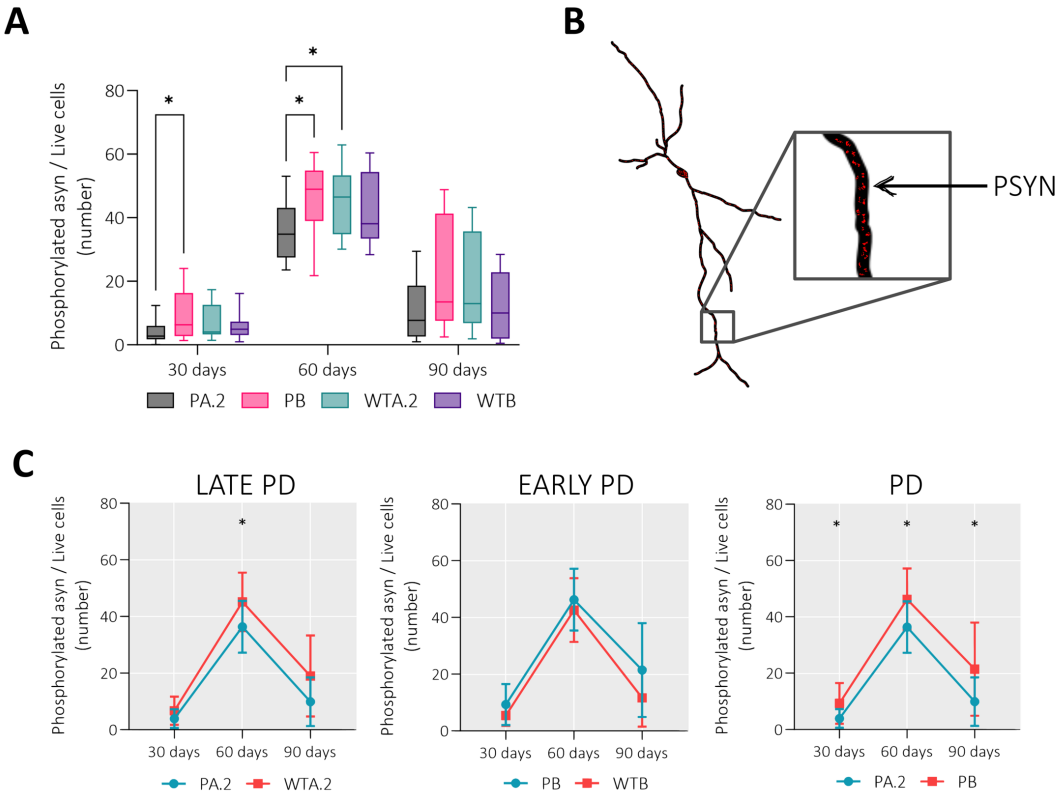

Figure 20. Analysis of the phosphorylated alpha synuclein phenotype. Based on the PSYN staining with MAP2 mask, the total number of phosphorylated alpha synuclein was extracted. (B) showed how the phenotype was analysed. (A) showed all four lines compared at each time point. (C) showed the patient-healthy and patient-patient comparisons. Significance was determined for all four lines with Tukey's multiple comparison test, then for the pairs with Šídák's multiple comparison test. * p≤0.05; ** p≤0.01; *** p≤0.001; **** p≤0.0001

Black neuron sourced from Oriol Pavon/SciDraw

4.5.3. MITOCHONDRIA

The TOMM20 staining was used for the mitochondria morphology. The number of mitochondria components within an overlay mask of MAP2 was counted for each line. (**Figure 21B**.) Between the four lines, initially the wild types had significantly higher amounts of mitochondria components than the patient neurons until day 90. (**Figure 21A**.) By day 90, PB (EARLY PD) saw an increase in their components to the levels comparable to the wild type neurons while PA.2 (LATE PD) did not.

For the comparisons among the targeted pairs, akin to what was seen between the four lines, the healthy counterparts had higher levels of mitochondria components than the patient neurons. Significance was seen for late-onset PD, at day 30 and 90. For comparing the etiologies, PB (EARLY PD) had higher levels of the organelle compared to PA.2 (LATE PD) and significantly at day 90.

TOMM20 stained the outer membrane of the mitochondria so each component was counted as an individual organelle within the neuron. Seeing that the PA.2 (LATE PD) neurons continuously having a low number of mitochondria, an impaired turnover rate and mitochondrial quality control proteins was suspected. (Chen, 2023.)

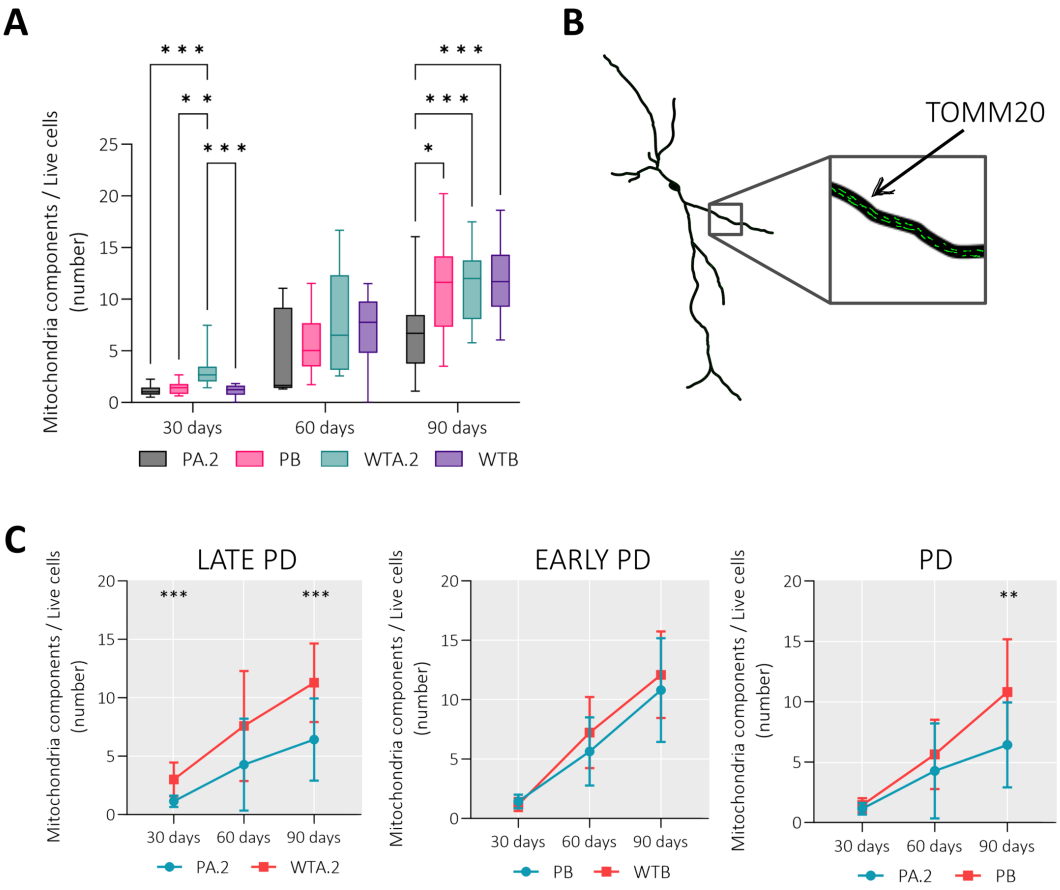

Figure 21. Analysis of the mitochondria phenotype. Based on the TOMM20 staining with MAP2 mask, the number of mitochondria components was extracted. (B) showed how the phenotype was analysed. (A) showed four lines compared at each time point. (C) showed the patient-healthy and patient-patient comparisons. Significance was determined for all four lines with Tukey's multiple comparison test, then for the pairs with Šídák's multiple comparison test. * p≤0.05; ** p≤0.01; *** p≤0.001; **** p≤0.0001

Black neuron sourced from Oriol Pavon/SciDraw

Putting it together, both the neurite and mitochondria morphologies were drastically altered in PA.2 (LATE PD) neurons compared to PB (EARLY PD) and wild type neurons. But the alpha synuclein morphology, both in their native and phosphorylated states, do not appear critical for the patient neurons.

4.6. MITOCHONDRIAL FUNCTION (INCOMPLETE)

We attempted to assess the mitochondrial function by measuring the oxygen consumption rate (OCR) with the Seahorse Mito Cell Stress test kit. The assay involved four sequential injections of drug compounds to influence mitochondrial respiration: oligomycin, FCCP, rotenone, and antimycin-a. By introducing the compounds, different aspects of the organelle were targeted so that the assay could evaluate several of their features: basal respiration, ATP production, maximal respiration, spare respiratory capacity, proton leak, and non-mitochondrial respiration. These altogether could offer a comprehensive view of the bioenergetics dynamics of the organelle.

The OCR measurements were obtained for all lines; however, no measurements were possible for PA.2 (LATE PD) neurons after day 30 despite having cells in the plate, which were confirmed with Hoechst staining. (**Figure 22A**.) What the Seahorse bioanalyzer showed instead was negative values for their OCR indicating that the cell density was too low for PA.2 (LATE PD) neurons. Nonetheless, the measurements continued for the remaining three lines for the last two time points and features were extracted. Although the significant analysis was not possible, each feature was plotted out for a visual assessment. (**Figure 22B**.) What appeared was the PA.2 (LATE PD) neurons had a potential defective mitochondrial health already at day 30 compared to PB (EARLY PD) and wild type neurons based on low basal and maximal respiration levels. Most strikingly, the PB (EARLY PD) neurons had a much higher maximum respiration level and spare respiratory capacity compared to the wild type neurons. Thus, only the early-onset PD pair (PB and WTB) were used for a targeted comparison. (**Figure 22C**.) The maximum respiration and spare capacity did not show any significant despite the striking visuals. Instead, the aging of the healthy neurons was confirmed in terms of mitochondrial health based on the basal respiration and proton leak.

Although the OCR measurements were incomplete, the partial results obtained showed potential differences in the mitochondrial function between the PA.2 (LATE PD) and PB (EARLY PD) neurons that would lend to the PD comparative analysis.

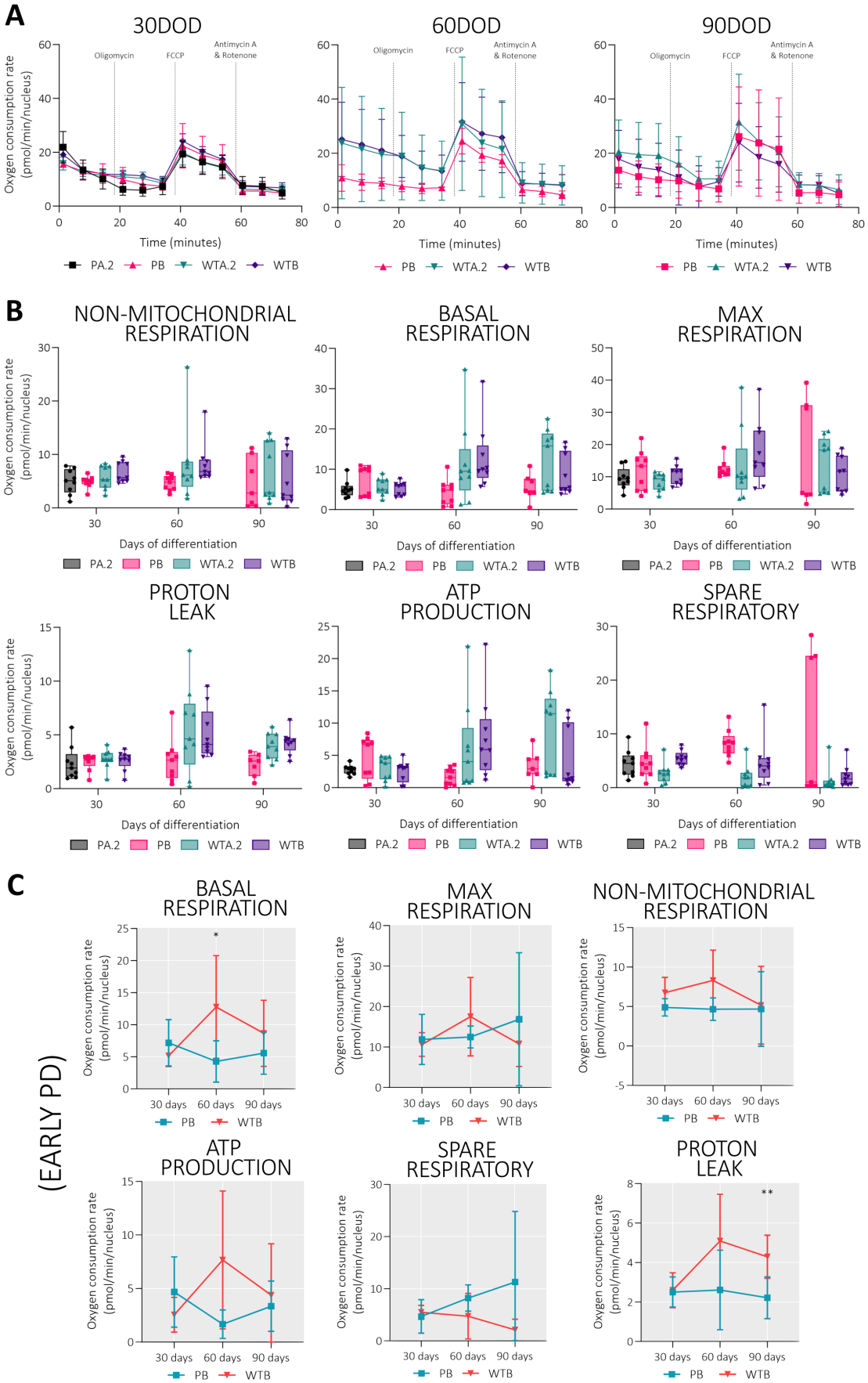
A
30DOD
60DOD
90DOD
Oligomycin
FCCP
Antimycin A & Rotenone
Oxygen consumption rate (pmol/min/nucleus)
Time (minutes)
PA.2
PB
WTA.2
WTB
B
NON-MITOCHONDRIAL RESPIRATION
BASAL RESPIRATION
MAX RESPIRATION
PROTON LEAK
ATP PRODUCTION
SPARE RESPIRATORY
Days of differentiation
C
(EARLY PD)
BASAL RESPIRATION
MAX RESPIRATION
NON-MITOCHONDRIAL RESPIRATION
ATP PRODUCTION
SPARE RESPIRATORY
PROTON LEAK
30 days
60 days
90 days
PB
WTB

Figure 22. The Seahorse Mito Cell Stress test. The oxygen consumption rate (OCR) was measured for all four lines; however, the OCR was unreadable for PA.2 (LATE PD) neurons after day 30. (A) showed overall OCR when the drugs were injected. (B) showed the mitochondrial features based on OCR measurements. (C) showed the analysis of early-onset PD pair (PB versus WTB). Significance was determined with Šídák's multiple comparison test. * $p \leq 0.05$; ** $p \leq 0.01$

4.7. TH+ YOUNG NEURONS (INCOMPLETE)

We attempted to obtain a population enriched with TH-positive neurons from the project lines for a closer investigation. To achieve this, we explored neural surface markers: atrial natriuretic peptide-converting enzyme (CORIN), activated leukocyte cell adhesion molecule (ALCAM), and leucine rich repeats and transmembrane domains 1 (LRTM1). (**Figure 23**.)

CORIN is a serine protease usually found in the heart but during embryo development, CORIN is also an early floor plate marker expressed over the entire neural tube. Previous studies have successfully used this surface marker with labelled LMX1A, a classical intracellular ventral midbrain marker, for generating a larger population of the midbrain neural progenitor cells that gave rise to TH+ neurons more efficiently; however, they were not entirely dopaminergic as serotonergic neurons and other non-specific neurons were identified as well. (Doi, 2014.) (Kirkeby, 2017.)

Building on top of that, the ALCAM and LRTM1 surface markers were incorporated for further specificity of the neural progenitor cells in differentiating to TH+ dopaminergic neurons. (Bye, 2014.) (Kumar A. T., 2023.) (Paik, 2018.) (Samata, 2016.) ALCAM are cell-cell adhesion molecules that are not tissue-specific but during the embryo development, ALCAM is a mesencephalic precursor marker within the midbrain region of the neural tube that give rise to the sensory neurons within the muscles of the face and neck. (Seigfried, 2017.) LRTM1 are transmembrane proteins that modulate the synaptic cell adhesion molecules but during embryo development, LRTM1 is expressed selectively in the ventral midbrain region of the neural tube. (Linhoff, 2009.)

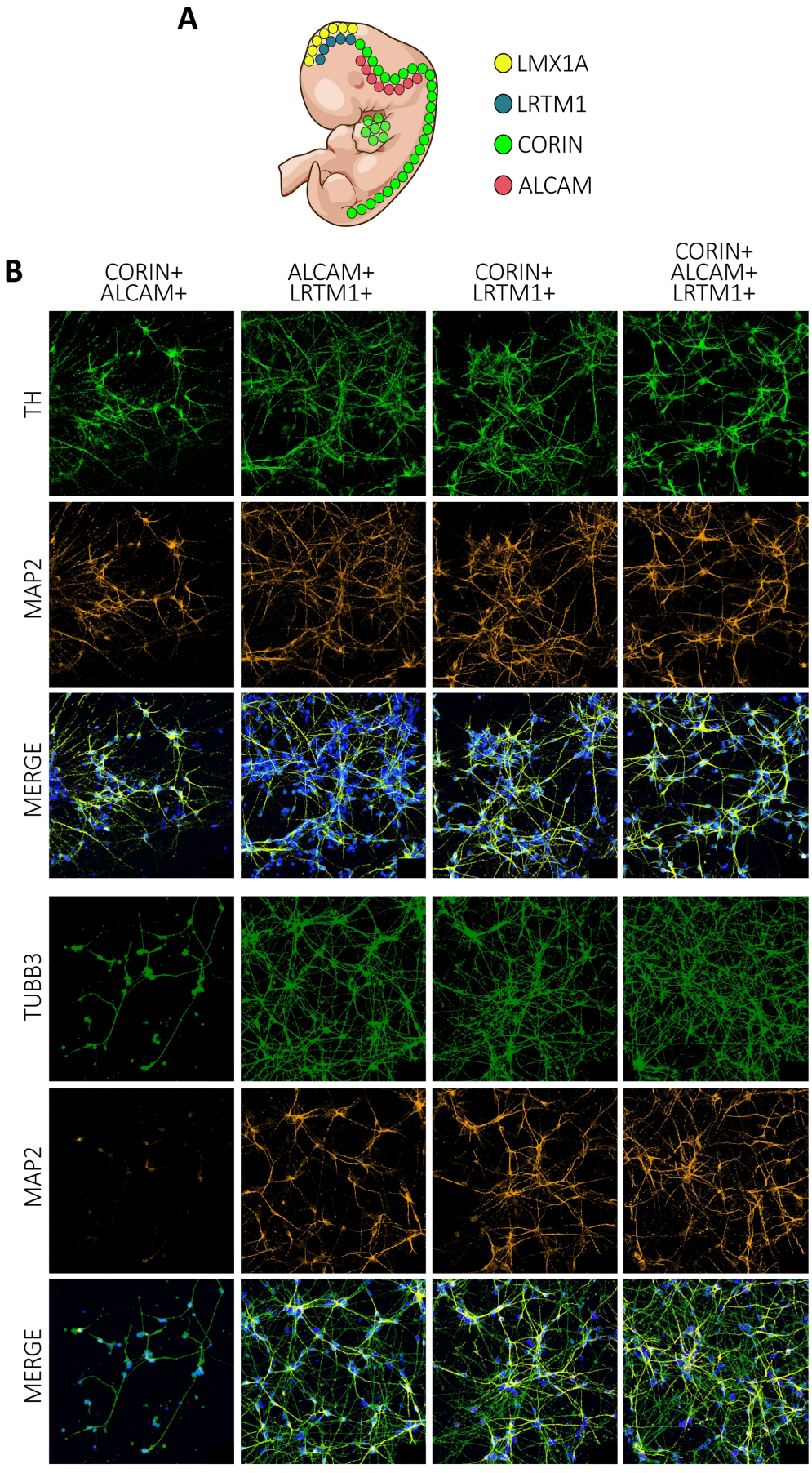
A
LMX1A
LRTM1
CORIN
ALCAM
B
CORIN+ ALCAM+
ALCAM+ LRTM1+
CORIN+ LRTM1+
CORIN+ ALCAM+ LRTM1+
TH
MAP2
MERGE
TUBB3
MAP2
MERGE

Figure 23. The sorting of the young TH+ neurons at 15DOD. CORIN, ALCAM, and LRTM1 were the surface markers used to sort for TH+ neurons at 15DOD. (A) showed a visual depiction of the markers' expression during neural tube development. (B) showed different combinations of the markers for sorting and staining afterward to confirm TH expression.

Embryo art sourced from © Oleksandr Pokusai/Adobe Stock

4.8. PROTEOMIC ANALYSIS (FAILED)

We attempted to extract the human peptides for proteomic analysis. Doing so required a method to distinguish between the human and bovine peptides because the neurons were cultured on Geltrex-coated surfaces, materials made of bovine-derived extracellular matrices. In addition, ideally, two peptide samples would be measured simultaneously in the mass spectrometry. With that said, stable isotope labelling by amino acids in cell culture (SILAC) technique was utilized. In theory, the human peptides would be labelled with medium and heavy lysine and arginine amino acids while the neurons were cultured in labelling medium. Then the extracted human peptides could be discerned and measured.

Usually, the cells would have been passaged a few times in the labelling medium to ensure a maximum incorporation of tagged amino acids. This was not possible with dopaminergic neurons due to their post-mitotic state, but previous studies were able to label the primary neurons. (Liao, 2008.) (Spellman, 2008.) (Zhang G. D., 2011.) Here, we attempted to do the same with iPSC-derived neurons. At this time, no literature reported similar experiments with similar parameters such as doing the labelling with medium and heavy amino acids on iPSC-derived neurons.

First, labelling efficiency for the iPSC-derived neurons was determined with K7 line, the outside control line. (**Figure 24**.) Young K7 neurons were cultured in SILAC medium between 12 to 16 days total before protein extraction. The maximum efficiency was seen at 12 days with 42.52% of peptides labelled. Unexpectedly the percentage decreased afterward, marking a possible difference between primary neurons and iPSC-derived neurons in SILAC culture, where the former had its efficiency plateaued. (Spellman, 2008.)

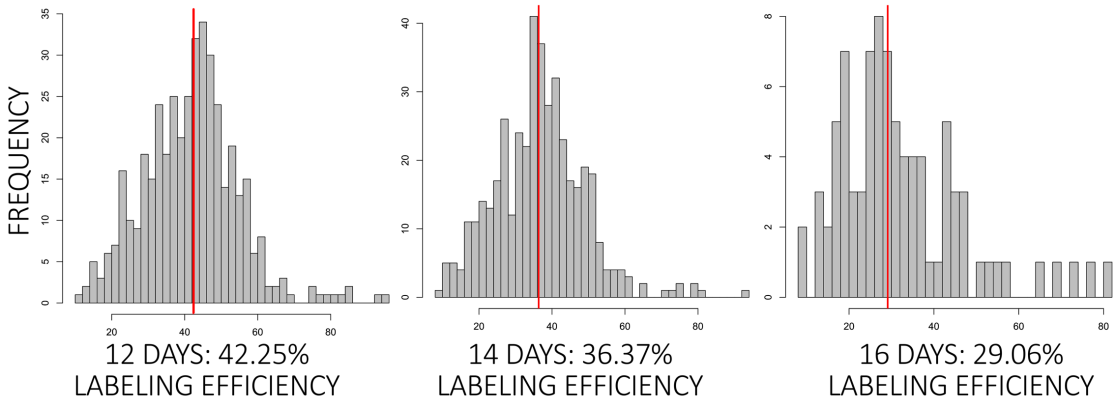

Figure 24. The labelling efficiency of K7 dopaminergic neurons. The K7 control neurons were used to determine the percentage of peptides labelled with heavy and medium amino acids. Different durations were tested to find maximum labelling efficiency possible.

The labelling scheme was set up so that each line was cultured with either medium or heavy amino acids to achieve forward-reverse labelling of their peptides. After twelve days of labelling, the protein extraction was done, and the samples were created where each pair had one line with the medium-labelled peptides and the other with heavy-labelled peptides. A total of twelve samples were created:

- PA.2 versus PB for 30DOD, 60DOD, and 90DOD each
- PA.2 versus WTA.2 for 30DOD, 60DOD, and 90DOD each
- PB versus WTB for 30DOD, 60DOD, and 90DOD each
- WTA.2 versus WTB for 30DOD, 60DOD, and 90DOD each

Then the measurements were done with mass spectrometry. Looking at the results, the forward-reverse labelling was achieved in each sample but not equally, even after normalization. (**Figure 25**.) The R correlation scores were calculated for each sample and only the healthy pairs (WTA.2 versus WTB) had a minimal passable score for all time points.

Although failed, with technical adjustments, there is a possibility for SILAC to be done on the iPSC-derived neurons and label the human peptides to a degree. A near-complete incorporation of the amino acids may not be possible as it was for primary neurons but that remain to be seen.

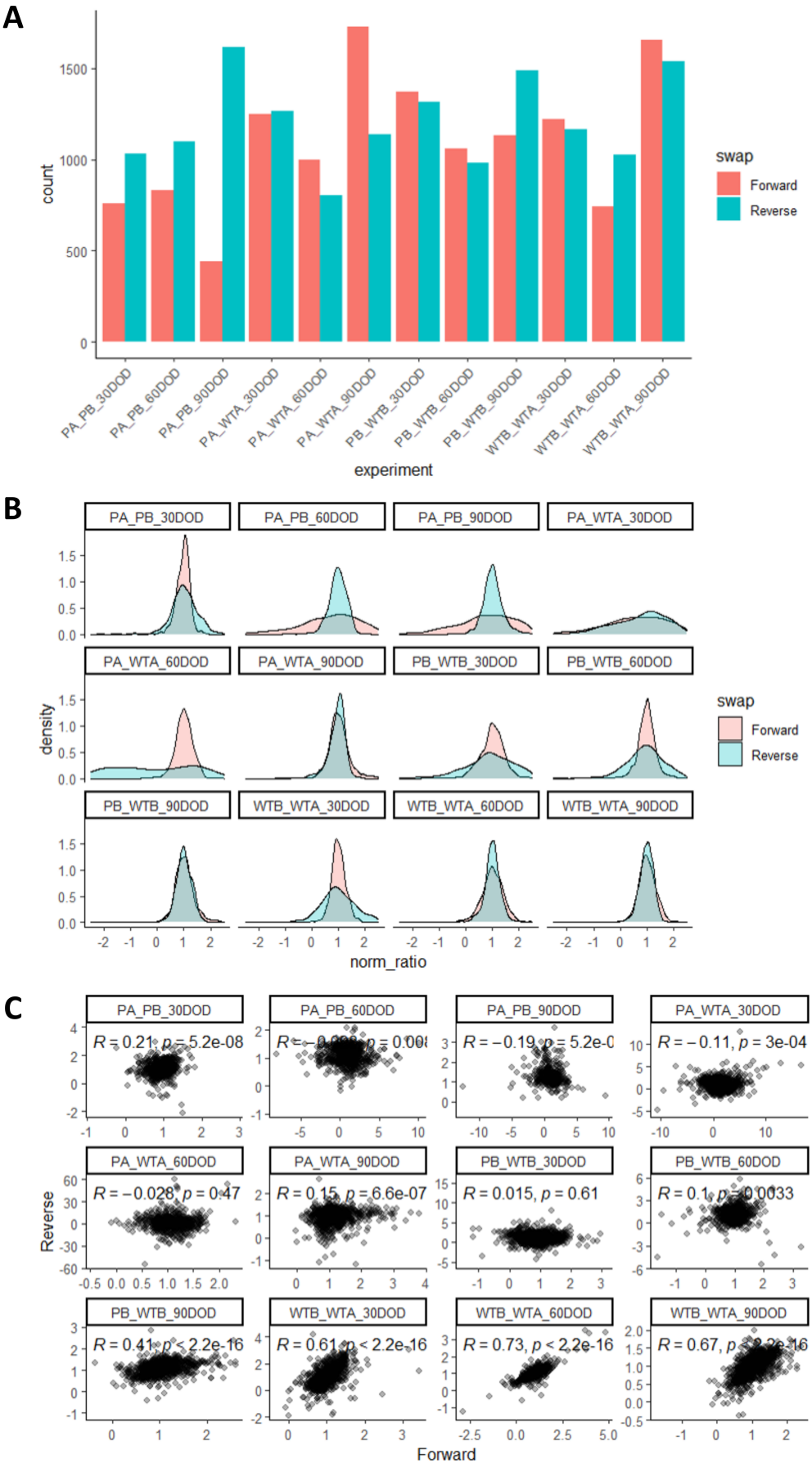
A
count
1500
1000
500
0
PA_PB_30DOD
PA_PB_60DOD
PA_PB_90DOD
PA_WTA_30DOD
PA_WTA_60DOD
PA_WTA_90DOD
PB_WTB_30DOD
PB_WTB_60DOD
PB_WTB_90DOD
WTB_WTA_30DOD
WTB_WTA_60DOD
WTB_WTA_90DOD
experiment
swap
Forward
Reverse
B
density
norm_ratio
C
Reverse
Forward
R = 0.21, p = 5.2e-08
R = −0.19, p = 5.2e-0
R = −0.11, p = 3e-04
R = −0.028, p = 0.47
R = 0.15, p = 6.6e-07
R = 0.015, p = 0.61
R = 0.1, p = 0.0033
R = 0.41, p < 2.2e-16
R = 0.61, p < 2.2e-16
R = 0.73, p < 2.2e-16
R = 0.67, p < 2.2e-16

Figure 25. The SILAC attempt. The labelling of iPSC-derived dopaminergic neurons was done as previous described. (A) showed the forward-reverse labelling of each sample. (B) showed the forward-reverse labelling in normalized samples. (C) showed the R correlation scores for normalized samples.

5. DISCUSSION

The influence of age on Parkinson's is a multifaceted aspect of the disease that shapes their onset, progression, and clinical manifestation. As a neurodegenerative disease that is predominately associated with the aging process, PD unfolds with distinct features in different age groups, ending up with the early-onset and late-onset PD patients. Despite the many clinical-pathological studies conducted on patients covering the diverse age spectrum, not many have been made on the biological aspect or in comparison. This is essential for understanding the heterogeneity of the symptoms, underlying pathology, and challenges associated with diagnosis and management.

In this study, we sought to fill in the gap in cellular/molecular understanding of the two PD etiologies.

5.1. NEURITE PLASTICITY

As seen from phenotypic analysis, the neurite plasticity was significantly affected for the late-onset PD compared to the early-onset PD neurons based on the features derived from MAP2 staining. In addition, many signalling-related processes were enriched with upregulated DEGs in PA.2 (LATE PD) compared to PB (EARLY PD) neurons. Most of these signalling pathways fall under the umbrella of RHO family of GTPases and their many associated processes. This could be refreshed by referring to **Figure 13**.

5.1.1. FROM THE PHENOTYPIC POINT OF VIEW

MAP2 are neuron-specific cytoskeletal proteins influencing microtubule dynamics within the neurites and synaptic terminal buttons. To that end, those proteins

malfunctioning would hurt the neuron plasticity. (Li Y. J., 1998.) We have seen the MAP2 marker showing a significant decline in expression within PA.2 (LATE PD) compared to PB (EARLY PD) neurons at day 90, stating a process of degeneration. The next step could be to take a closer look into the dendritic morphology, including their spines, or the interaction between MAP2 and tau proteins.

The spines are tiny protrusions from the dendrites that form functional contacts with neighbouring neurons. This occurs with the dendrites of a neuron receiving excitatory signals from adjacent axon terminals and then integrating them into the said neuron. The spines come in different shapes corresponding to their functional state, ranging from thin, stubby, mushroom or cup. They are dynamic and constantly changing according to the environment such as the aging process. Studies have established a direct proportional link between the dendritic spines and cognitive processes such as learning and memory. (Hering, 2001.) (Runge, 2020.) Considering the slow decline of the cognitive state for early-onset PD, observing the spines would create a clearer picture of the contrasting neurite plasticity occurring between PA.2 (LATE PD) and PB (EARLY PD) neurons.

In addition, these spiny structures can be used to investigate the alpha synuclein and phosphorylated alpha synuclein morphologies further. These two proteins showed interesting behaviour in the patient neurons, indicating they may not be as usually pathogenic as otherwise believed. Their normal functions are poorly understood but given that their localization is in the synaptic terminals, studying the spines may clarify their activities in the neurons. (Burré, 2015.) (Butler, 2015.) (Kontaxi, 2023.) (Ramalingam, 2023.)

On top of that, another well-known microtubule-associated protein could be perused: the tau protein. These stabilizing proteins work to support the microtubule highway system, therefore maintaining the neurite plasticity. (Kaech, 1996.) When abnormal, these proteins detach from the microtubules and form aggregates within the neurons. This is a hallmark of Alzheimer's disease and now possibly a symptom of Parkinson's as well based on the accumulating evidence. (Pan, 2021.) (Zhang J. J., 2023.) (Zhang X. G., 2018.) We have seen that the alpha synuclein pathology was not significant between these patient and healthy

neurons. Instead, it may be the tau pathology considering the significant degradation of MAP2 or a combination of both microtubule proteins.

5.1.2. FROM THE TRANSCRIPTOMIC POINT OF VIEW

Another supporting claim for neurite plasticity being one of the key signatures between early-onset and late-onset PD comes from the transcriptomic analysis. The activity of MAP2 is dependent on their phosphorylation, which is in part mediated by the RAS/MAPK pathway. (DeGiosio, 2022.) (Llansol, 2001.) This was enriched with downregulated DEGs in PB (EARLY PD) compared to PA.2 (LATE PD) neurons, which meant the RAS/MAPK pathway had the upregulated DEGS in PA.2 (LATE PD) neurons. Aside from the RNAs involved in the MAPK downstream signalling cascades, the MAPK1/MAPK3 signalling pathway was enriched with downregulated DEGs in PA.2 (LATE PD) neurons. Alterations in these upstream MAPK1/MAPK3 kinases were implicated in schizophrenia and Alzheimer's disease. (Funk, 2012.) (Gerschüz, 2015.) Then there was the SLIT/ROBO pathway enriched with upregulated DEGs in PA.2 (LATE PD) neurons. This pathway influenced both the axonal guidance and regulation of dendrite development. Studies revealed that neuron recovery after brain injury such as ischemic stroke or spinal cord injury was achieved through the SLIT/ROBO pathway. (Kaneko, 2018.) (Sherchan, 2020.) Putting this information together, those upregulated DEGs in RAS/MAPK and SLIT/ROBO pathways and downregulated DEGs in MAPK1/MAPK3 pathway were highly likely to be working against the neurite plasticity in the PA.2 (LATE PD) neurons.

When looking at the transcriptomic data, having many upregulated DEGs in the mentioned pathways is not always positive; instead, those DEGs could have an inhibitory role or work in a negative feedback loop within those pathways. This can be assessed at different parts by choosing the commercially available inhibitors or activators for the individual components within the pathways and seeing their effect on the MAP2 morphology. Specifically, it would be curious to assess the RNAs and their functional capacity within the RAS/MAPK, MAPK1/MAPK3 or SLIT/ROBO pathways. Some of them include SLIT2, RAC1,

CDC42, RASGRP1, RASGRP3 or RASGRF1. The SLIT, RAC1, and CDC42 work together to regulate the actin dynamics while the guanine-releasing- protein/factors (GRPs/GRFs) regulate the kinases for the downstream effectors on microtubule dynamics. (Gonda, 2020.) (Haberman, 2008.) (Roberts, 2004.) (Umeda, 2019.)

5.2. NEUROINFLAMMATION

Neuroinflammation is another process involved in the disease pathogenesis. Neuroinflammation, as the name implies, is an inflammatory reaction in the central nervous system that activates neuroprotective mechanisms while inducing damage to nervous tissue, thus contributing to the neurodegeneration process. Their induction can be due to various factors including the environment such as the glial cells or the gut microbiome. This gut-brain axis refers to the bidirectional communication between the gastrointestinal tract and the brain. In PD, the blood-brain barrier becomes compromised, allowing the gut microbial-derived products or byproducts leak into the brain and augment the neuroinflammation. (Arena, 2022.) For the glial cells, a postmortem tissue analysis uncovered an increase in the pro-inflammatory cytokines from the astrocytes and microglia in the PD brain. (Wang Q. L., 2015.)

5.2.1. FROM THE TRANSCRIPTOMIC POINT OF VIEW

Another signature of interest was extracted from the transcriptomic analysis, the noncanonical NF-κB pathways enriched with upregulated RNAs in the PB (EARLY PD) compared to WTB (HEALTHY), their healthy counterpart, and PA.2 (LATE PD) neurons. The ones presented were NIK, TNFR2, and DECTIN-1 mediated NF-κB signalling processes, all of which were part of the noncanonical side of the activation machinery. The NF-κB inducing kinase (NIK) is a central component controlling the activation together with IκB kinase complex α (IKKα), while the tumour necrosis factor receptor (TNFR) family have a subset of ligands that are the usual inducers of the said pathway, and lastly, the dendritic cell-associated C-type lectin-1 (DECTIN-1) are transmembrane receptors that recognize danger-

associated molecular patterns (DAMPs) to trigger an inflammatory response. (Deerhake, 2021.) (Kingeter, 2012.) (Sun, 2017.) Considering that early-onset and late-onset PD patients have different inflammatory profiles, this would be an inquisitive avenue to explore.

NF-κB is a family of transcription factors involved in different processes of the immune and inflammatory responses. The activation method of NF-κB can be of two ways: canonical or noncanonical. The former is stimulation from various immune receptors and inflammatory cytokines while the latter requires stimulation from specific cytokine/receptor pairs. (Trares, 2022.) The physiological responses from either method can be rapid and transient or slow and persistent respectively. This is dependent on the downstream target, the IκB kinase complex (IKK) but in different parts, the IKKα/IKKβ pair or the IKKα/IKKα pair respectively. As the name suggests, the noncanonical NF-κB appears to be an auxiliary pathway to canonical NF-κB; however, recent studies have established the connection between faulty activation of the noncanonical NF-κB to autoimmune and inflammatory disorders. (Barnabei, 2021.) (Liu T. Z., 2017.)

Several studies disclosed the molecular mechanism showing how PARK2 add onto the neurodegeneration through NF-κB pathway. The wild-type PARK2 in neuroblastoma had NF-κB activation yet it was inhibited in pathogenic PARK2 in response to cellular stress. (Henn, 2007.) On the other hand, the activation of NF-κB by nuclear translocation was observed in the postmortem brain tissue of PD patients and animal models. (Dresselhaus, 2019.) Those changes were not characterized to a specific disease state such as early-onset versus late-onset. For example, patients with schizophrenia who had a high cortical expression of pro-inflammatory cytokines were associated with elevated noncanonical NF-κB activities compared to non-schizophrenia controls with similar neuroinflammatory status. (Murphy, 2020.) Perhaps the noncanonical NF-κB activation level or activities could be higher in PB (EARLY PD) neurons during the disease progression or triggered the progression. Another possibility could be the noncanonical NF-κB being triggered after the onset of the disease like the increased DECTIN-1 expression triggering neuroinflammation

in mice after ischemic stroke. (Ye, 2020.) On the other end of the spectrum, there could be benefits to being enriched with upregulated DEGs in noncanonical NF-κB pathways as they have neuroprotective properties given that early-onset PD has a slower progression of the disease. (Cao, 2008.) (Kaltschmidt, 2022.)

5.2.2. FROM THE MITOCHONDRIAL POINT OF VIEW

Supporting the claim that the noncanonical NF-κB pathway could be prevalent in early-onset PD, we have the partial results from the Seahorse Mito Cell Stress test. Most of the mitochondrial features were compromised in PB (EARLY PD) compared to the healthy neurons; however, the maximum and spare respiration levels appeared to be high and pose an interesting question of how the mitochondria would function in stress given that the neurons normally run on a fraction of their mitochondrial energy capacity. Additionally, the mitochondria were also affected by NF-κB signalling. The overall mitochondria function could be impacted in the PB (EARLY PD) neurons and given the potential large spare respiratory, the implication of this specific feature could be a contributing factor to the neuroinflammation from noncanonical NF-κB signalling.

Both the NF-κB and IKKα were found in the mitochondria and interact with the organelle in several ways. (Cogswell, 2003.) (Pazarentzos, 2014.) (Puri, 2019.) For one, there was an intrinsic regulatory loop between the damaged mitochondria, the PARK2-dependent ubiquitination, and NF-κB that activate the latter signalling and the following inflammatory response could be restricted by NF-κB through damaged mitochondria clearance. (Harding, 2023.) (Zhong, 2016.) Concerning the organelle's activity, studies have established a role for the noncanonical NF-κB pathway in mitochondrial dynamics, especially the interactions with the optic atrophy 1 (OPA1) protein within the organelle, a key element in regulating the said dynamics. (Laforge, 2016.) (Nan, 2017.) Outside of the pathway, several associated molecules were involved in mitochondrial respiration such as NIK. (Jung, 2016.) (Pflug, 2023.) (Willmann, 2016.) To that point, the NIK molecule enhanced the mitochondrial spare respiratory capacity and reduced the proton leak as well as increasing fission by interacting

with the dynamin-related protein 1 (DRP1). (Jung, 2016.) (Pflug, 2023.) This could be further investigated by taking advantage of the many NIK inhibitors commercially available and applying them to the project's neurons.

Although all these studies were done with different cell types, they can be taken as a reference to the potential activities occurring between noncanonical NF-κB pathway and mitochondria toward neuroinflammation.

5.3. REST OF THE GOALS

Unfortunately, not all the goals for this project were achieved. In this section, the rest of the goals are briefly discussed in terms of their results obtained so far, the intended outcomes, and further troubleshooting suggestions if any.

5.3.1. TH+ YOUNG NEURONS

The affected cells in Parkinson's are primarily the midbrain dopaminergic neurons, therefore it would be ideal to work with a population containing a relatively high percentage of those types of neurons. The protocol used for neuron differentiation was expected to result in a heterogeneous population including astrocytes. (Reinhardt, 2013.) Given the cell culture limitations, we thought to extract the TH-positive neurons based on their surface markers, focusing on the young neurons at 15DOD where they were robust and more likely to survive in culture post-sorting.

According to the literature, three markers were chosen to sort the dopaminergic neuron progenitors or young neurons: ALCAM, CORIN, and LRTM1. Different combinations were made, either in pairs or all three, and all achieved a population of TH-positive neurons. Any of them could be considered for deriving the dopaminergic neuron progenitors, depending on the experimental settings and needs.

Despite the initial success of sorting for the young neurons with the project cell lines, the FACSAria III instrument kept breaking down at times and this was not ideal given that several differentiation batches were ongoing in parallel that could not be stopped. So, this protocol had to be removed for time's sake. However, it is a protocol proposed as an alternative to the generation of TH-reporter neurons that comes with some disadvantages such as background noise, low signal-to-noise ratio, and tedious assays.

5.3.2. MITOCHONDRIAL FUNCTION

Mitochondrial function is one of the fundamental elements for the central nervous system activity and their dysfunction has been strongly implicated in Parkinson's. All cells rely on the ATP production from the organelle, but the neurons are distinct regarding their bioenergetics needs. This is constantly challenged by neural activities ranging from the generation of electrical impulses, the packing and trafficking of vesicles, up to maintenance and repair of the neurotransmitter-release machinery. (Henrich, 2023.) Aside from fulfilling the energy demand, the mitochondria also play a role in calcium buffer and metabolic signalling. (Walters, 2023.) (Yin, 2014.)

To assess the function, we were able to measure the oxygen consumption rate for all the lines; however, the OCR measurements were unreadable for the PA.2 (LATE PD) neurons after day 30. The presence of the PA.2 (LATE PD) neurons in the Seahorse culture plate was confirmed with the Hoechst staining, so it was hypothesized that their mitochondria function had declined drastically. The density could be increased but it was not in line with the manufacturer's suggestion of keeping an even monolayer for the wells of the culture plate. Another issue was the coating material as a dense neuron layer could easily detach from the well at slight agitations.

One of the suggestions for further experiments would be to consider a spheroid culture and Agilent does have specific Seahorse culture plates for them. The influence of structural differences of the spheroid must be considered but if the 2D cultured neurons were to form

into a spheroid shortly before the assay then the influence may be negligible. 3D scaffolding materials have been used to construct such designs. (Dingle, 2015.) (Strong, 2023.) On the other hand, if an increased cell density is attempted then a stronger coating material is required. A suggestion for this would be the coating protocol that was used for the phenotypic analysis, which was sought for that reason specifically. A short reminder of this is an overnight coating of PDL then another overnight coating of Geltrex. In line with this suggestion, the NESCs could be directly differentiated in the wells of the Seahorse culture plate.

With the partial success with the Seahorse Mito Cell Stress test, a repeat of this experiment should achieve a complete set of measurements with the troubleshooting suggestions. To predict the results, the PA.2 (LATE PD) neurons should have a significantly lower overall oxygen consumption rate compared to the PB (EARLY PD) and wild type neurons. With regards to the derived mitochondrial features, the basal respiration and ATP production should be significantly lower while the proton leak being significantly higher. The max and spare respiratory capacity levels may be as surprising as it was for the PB (EARLY PD) neurons.

5.3.3. PROTEOMIC ANALYSIS

It was with hope that integrating the transcriptomic and proteomic analyses may identify some of the RNA-protein pairs to elucidate the molecular mechanism underlying early-onset and late-onset PD. Indeed, the proteomic analysis is not without its challenges as the peptides are much more complex with a code of 20 amino acids and a diverse range of folding conformations, chemical modifications, and multiple isoforms. (Manzoni, 2016.) Furthermore, the interaction between the mRNA and proteins is highly debated but some progress has been made in establishing the positive correlation between the two states. (Du Y. C., 2019.) (Kumar D. Y., 2016.) (Nie, 2008.)

The attempted SILAC neuron culture ultimately did not work out. With few exceptions, nearly all the forward-reverse labelling of the samples was not successful as they had poor R correlation scores. Interestingly, the pairs with WTA.2 and WTB neurons (HEALTHY) had the best R score out of all samples so potentially, the labelling efficiency may be impacted in the patient neurons. Hence, the labelling efficiency should be repeated with the project cell lines as a general timeframe was already established with the K7 neurons, the outside control cell line. An initial inquiry was made with the proteomic analysis on WTA.2 and WTB (HEALTHY) pairs for all three time points and several differentially expressed peptides were found. With a better R score for future SILAC experiments, these data could be integrated into the analysis.

Given the complete failure of the SILAC experiment, some troubleshooting suggestions are made with the guidance of Dr. Gunnar of the Proteomics of Cellular Signalling group. A smaller tissue culture flask or plate with stronger coating material that the older neurons could withstand some washing should be the cell culture setup. Again, the coating protocol for the phenotypic analysis can be used. When collecting the neurons, more gentle washes with the SILAC DMEM/F-12 medium should be done to ensure the complete removal of the normal N2B27 maintenance medium. If detachment does occur, the neurons may still be usable, but their good viability must be doubly confirmed as the peptides from dead cells will skew the measurements. Another suggestion would be to seed a new flask with the neurons in the SILAC medium in their entirety: detach the neurons from their usual flask while using the SILAC DMEM/F-12 basal medium as their vehicle. Additional advantages to this are being able to control the number of live neurons and having an even layer in the flask when labelling them.

Despite the failure, this SILAC protocol could be feasible for the iPSC-derived neuronal culture considering slight success with WTA.2 and WTB (HEALTHY) neurons. Additional encouragement can be found from previous success with other neural types such as the primary cultured neurons or other SILAC labelling methods for iPSC-derived neurons. With further optimization, the differentially expressed peptides can be obtained for proteomics

analysis and provide supplementary information for the pathway analysis in conjunction with the RNA data.

Altogether, what potentially set apart the two PD etiologies are two key signatures: neurite plasticity and neuroinflammation, both showing an inverse relationship between early-onset and late-onset PD patient neurons during their progression. The clinical assessment of early-onset and late-onset PD is well established; however, the biological backgrounds of either etiologies remain vague. These results can help elucidate their biological backgrounds.

6. CONCLUSIONS&PERSPECTIVES

In conclusion, we have made one of the few expeditions to investigate the molecular and cellular mechanisms underlying the neurons of early-onset and late-onset Parkinson's. The transcriptomic and phenotypic analyses were utilized here in attempt to understand the unique circumstances of how the disease progresses in each etiology.

The dichotomous nature of the neurites showcased the flawed neural network within late-onset PD neurons while they remained somewhat in good health in the early-onset PD neurons. A closer look into the structural components and their innards can reveal compromised parts or molecules that degrade the neural network. Examples include all parts of the neuron starting from the dendrites and their spines to the axon and their traffic highways, and lastly down to the terminals with their junctions formed with neighbouring neurons. Most notably, the nature of alpha synuclein should be scrutinized between early-onset and late-onset PD. Whether those molecules are pathogenic or physiological, is a question that should be answered.

With the defence mechanisms of the immune system, various components can be working against the central nervous system. And all mechanisms are candidates including the noncanonical ones, despite their name. The autophagic flux is one mechanism that could be gauged with luminescence assays, or the ubiquitin-proteasome activity can be tested with in vitro high-throughput screening of ubiquitination assays that exploit different substrates and inhibitors. In addition, molecular subunits of the activation machinery should be probed for their functions outside of their role in the inflammatory responses such as NIK molecule of the noncanonical NF-κB pathway.

This project is not without its challenges. The samples are unique that they must be in a specific range for their age of onset. The project's samples happen to have mutations in the

same gene but PARK2 is not the only gene implicated in early-onset PD. These two limiting factors may be what prevent the results from being an overarching representative of the differences in the biological mechanism beneath the PD etiologies. Future experiments for the comparative analysis should be designed with that caveat in mind. And of course, the remaining goals of this project should be completed. Obtaining a population rich with TH+ dopaminergic neurons, determining the mitochondrial function, and extracting the human peptides for proteomic analysis are all potential results that will go into ascertaining how the disease manifests itself differently. Connections can be established within the system to explain different ramifications such as the NF-κB or neurites with the mitochondria or integrating proteomic with transcriptomic. Moreover, investigating just the TH+ dopaminergic neurons can paint the clearest picture of early-onset PD versus late-onset PD. But that is in the 2D culture, organoids can be considered here as well to recapitulate the anatomical complexity of the brain.

The recognition of early-onset and late-onset forms of Parkinson's underscores their variability and reflects the intricate interplay of factors shaping their clinical landscape. Understanding the subtleties and nuances of different cellular systems within the PD neurons will go far in developing personalized diagnostics and interventions. As research progresses, the evolving comprehension of the disease offers hope for improved outcomes, and enhanced quality of life for individuals at different stages of this complex neurological condition.

7. REFERENCES

Abujarour, R. V. (2013.). Optimized Surface Markers for the Prospective Isolation of High-Quality hiPSCs using Flow Cytometry Selection. *Scientific Reports.* doi:10.1038/srep01179

Akkaoui, M. G. (2019.). Functional Motor Symptoms in Parkinson's Disease and Functional Parkinsonism: A Systematic Review. *Journal of Neuropsychiatry and Clinical Neurosciences., 1.*, 4-13. doi:10.1176/appi.neuropsych.19030058

Alexander, G. (2004.). Biology of Parkinson's disease: pathogenesis and pathophysiology of a multisystem neurodegenerative disorder. *Dialogues in Clinical Neuroscience., 6.*, 259-280. doi:10.31887/DCNS.2004.6.3/galexander

Amm, I. S. (2014.). Protein quality control and elimination of protein waste: The role of the ubiquitin–proteasome system. *BBA - Molecular Cell Research., 1843.*, 182-196. doi:10.1016/j.bbamcr.2013.06.031

Arena, G. S. (2022.). Neurodegeneration and Neuroinflammation in Parkinson's Disease: a Self-Sustained Loop. *Current Neurology and Neuroscience Reports., 22.*, 427-440. doi:10.1007/s11910-022-01207-5

Armstrong, M. &. (2020.). Diagnosis and Treatment of Parkinson Disease. *JAMA., 323.*, 548-560. doi:10.1001/jama.2019.22360

Ball, N. T. (2019.). Parkinson's Disease and the Environment. *Frontiers in Neurology., 10.* doi:10.3389/fneur.2019.00218

Barnabei, L. L.-L. (2021.). NF-κB: At the Borders of Autoimmunity and Inflammation. *Frontiers in Immunology., 12.* doi:10.3389/fimmu.2021.716469

Becker, A. M. (1963.). Cytological Demonstration of the Clonal Nature of Spleen Colonies Derived from Transplanted Mouse Marrow Cells. *Nature., 197.*, 452-454. doi:10.1038/197452a0

Bélanger, M. A. (2011.). Brain Energy Metabolism: Focus on Astrocyte-Neuron Metabolic Cooperation. *Cell Metabolism., 14.*, 724-738. doi:10.1016/j.cmet.2011.08.016

Bellucci, A. M. (2016.). Review: Parkinson's disease: from synaptic loss to connectome dysfunction. *Neuropathology and Applied Neurobiology., 42.*, 77-94. doi:10.1111/nan.12297

Bendor, J. L. (2013.). The Function of α-Synuclein. *Neuron., 79.* doi:10.1016/j.neuron.2013.09.004

Bernal-Conde, L. R.-A.-H.-O.-M.-S.-C. (2020.). Alpha-Synuclein Physiology and Pathology: A Perspective on Cellular Structures and Organelles. *Frontiers in Neuroscience., 13.* doi:10.3389/fnins.2019.01399

Birbrair, A. (Ed.). (2021.). *iPSC Derived Progenitors.* (Vol. 13.). doi:10.1016/C2020-0-02641-1

Buganim, Y. F. (2013.). Mechanisms and models of somatic cell reprogramming. *Nature Reviews Genetics., 14.*, 427-439. doi:10.1038/nrg3473

Burré, J. (2015.). The Synaptic Function of α-Synuclein. *Journal of Parkinson's Disease., 5.*, 699-713. doi:10.3233/JPD-150642

Butler, B. S. (2015.). Dopamine Transporter Activity Is Modulated by α-Synuclein. *Journal of Biological Chemistry., 290.* , 29542-29554. doi:10.1074/jbc.M115.691592

Bye, C. J. (2014.). Transcriptome analysis reveals transmembrane targets on transplantable midbrain dopamine progenitors. *PNAS., 112.*, 1946-1955. doi:10.1073/pnas.1501989112

Cao, J. W. (2008.). The involvement of NF-kappaB p65/p52 in the effects of GDNF on DA neurons in early PD rats. *Brain Research Bulletin., 76.*, 505-511. doi:10.1016/j.brainresbull.2008.03.007

Chen, C. M. (2023.). Parkinson’s disease neurons exhibit alterations in mitochondrial quality control proteins. *npj Parkinson's Disease., 9.* doi:10.1038/s41531-023-00564-3

Cogswell, P. K. (2003.). NF-κB and IκBα Are Found in the Mitochondria. *Journal of Biological Chemistry., 278.*, 2963-2968. doi:10.1074/jbc.M209995200

Cooke, S. &. (2006.). Plasticity in the human central nervous system. *Brain., 129.*, 1659-1673. doi:10.1093/brain/awl082

Daubner, S. L. (2011.). Tyrosine Hydroxylase and Regulation of Dopamine Synthesis. *Archives of Biochemistry and Biophysics., 508.*, 1-12. doi:10.1016/j.abb.2010.12.017

Day, J. &. (2021.). The Genetics of Parkinson’s Disease and Implications for Clinical Practice. *Genes., 17.* doi:10.3390/genes12071006

De Miranda, B. G. (2022.). Preventing Parkinson’s Disease: An Environmental Agenda. *Journal of Parkinson's Disease., 12.*, 45-68. doi:10.3233/JPD-212922

Deerhake, M. &. (2021.). Emerging roles of Dectin-1 in noninfectious settings and in the CNS. *Trends in Immunology., 42.*, 891-903. doi:10.1016/j.it.2021.08.005

DeGiosio, R. G. (2022.). More than a marker: potential pathogenic functions of MAP2. *Frontiers in Molecular Neuroscience., 15.* doi:10.3389/fnmol.2022.974890

Dingle, Y. B.-K. (2015.). Three-Dimensional Neural Spheroid Culture: An In Vitro Model for Cortical Studies. *Tissue Engineering Part C: Methods., 21.*, 1274-1283. doi:10.1089/ten.tec.2015.0135

Doi, D. S. (2014.). Isolation of Human Induced Pluripotent Stem Cell-Derived Dopaminergic Progenitors by Cell Sorting for Successful Transplantation. *Stem Cell Reports., 2.*, 337-350. doi:10.1016/j.stemcr.2014.01.013

Doss, M. &. (2019.). Current Challenges of iPSC-Based Disease Modeling and Therapeutic Implications. *Cells., 8.* doi:10.3390/cells8050403

Doucet-Beaupré, H. A. (2015.). Cell fate determination, neuronal maintenance and disease state: The emerging role of transcription factors Lmx1a and Lmx1b. *FEBS Letters., 589.*, 3727-3738. doi:10.1016/j.febslet.2015.10.020

Dresselhaus, E. &. (2019.). Cellular Specificity of NF-κB Function in the Nervous System. *Frontiers in Immunology., 10.* doi:10.3389/fimmu.2019.01043

Du, D. S. (2022.). Biomimetic synthesis of L-DOPA inspired by tyrosine hydroxylase. *Journal of Inorganic Biochemistry., 234.* doi:10.1016/j.jinorgbio.2022.111878

Du, Y. C. (2019.). Integration of transcriptomic and proteomic data identifies biological functions in cell populations from human infant lung. *American Journal of Physiology Lung Cellular and Molecular Physiological., 317.*, 347-360. doi:10.1152/ajplung.00475.2018

Dulski, J. U. (2022.). Genetic architecture of Parkinson’s disease subtypes – Review of the literature. *Frontiers in Aging Neuroscience.*, 14. doi:10.3389/fnagi.2022.1023574

Eeden, S. T. (2003.). Incidence of Parkinson's Disease: Variation by Age, Gender, and Race/Ethnicity. *American Journal of Epidemiology., 157.*, 1015-1022. doi:10.1093/aje/kwg068

Ewels, P. M. (2016.). MultiQC: Summarize analysis results for multiple tools and samples in a single report. *Bioinformatics.* doi:10.1093/bioinformatics/btw354

Ferguson, L. R. (2016.). Early-onset vs. Late-onset Parkinson's disease: A Clinical-pathological Study. *Canadian Journal of Neurological Sciences., 43.*, 113-119. doi:10.1017/cjn.2015.244

Funk, A. M.-W. (2012.). Abnormal Activity of the MAPK- and cAMP-Associated Signaling Pathways in Frontal Cortical Areas in Postmortem Brain in Schizophrenia. *Neuropsychopharmacology., 37.*, 896-905. doi:10.1038/npp.2011.267

Gale, E. &. (2008.). Midbrain dopaminergic neuron fate specification: Of mice and embryonic stem cells. *Molecular Brain.* doi:10.1186/1756-6606-1-8

Ganley, I. (2022.). Strengthening the link between mitophagy and Parkinson's disease. *Brain., 145.*, 4154-4156. doi:10.1093/brain/awac405

Garcia-Ruiz, P. C.-M. (2014.). Non-motor symptoms of Parkinson's disease A review…from the past. *Journal of the Neurological Sciences., 338.*, 30-33. doi:10.1016/j.jns.2014.01.002

Gerritzen, E. L. (2022.). Online Peer Support for People With Parkinson Disease: Narrative Synthesis Systematic Review. *JMIR Aging., 5.* doi:10.2196/35425

Gerschüz, A. H.-S. (2015.). Neuron-Specific Alterations in Signal Transduction Pathways associated with Alzheimer's Disease. *Journal of Alzheimer's Disease., 40.*, 135-142. doi:10.3233/JAD-131280

Gonda, Y. N. (2020.). Beyond Axon Guidance: Roles of Slit-Robo Signaling in Neocortical Formation. *Frontiers in Cell and Developmental Biology., 8.* doi:10.3389/fcell.2020.607415

Gonzalez-Suarez, A. Z.-V. (2022.). Excitatory and inhibitory neural dynamics jointly tune motion detection. *Current Biology., 32.*, 3659-3675. doi:10.1016/j.cub.2022.06.075

Green, M. &. (2016.). Precipitation of RNA with Ethanol. *Cold Spring Harbor Laboratory Press.* doi:10.1101/pdb.prot093377

Haberman, R. L. (2008.). Rapid encoding of new information alters the profile of plasticity-related mRNA transcripts in the hippocampal CA3 region. *PNAS., 105.* doi:10.1073/pnas.0804292105

Harding, O. H. (2023.). Damaged mitochondria recruit the effector NEMO to activate NF-kB signaling. *Molecular Cell., 83.*, 3188-3204. doi:10.1016/j.molcel.2023.08.005

Hauser, D. P. (2017.). The effects of variants in the PARK2 (parkin), PINK1, and PARK7 (DJ-1) genes along with evidence for their pathogenicity. *Current Protein & Peptide Science., 18.*, 702-714. doi:10.2174/1389203717666160311121954

Haxhiu, M. K. (2005.). Brain stem excitatory and inhibitory signaling pathways regulating bronchoconstrictive responses. *Journal of Applied Physiology., 98.*, 1961-1982. doi:10.1152/japplphysiol.01340.2004

Heetun, Z. &. (2012.). Gastroparesis and Parkinson's disease: A systematic review. *Parkinsonism & Related Disorders., 18.*, 433-440. doi:10.1016/j.parkreldis.2011.12.004

Hely, M. R. (2008.). The Sydney Multicenter Study of Parkinson's Disease: The Inevitability of Dementia at 20 years. *Movement Disorders., 23.*, 837-844. doi:10.1002/mds.21956

Henderson, J. D. (2002.). Preimplantation Human Embryos and Embryonic Stem Cells Show. *Stem Cells., 20.*, 329-337. doi:10.1634/stemcells.20-4-329

Henn, I. B. (2007.). Parkin mediates neuroprotection through activation of IkappaB kinase/nuclear factor-kappaB signaling. *Journal of Neuroscience., 27.*, 1868-1878. doi:10.1523/JNEUROSCI.5537-06.2007

Henrich, M. O. (2023.). Mitochondrial dysfunction in Parkinson's disease – a key disease hallmark with therapeutic potential. *Molecular Neurodegeneration., 18.* doi:10.1186/s13024-023-00676-7

Hering, H. &. (2001.). Dentritic spines: structure, dynamics and regulation. *Nature Reviews Neuroscience., 2.*, 880-888. doi:10.1038/35104061

Hilger, D. M. (2018.). Structure and dynamics of GPCR signaling complexes. *Nature Structural & Molecular Biology., 25.*, 4-12. doi:10.1038/s41594-017-0011-7

Howell, J. &. (2009.). Nuclear Export-independent Inhibition of Foxa2 by Insulin. *Journal of Biological Chemistry., 284.*, 24816–24824. doi:10.1074/jbc.M109.042135

Huang, Y. &. (2015.). Regulation of neuronal communication by G protein-coupled receptors. *FEBS Letters., 589.*, 1607-1619. doi:10.1016/j.febslet.2015.05.007

Huang, Y. W. (2023.). Parkinson's disease: From genetics to molecular dysfunction and targeted therapeutic approaches. *Genes & Diseases., 10.*, 786-798. doi:10.1016/j.gendis.2021.12.015

Jankovic, J. &. (2020.). Parkinson's disease: etiopathogenesis and treatment. *Journal of Neurology, Neurosurgery & Psychiatry., 91.*, 795-808. doi:10.1136/jnnp-2019-322338

Juengst, E. &. (2000.). The Ethics of Embryonic Stem Cells—Now and Forever, Cells Without End. *JAMA., 284.*, 3180-3184. doi:10.1001/jama.284.24.3180

Jung, J. R. (2016.). NIK/MAP3K14 Regulates Mitochondrial Dynamics and Trafficking to Promote Cell Invasion. *Current Biology., 26.*, 3288-3302. doi:10.1016/j.cub.2016.10.009

Kaech, S. L. (1996.). Cytoskeletal Plasticity in Cells Expressing Neuronal Microtubule-Associated Proteins. *Neuron., 17.*, 1189-1199. doi:10.1016/S0896-6273(00)80249-4

Kaltschmidt, B. H. (2022.). NF-κB in neurodegenerative diseases: Recent evidence from human genetics. *Frontiers in Molecular Neuroscience., 15.* doi:10.3389/fnmol.2022.954541

Kaneko, N. H.-P.-V. (2018.). New neurons use Slit-Robo signaling to migrate through the glial meshwork and approach a lesion for functional regeneration. *Cellular Neuroscience., 4.* doi:10.1126/sciadv.aav0618

Kawahata, I. F. (2022.). Pathogenic Impact of α-Synuclein Phosphorylation and Its Kinases in α-Synucleinopathies. *International Journal of Molecular Sciences., 23.* doi:10.3390/ijms23116216

Keller, G. (2005.). Embryonic stem cell differentiation: emergence of a new era in biology and medicine. *Genes & Development., 19.*, 1129-1155. doi:10.1101/gad.1303605

Kim, Y. J. (2020.). Microtubule-associated protein 2 mediates induction of long-term potentiation in hippocampal neurons. *FASEB., 34.*, 6965-6983. doi:10.1096/fj.201902122RR

Kingeter, L. &. (2012.). C-type lectin receptor-induced NF-kB activation in innate immune and inflammatory responses. *Cellular & Molecular Immunology., 9.*, 105-112. doi:10.1038/cmi.2011.58

Kinter, C. (2022.). Neurogenesis in Embryos and in Adult Neural Stem Cells. *Journal of Neuroscience., 22.*, 639-643. doi:10.1523/JNEUROSCI.22-03-00639.2002

Kirkeby, A. N. (2017.). Predictive Markers Guide Differentiation to Improve Graft Outcome in Clinical Translation of hESC-Based Therapy for Parkinson's Disease. *Cell Stem Cell., 20.*, 135-148. doi:10.1016/j.stem.2016.09.004

Klann, E. D.-Z.-M. (2021.). The Gut-Brain Axis and Its Relation to Parkinson's Disease: A Review. *Frontiers in Aging Neuroscience., 13.* doi:10.3389/fnagi.2021.782082

Knight, E. G. (2022.). The Role of Diet and Dietary Patterns in Parkinson's Disease. *Nutrients., 14.* doi:10.3390/nu14214472

Knoepfler, P. (2009.). Deconstructing Stem Cell Tumorigenicity: A Roadmap to Safe Regenerative Medicine. *Stem Cells., 27.*, 1050-1056. doi:10.1002/stem.37

Kontaxi, C. &. (2023.). Synuclein phosphorylation: pathogenic or physiologic? *npj Parkinson's Disease., 9.* doi:10.1038/s41531-023-00487-z

Kreutz, A. H. (2023.). Pluripotent Stem Cell-derived Dopaminergic Neurons for Studying Developmental Neurotoxicity. *Stem Cell Reviews and Reports., 19.*, 2120-2130. doi:10.1007/s12015-023-10555-9

Kumar, A. T. (2023.). Spatiotemporal transcriptomic maps of whole mouse embryos at the onset of organogenesis. *Nature Genetics., 55.*, 117-1185. doi:10.1038/s41588-023-01435-6

Kumar, D. Y. (2016.). Integrated Transcriptomic-Proteomic Analysis Using a Proteogenomic Workflow Refines Rat Genome Annotation. *Molecular and Cellular Proteomics., 15.*, 329-339. doi:10.1074/mcp.M114.047126

Laforge, M. R. (2016.). NF-κB pathway controls mitochondrial dynamics. *Cell Death & Differentiation., 23.*, 89-98. doi:10.1038/cdd.2015.42

Li, M. Z. (2016.). Efficient derivation of dopaminergic neurons from SOX1− floor plate cells under defined culture conditions. *Journal of Biomedical Science., 23.* doi:10.1186/s12929-016-0251-6

Li, Y. J. (1998.). Neuronal Damage and Plasticity Identified by Microtubule-Associated Protein 2, Growth-Associated Protein 43, and Cyclin D1 Immunoreactivity After Focal Cerebral Ischemia in Rats. *Stroke., 29.*, 1972-1981. doi:10.1161/01.STR.29.9.1972

Liao, L. P. (2008.). Quantitative proteomic analysis of primary neurons reveals diverse changes in synaptic protein content in fmr1 knockout mice. *PNAS., 105.*, 15281-15286. doi:10.1073/pnas.0804678105

Lim, K. N. (2012.). Mitochondrial Dynamics and Parkinson's Disease: Focus on Parkin. *Antioxidants & Redox Signaling., 16.*, 935-949. doi:10.1089/ars.2011.4105

Linhoff, M. L. (2009.). An Unbiased Expression Screen for Synaptogenic Proteins Identifies the LRRTM Protein Family as Synaptic Organizers. *Neuron., 61.*, 734-749. doi:10.1016/j.neuron.2009.01.017

Liu, C. O. (2018.). Modeling human diseases with induced pluripotent stem cells: from 2D to 3D and beyond. *Development., 145.* doi:10.1242/dev.156166

Liu, T. Z. (2017.). NF-κB signaling in inflammation. *Signal Transduction and Targeted Therapy., 2.* doi:10.1038/sigtrans.2017.23

Llansol, M. S. (2001.). NMDA-induced phosphorylation of the microtubule-associated protein MAP-2 is mediated by activation of nitric oxide synthase and MAP kinase. *European Journal of Neuroscience., 13.*, 1283-1291. doi:10.1046/j.0953-816x.2001.01497.x

Loewa, A. F. (2023.). Human disease models in drug development. *Nature Reviews Bioengineering., 1.*, 545-559. doi:10.1038/s44222-023-00063-3

Love, M. H. (2014.). Moderated estimation of fold change and dispersion for RNA-seq data with DESeq2. *Genome Biology., 15.* doi:10.1186/s13059-014-0550-8

Malecki, M. A. (2012.). TRA-1-60+, SSEA-4+, Oct4A+, Nanog+ Clones of Pluripotent Stem Cells in the Embryonal Carcinomas of the Ovaries. *Journal of Stem Cell Research & Therapy.* Retrieved from https://pubmed.ncbi.nlm.nih.gov/23293749/

Manzoni, C. K. (2016.). Genome, transcriptome and proteome: the rise of omics data and their integration in biomedical sciences. *Briefings in Bioinformatics., 19.*, 286-302. doi:10.1093/bib/bbw114

Martello, G. &. (2014.). The Nature of Embryonic Stem Cells. *Annual Review of Cell and Developmental Biology., 30.*, 647-675. doi:10.1146/annurev-cellbio-100913-013116

Maynard, S. R. (2023.). Quantifying postsynaptic receptor dynamics: insights into synaptic function. *Nature Reviews Neuroscience., 24.*, 4-22. doi:10.1038/s41583-022-00647-9

McNaught, K. O. (2001.). Failure of the ubiquitin–proteasome system in Parkinson's disease. *Nature Reviews Neuroscience., 2.*, 589-594. doi:10.1038/35086067

Mehanna, R. &. (2019.). Young-onset Parkinson's disease: Its unique features and their impact on quality of life. *Parkinsonism & Related Disorders., 65.*, 39-48. doi:10.1016/j.parkreldis.2019.06.001

Mehanna, R. M. (2014.). Comparing clinical features of young onset, middle onset and late onset Parkinson's disease. *Parkinsonism & Related Disorders., 20.*, 530-534. doi:10.1016/j.parkreldis.2014.02.013

Mishra, A. &. (2022.). Dopaminergic Axons: Key Recitalists in Parkinson’s Disease. *Neurochemical Research., 47.*, 234-248. doi:10.1007/s11064-021-03464-1

Moustafa, A. C. (2016.). Motor symptoms in Parkinson's disease: A unified framework. *Neuroscience & Biobehavioral Reviews., 68.*, 727-740. doi:10.1016/j.neubiorev.2016.07.010

Mu, J. Z. (2022.). The physiological and pathological mechanisms of early embryonic development. *Fundamental Research., 2.*, 859-872. doi:10.1016/j.fmre.2022.08.011

Murphy, C. L. (2020.). Nuclear factor kappa B activation appears weaker in schizophrenia patients with high brain cytokines than in non-schizophrenic controls with high brain cytokines. *Journal of Neuroinflammation., 17.* doi:10.1186/s12974-020-01890-6

Najafi, F. M. (2023.). Association between socioeconomic status and Parkinson’s disease: findings from a large incident case–control study. *BMJ Neurology Open., 5.* doi:10.1136/bmjno-2022-000386

Nan, J. H. (2017.). TNFR2 Stimulation Promotes Mitochondrial Fusion via Stat3- and NF-kB–Dependent Activation of OPA1 Expression. *Circulation Research., 121.*, 392-410. doi:10.1161/CIRCRESAHA.117.311143

Nelson, A. &. (2017.). Axonal Membranes and Their Domains: Assembly and Function of the Axon Initial Segment and Node of Ranvier. *Frontiers in Cellular Neuroscience., 11.* doi:10.3389/fncel.2017.00136

Ng, J. &. (2004.). Rho GTPases Regulate Axon Growth through Convergent and Divergent Signaling Pathways. *Neuron., 44.*, 779-793. doi:10.1016/j.neuron.2004.11.014

Nie, L. W. (2008.). Integrative Analysis of Transcriptomic and Proteomic Data: Challenges, Solutions and Applications. *Critical Reviews in Biotechnology., 27.*, 63-75. doi:10.1080/07388550701334212

Olanow, W. &. (2006.). Ubiquitin–proteasome system and Parkinson's disease. *Movement Disorders., 21.*, 1806-1823. doi:10.1002/mds.21013

Pagin, M. P. (2021.). Sox2 controls neural stem cell self-renewal through a Fos-centered gene regulatory network. *Stem Cells., 39.*, 1107–1119. doi:10.1002/stem.3373

Paik, E. O. (2018.). Using intracellular markers to identify a novel set of surface markers for live cell purification from a heterogeneous hIPSC culture. *Scientific Reports., 8.* doi:10.1038/s41598-018-19291-4

Pan, L. M. (2021.). Tau in the Pathophysiology of Parkinson's Disease. *Journal of Molecular Neuroscience., 71.*, 2179-2191. doi:10.1007/s12031-020-01776-5

Park, D. X. (2010.). Nestin is required for the proper self-renewal of neural stem cells. *Stem Cells.* doi:10.1002/stem.541

Park, S. G. (2023.). Engineering considerations of iPSC-based personalized medicine. *Biomaterials Research., 27.* doi:10.1186/s40824-023-00382-x

Parkinson, J. (1817.). An Essay on the Shaking Palsy. *Sherwood, Neely, and Jones.*

Pazarentzos, E. M.-M.-R.-A. (2014.). IκBα inhibits apoptosis at the outer mitochondrial membrane independently of NF-κB retention. *The EMBO Journal., 33.*, 2814-2828. doi:10.15252/embj.201488183

Pflug, K. L. (2023.). NF-κB-inducing kinase maintains mitochondrial efficiency and systemic metabolic homeostasis. *BBA - Molecular Basis of Disease., 1869.* doi:10.1016/j.bbadis.2023.166682

Picconi, B. P. (2012.). Synaptic Dysfunction in Parkinson's Disease. *Synaptic Plasticity., 970.*, 553-572. doi:10.1007/978-3-7091-0932-8_24

Pigott, J. K. (2022.). Systematic review and meta-analysis of clinical effectiveness of self-management interventions in Parkinson's disease. *BMC Geriatrics., 22.* doi:10.1186/s12877-021-02656-2

Piredda, R. D.-S. (2019.). Cognitive and psychiatric symptoms in genetically determined Parkinson's disease: a systematic review. *European Journal of Neurology., 27.*, 229-234. doi:10.1111/ene.14115

Pittenger, M. D. (2019.). Mesenchymal stem cell perspective: cell biology to clinical progress. *npj Regenerative Medicine., 4.* doi:10.1038/s41536-019-0083-6

Pohl, C. &. (2019.). Cellular quality control by the ubiquitin-proteasome system and autophagy. *Science., 366.*, 818-822. doi:10.1126/science.aax3769

Post, B. H. (2020.). Young Onset Parkinson's Disease: A Modern and Tailored Approach. *Journal of Parkinson's Disease., 10.*, 29-36. doi:10.3233/JPD-202135

Prakash, N. &. (2006.). Development of dopaminergic neurons in the mammalian brain. *Cellular and Molecular Life Sciences., 63.*, 187-206. doi:10.1007/s00018-005-5387-6

Puri, R. C. (2019.). Mul1 restrains Parkin-mediated mitophagy in mature neurons by maintaining ER-mitochondrial contacts. *Nature Communications., 10.* doi:10.1038/s41467-019-11636-5

Ramalingam, N. J.-O. (2023.). Dynamic physiological α-synuclein S129 phosphorylation is driven by neuronal activity. *npj Parkinson's Disease., 9.* doi:10.1038/s41531-023-00444-w

Reinhardt, P. G. (2013.). Derivation and Expansion Using Only Small Molecules of Human Neural Progenitors for Neurodegenerative Disease Modeling. *PLoS ONE.* doi:10.1371/journal.pone.0059252

Riboldi, G. F. (2022.). A Practical Approach to Early-Onset Parkinsonism. *Journal of Parkinson's Disease., 12.*, 1-26. doi:10.3233/JPD-212815

Roberts, D. A. (2004.). A Vascular Gene Trap Screen Defines RasGRP3 as an Angiogenesis-Regulated Gene Required for the Endothelial Response to Phorbol Esters. *Molecular*

and Cellular Biology., 24., 10515-10528. doi:10.1128/MCB.24.24.10515-10528.2004

Rohani, L. J. (2018.). Concise Review: Molecular Cytogenetics and Quality Control: Clinical Guardians for Pluripotent Stem Cells. *Stem Cells Translational Medicine., 7.*, 867-875. doi:10.1002/sctm.18-0087

Runge, K. C. (2020.). Dendritic Spine Plasticity: Function and Mechanisms. *Frontiers in Synaptic Neuroscience., 12.* doi:10.3389/fnsyn.2020.00036

Saab, A. &. (2017.). Myelin dynamics: protecting and shaping neuronal functions. *Current Opinion in Neurobiology., 47.*, 104-112. doi:10.1016/j.conb.2017.09.013

Sadler, T. (2005.). Embryology of neural tube development. *American Journal of Medical Genetics Part C., 135C.*, 2-8. doi:10.1002/ajmg.c.30049

Samata, B. D. (2016.). Purification of functional human ES and iPSC-derived midbrain dopaminergic progenitors using LRTM1. *Nature Communications., 7.* doi:10.1038/ncomms13097

Schirinzi, T. L. (2020.). Young-onset and late-onset Parkinson's disease exhibit a different profile of fluid biomarkers and clinical features. *Neurobiology of Aging.*, 119-124. doi:10.1016/j.neurobiolaging.2020.02.012

Seigfried, F. C. (2017.). Frizzled 3 acts upstream of Alcam during embryonic eye development. *Developmental Biology., 426.*, 69-83. doi:10.1016/j.ydbio.2017.04.004

Sharma, A. S. (2020.). Multi-lineage Human iPSC-Derived Platforms for Disease Modeling and Drug Discovery. *Cell Stem Cell., 26.*, 309-329. doi:10.1016/j.stem.2020.02.011

Sheng, M. &. (2002.). Postsynaptic Signaling and Plasticity Mechanisms. *Science., 298.*, 776-780. doi:10.1126/science.1075333

Sherchan, P. T. (2020.). The potential of slit2 as a therapeutic target for central nervous system disorders. *Expert Opinion on Therapeutic Targets., 24.*, 805-818. doi:10.1080/14728222.2020.1766445

Shi, Y. I. (2017.). Induced pluripotent stem cell technology: a decade of progress. *Nature Reviews Drug Discovery., 16.*, 115-130. doi:10.1038/nrd.2016.245

Spellman, D. D. (2008.). Stable Isotopic Labeling by Amino Acids in Cultured Primary Neurons. *Molecular & Cellular Proteomics., 7.*, 1067-1076. doi:10.1074/mcp.M700387-MCP200

Spillane, M. &. (2014.). Involvement of Rho-family GTPases in axon branching. *Small GTPases., 5.* doi:10.4161/sgtp.27974

Strong, C. Z. (2023.). Functional brain region-specific neural spheroids for modeling neurological diseases and therapeutics screening. *Communications Biology., 6.* doi:10.1038/s42003-023-05582-8

Sulzer, D. &. (2013.). Neuronal vulnerability, pathogenesis, and Parkinson's disease. *Movement Disorders., 28.*, 715-724. doi:10.1002/mds.25187

Sun, S. (2017.). The non-canonical NF-κB pathway in immunity and inflammation. *Nature Reviews Immunology., 17.*, 545-558. doi:10.1038/nri.2017.52

Sund, N. V. (2001.). Tissue-specific deletion of Foxa2 in pancreatic β cells results in hyperinsulinemic hypoglycemia. *Genes & Development., 15.*, 1706-1715. doi:10.1101/gad.901601

Swain, N. T. (2020.). The core embryonic stem cell pluripotency regulators in oral carcinogenesis. *Journal of Oral and Maxillofacial Pathology., 24*, 368-373. doi:10.4103/jomfp.JOMFP_22_20

Tagliaferro, P. &. (2016.). Retrograde Axonal Degeneration in Parkinson Disease. *Journal of Parkinson's Disease., 6.*, 1-15. doi:10.3233/JPD-150769

Takahashi, K. T. (2007.). Induction of pluripotent stem cells from adult human fibroblasts by defined factors. *Cell., 131.*, 861-872. doi:10.1016/j.cell.2007.11.019

Tan, A. L. (2022.). The microbiome–gut–brain axis in Parkinson disease — from basic research to the clinic. *Nature Reviews Neurology., 18.*, 476-495. doi:10.1038/s41582-022-00681-2

Thakurela, S. T. (2016.). Mapping gene regulatory circuitry of Pax6 during neurogenesis. *Cell Discovery.* doi:10.1038/celldisc.2015.45

Tian, C. L. (2015.). Selective Generation of Dopaminergic Precursors from Mouse Fibroblasts by Direct Lineage Conversion. *Scientific Reports.* doi:10.1038/srep12622

Tong, M. J. (2019.). The Role of the Slit/Robo Signaling Pathway. *Journal of Cancer., 10.*, 2694-2705. doi:10.7150/jca.31877

Trares, K. A. (2022.). The canonical and non-canonical NF-κB pathways and their crosstalk: A comparative study based on Petri nets. *Biosystems., 211.* doi:10.1016/j.biosystems.2021.104564

Truban, D. H. (2017.). PINK1, Parkin, and Mitochondrial Quality Control: What can we Learn about Parkinson's Disease Pathobiology? *Journal of Parkinson's Disease., 7.*, 13-29. doi:10.3233/JPD-160989

Umeda, K. N. (2019.). RasGRF1 mediates brain-derived neurotrophic factor-induced axonal growth in primary cultured cortical neurons. *Biochemistry and Biophysics Reports., 17.*, 56-64. doi:10.1016/j.bbrep.2018.11.011

Verneri, P. E. (2020.). Dynamical reorganization of the pluripotency transcription factors Oct4 and Sox2 during early differentiation of embryonic stem cells. *Scientific reports., 10.* doi:10.1038/s41598-020-62235-0

Villalba, R. &. (2010.). Striatal spine plasticity in Parkinson's disease. *Frontiers in Neuroanatomy., 4.* doi:10.3389/fnana.2010.00133

Vuidel, A. C.-D. (2022.). High-content phenotyping of Parkinson's disease patient stem cell-derived midbrain dopaminergic neurons using machine learning classification. *Stem Cell Reports., 17.*, 2349–2364. doi:10.1016/j.stemcr.2022.09.001

Walters, G. &. (2023.). Mitochondrial calcium cycling in neuronal function and neurodegeneration. *Frontiers in Cell and Developmental Biology., 11.* doi:10.3389/fcell.2023.1094356

Wang, H. G.-J. (2002.). Foxa2 (HNF3β) Controls Multiple Genes Implicated in Metabolism-Secretion Coupling of Glucose-induced Insulin Release. *The Journal of Biological Chemistry., 277.*, 17564-17570. doi:10.1074/jbc.M111037200

Wang, Q. L. (2015.). Neuroinflammation in Parkinson's disease and its potential as therapeutic target. *Translational Neurodegeneration., 4.* doi:10.1186/s40035-015-0042-0

Weatherbee, B. C.-G. (2021.). Modeling human embryo development with embryonic and extra-embryonic stem cells. *Developmental Biology., 474.*, 91-99. doi:10.1016/j.ydbio.2020.12.010

Weihe, E. D. (2006.). Three Types of Tyrosine Hydroxylase-Positive CNS Neurons Distinguished by Dopa Decarboxylase and VMAT2 Co-Expression. *Cellular and Molecular Neurobiology., 26.*, 659-678. doi:10.1007/s10571-006-9053-9

Wert, G. &. (2003.). Human embryonic stem cells: research, ethics and policy. *Human Reproduction., 18.*, 672-682. doi:10.1093/humrep/deg143

Wickham, H. (2016.). *ggplot2: Elegant Graphics for Data Analysis.* Springer-Verlag New York. Retrieved from https://ggplot2.tidyverse.org

Wickremaratchi, M. K.-S. (2011.). The motor phenotype of Parkinson's disease in relation to age at onset. *Movement Disorders., 26.*, 457-463. doi:10.1002/mds.23469

Willis, A. E. (2010.). Geographic and Ethnic Variation in Parkinson Disease: A Population-Based Study of US Medicare Beneficiaries. *Neuroepidemiology., 34.*, 143-151. doi:10.1159/000275491

Willmann, K. S. (2016.). Expanding the Interactome of the Noncanonical NF-κB Signaling Pathway. *Journal of Proteome Research., 15.* doi:2900-2909.

Wolfrum, C. A. (2004.). Foxa2 regulates lipid metabolism and ketogenesis in the liver during fasting and in diabetes. *Nature., 432.*, 1027-1032. doi:10.1038/nature03047

Wolfrum, C. B. (2003.). Insulin regulates the activity of forkhead transcription factor Hnf-3β/Foxa-2 by Akt-mediated phosphorylation and nuclear/cytosolic localization. *PNAS., 100.*, 11624–11629. doi:10.1073/pnas.1931483100

Yang, F. J. (2016.). Socioeconomic status in relation to Parkinson's disease risk and mortality. *Medicine., 95.* doi:10.1097/MD.0000000000004337

Ye, X. H. (2020.). Dectin-1/Syk signaling triggers neuroinflammation after ischemic stroke in mice. *Journal of Neuroinflammation., 17.* doi:10.1186/s12974-019-1693-z

Yin, F. B. (2014.). Mitochondrial Energy Metabolism and Redox Signaling in Brain Aging and Neurodegeneration. *Antioxidants & Redox Signaling., 20.* doi:10.1089/ars.2012.4774

Zakrzewski, W. D. (2019.). Stem cells: past, present, and future. *Stem Cell Research & Therapy., 10.* doi:10.1186/s13287-019-1165-5

Zhai, J. X. (2022.). Human embryonic development: from peri-implantation to gastrulation. *Trends in Cell Biology., 32.*, 18-29. doi:10.1016/j.tcb.2021.07.008

Zhang, G. D. (2011.). Study of neurotrophin 3 signaling in primary cultured neurons using multiplex stable isotope labeling with amino acids in cell culture. *Journal of Proteome Research., 10.*, 2546-2554. doi:10.1021/pr200016n

Zhang, J. J. (2023.). Tau-PET imaging in Parkinson's disease: a systematic review and meta-analysis. *Frontiers in Neurology., 14.* doi:10.3389/fneur.2023.1145939

Zhang, X. G. (2018.). Tau Pathology in Parkinson's Disease. *Frontiers in Neurology., 9.* doi:10.3389/fneur.2018.00809

Zheng, Y. Z. (2019.). Mitochondrial transport serves as a mitochondrial quality control strategy in axons: Implications for central nervous system disorders. *CNS Neuroscience & Therapeutics., 25.*, 876-886. doi:10.1111/cns.13122

Zhong, Z. U.-L.-M. (2016.). NF-kB Restricts Inflammasome Activation via Elimination of Damaged Mitochondria. *Cell., 164.*, 896-910. doi:10.1016/j.cell.2015.12.057